SYNTHESIS AND CHARACTERIZATION OF UNSYMMETRICAL PORPHYRINS AND THEIR ZINC COMPLEXES

BY

MISS JANTIMA SUKJAN

A THESIS SUBMITTED IN PARTIAL FULFILLMENT OF THE REQUIREMENTS FOR THE DEGREE OF MASTER OF SCIENCE IN CHEMISTRY FACULTY OF SCIENCE AND TECHNOLOGY THAMMASAT UNIVERSITY ACADEMIC YEAR 2014

SYNTHESIS AND CHARACTERIZATION OF UNSYMMETRICAL PORPHYRINS AND THEIR ZINC COMPLEXES

BY

MISS JANTIMA SUKJAN

A THESIS SUBMITTED IN PARTIAL FULFILLMENT OF THE REQUIREMENTS FOR THE DEGREE OF MASTER OF SCIENCE IN CHEMISTRY FACULTY OF SCIENCE AND TECHNOLOGY THAMMASAT UNIVERSITY ACADEMIC YEAR 2014

THAMMASAT UNIVERSITY
FACULTY OF SCIENCE AND TECHNOLOGY

THESIS

BY

MISS JANTIMA SUKJAN

ENTITLED

SYNTHESIS AND CHARACTERIZATION OF UNSYMMETRICAL PORPHYRINS AND THEIR ZINC COMPLEXES

was approved as partial fulfillment of the requirements for
the degree of master of science in chemistry

on July, 2015

Chairman _____
(Assistant Professor Kittipong Chainok, Ph.D.)

Member and Advisor _____
(Assistant Professor Supakorn Boonyuen, Ph.D.)

Member and Co-advisor _____
(Nanthawat Wannarit, Ph.D.)

Member _____
(Parichatr Vanalabhpatana, Ph.D.)

Dean _____
(Associate Professor Pakorn Sermsuk)

Thesis Title	SYNTHESIS AND CHARACTERIZATION OF UNSYMMETRICAL PORPHYRINS AND THEIR ZINC COMPLEXES
Author	Miss Jantima Sukjan
Degree	Master of Science
Department/Faculty/University	Chemistry Science and Technology Thammasat University
Thesis Advisor	Assistant Professor Supakorn Boonyuen, Ph.D.
Thesis Co-Advisor	Nanthawat Wannarit, Ph.D.
Academic Year	2014

ABSTRACT

Porphyrins have attracted considerable attention because they are an important class of naturally occurring macrocyclic compounds found in biological molecules that play very important roles in several life processes. They have biological importance and fascinating physical, chemical, and spectroscopic properties. Porphyrins have wide prospective applications in many fields such as biomimetic catalysis, electrocatalysis, biological sensors, and so on. In particular, dye-sensitized solar cells using porphyrins have gained widespread attention in recent years because of their low production costs, ease of fabrication, and tunable optical properties such as color and transparency.

In the current study, a series of metal-free tetrasubstituted phenylporphyrins containing one group of alkoxy and carboxyl on the *para* position of the phenyl rings were successfully synthesized by condensing a mixture of pyrrole and benzaldehyde using the modified Adler-Longo method. The Zinc complexes were prepared by adding Zinc ion (Zn^{2+}) into the central hole of mentioned free base porphyrins. To examine the structure and study the effect of different peripheral substitution on the *para* position of the phenyl rings, reference tetraphenylporphyrins were prepared as described. All the synthesized porphyrins were characterized by UV-Vis, fluorescence, infrared and nuclear magnetic resonance spectroscopy. The elemental analysis and X-ray

crystallography were used to confirm the structure. Mass spectrometry was selected as a tool for molecular mass analysis of complexes fragmentation patterns. Finally, the thermal stability of synthesized porphyrins was studied by using thermal gravimetric analysis.

Keywords: Porphyrins, Adler-Longo method, asymmetric

“….สิ่งที่มิได้คิดไว้ จะมีก็ได้ สิ่งที่คิดไว้ จะพินาศไปก็ได้ โภคะ

ทั้งหลายของหญิงก็ตาม ของชายก็ตาม มิได้สำเร็จด้วยเพียงคิดเท่านั้น.”

“Things that we do not plan may well happen. Things that we do plan may well meet with disaster. Wealth will not come to anybody by just dreaming about it.”

His Majesty King Bhumibol Adulyadej

The Story of Mahajanaka

ACKNOWLEDGEMENTS

Many people have been very supportive me in various way. I would like to begin by thanking Assistant Professor Dr.Supakorn Boonyuen for being the best advisor anyone could ever ask for. I was so lucky to have him as my advisor. He provided me with opportunities to know porpyrins and to enjoy porphyrin research. He provided me with abundant guidance and support, and always believed in me and encouraged me to do my best. He is always there for me to help me with my research. It was a great pleasure and privilege to study under his mentorship.

I also wish to thank my co-advisor, Dr.Nanthawat Wannarit, for his guidance, insight, and support throughout this research endeavor. I truly appreciate the time they have devoted to helping me. My special thanks go to Assistant Professor Dr.Kittipong Chainok and Dr. Parichatr Vanalabhpatana for the time and patience they have spent reading and editing the manuscript of this Dissertation. Thank you for their invaluable discussions about crystallography, which was very valuable for my research. I want to thank the technical staffs at Thammasat and Chulalongkorn University. My thanks also to Central Scientific Instrument Center (CSIC), Faculty of Science and Technology, Thammasat University, for performing analyzed. Especialy, I would like to thank you The National Research Council of Thailand (NRCT) for supporting “FY2015 Thesis Grant for Master Degree Student” under the topic: Synthesis and Characterization of Unsymmetrical Porphyrins and Their Complexes.

I wish to thank all my friends and my research group, especially, Kamolnate Jansaeng and Wootthiphan Jantayot among many others, who have inspired, supported and encouraged me over the years. I would like to thank my wonderful family for their unconditional love and support. My grandmother deserves special recognition for being the best role models I could imagine, and also for encouraging my lifelong. Finally, I would like to thank the authors acknowledge the Department of Chemistry, Faculty of science and Thecnology, Thammasat University.

Miss Jantima Sukjan

TABLE OF CONTENTS

LIST OF TABLES

LIST OF FIGURES

LIST OF SCHEMES

LIST OF ABBREVIATIONS

Symbols/Abbreviations	Terms
^{1}H-NMR	Proton Nuclear Magnetic Resonance Spectroscopy
Å	Length
δ	Chemical shift
J	Coupling constant
°	Angle
calcd	Calculated
CTrPP	5-(4-Carboxyphenyl)-10,15,20-triphenylporphyrin
CTrPP-2	Bis(4-carboxyphenyl)-diphenylporphyrin or 5,15-bis(4-carboxyphenyl)-10,20-diphenylporphyrin
CTrPP-3	5,10,15-Tris(4-carboxyphenyl)-20-phenylporphyrin
ESI-MS	Electrospray Ionization Mass Spectrometry
HTrPP	5-(4-Hydroxyphenyl)-10,15,20-triphenylporphyrin
IR	Infrared
K	Kelvin
MeTrPP	5-(4-Methoxyphenyl)-10,15,20-triphenylporphyrin
MeTrPP-2	5,10-Bis(4-methoxyphenyl)-15,20-diphenylporphyrin or 5,15-bis(4-methoxy)-10,20-diphenylporphyrin
MeTrPP-3	5,10,15-Tris(4-methoxyphenyl)-20-phenylporphyrin

MTrPP	5-(4-Methylphenyl)-10,15,20-triphenylporphyrin
OTrPP	5-(4-Octyloxyphenyl)-10,15,20-triphenylporphyrin
TCPP	5,10,15,20-Tetrakis(4-carboxyphenyl) porphyrin
TGA	Thermogravimetric Analysis
TMePP	5,10,15,20-Tetrakis(4-methoxylphenyl) porphyrin
TPP	5,10,15,20-Tetraphenylporphyrin
ZnCTrPP	Zinc-5-(4-Carboxyphenyl)-10,15,20-triphenylporphyrin
ZnCTrPP-2	Zinc-5,10-bis(4-carboxyphenyl)-15,20-diphenylporphyrin or Zinc-5,15-bis(4-carboxyphenyl)-10,20-diphenylporphyrin
ZnCTrPP-3	Zinc-5,10,15-tris(4-carboxyphenyl)-20-phenylporphyrin
ZnHTrPP	Zinc-5-(4-hydroxyphenyl)-10,15,20-triphenylporphyrin
ZnMeTrPP	Zinc-5-(4-methoxyphenyl)-10,15,20-triphenylporphyrin
ZnMeTrPP-2	Zinc-5,10-bis(4-methoxyphenyl)-15,20-diphenylporphyrin or Zinc-5,15-bis(4-methoxy)-10,20-diphenylporphyrin
ZnMeTrPP-3	Zinc-5,10,15-tris(4-methoxyphenyl)-20-phenylporphyrin
ZnMTrPP	Zinc-5-(4-methylphenyl)-10,15,20-triphenylporphyrin

ZnOTrPP	Zinc-5-(4-octyloxyphenyl)-10,15,20-triphenylporphyrin
ZnTCPP	Zinc-5,10,15,20-tetrakis(4-carboxyphenyl) porphyrin
ZnTMePP	Zinc-5,10,15,20-tetrakis(4-methoxylphenyl) porphyrin
ZnTPP	Zinc-5,10,15,20-tetraphenylporphyrin

CHAPTER 1
INTRODUCTION

All organisms need energy to survive. Living things use energy to grow, to move around and to defend themselves. There are many forms of energy such as chemical energy, thermal energy, mechanical energy, radiant energy, electrical energy and nuclear energy. Especially the electrical energy is becoming more and more important for nearly everybody in daily life, communication, transportation, education and economic growth. The electrical energy is necessary for increasing the productivity from agriculture and industry. Accordingly, electrical energy is the one important factor in economic growth that leads to economic development. Many different energy resources can be used to make electricity. The energy resources include fossil fuels, wind, biomass, geothermal energy and solar energy. However, Thailand still imports fuel from abroad to produce energy. (EIA data, 2014) Therefore, Thailand needs to accelerate development for reduce expensive fuel imports and increases production of energy from alternative energy sources.

The sun is probably the most important source of renewable energy available today. The widespread use of solar energy as a clean, carbon-free, cost-effective electricity source will expand through the development of a variety of photovoltaic (PV) technologies. A solar cell, or photovoltaic cell, is an electrical device that converts the energy of light directly into electricity by the photovoltaic effect, which is a physical and chemical phenomenon. Whereas solar cell will continue to become cheaper and more efficient over time, fuel has the opposite effect – becoming more expensive. Dye-sensitized solar cells (DSSCs) are proposed as alternatives to conventional solar cells of silicon. DSSCs have numerous advantages over silicon based solar cells such as low materials cost, ease of production, and efficiencies out performing amorphous silicon solar cells.

Porphyrins are one of the important chemical parts essential for several life processes in the nature. They are aromatic macrocycles containing a total of 22 conjugated π electrons, 18 of which are incorporated into the delocalized pathway. Porphyrins are found in many natural systems, where they play an essential role as

photoactive, redox, guest-binding, and catalytic entities. They are immense biological importance and fascinating physical, chemical, and spectroscopic properties. Because of their special properties, porphyrins have wide applications in many fields such as biomimetic catalysis, electro catalysis, biological sensors, solar energy conversion, and so on. The aim of this thesis was to design and synthesize porphyrins as dye sensitizers.

1.1 Introduction to the porphyrin structure

Porphyrins are one of the important chemical parts essential for several life processes in the nature. Many biological molecules essentially made of these units. The most obvious example is heme, which is the pigment that gives red blood cells their color. Heme is as a component of hemoglobin that transports oxygen to animal tissues and as the central unit of myoglobin ensures the storage of oxygen [1-2]. Another relative of chlorophyll is vitamin B12. Vitamin B12 contains a cobalt ion at the center of the porphyrin [3]. It is essential to digestion and nutritional absorption in animals. Chlorophyll [4], the green pigment of plants is capable of channeling the energy of sunlight into chemical energy through the process of photosynthesis.

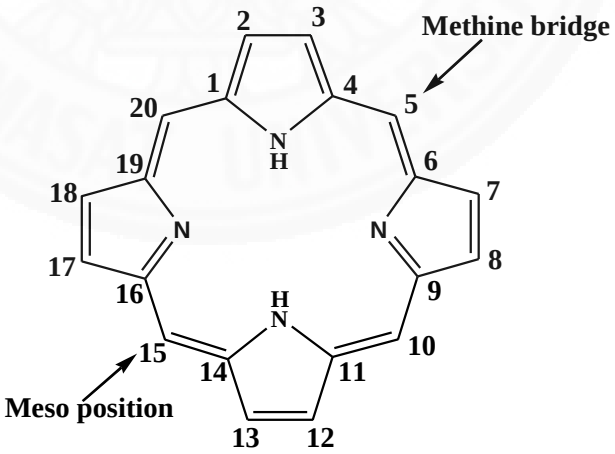

Figure 1. The structure of porphyrins

The name porphyrin has its origin in ancient Greece with the word *porphura* meaning purple. Porphyrin is the name given to a family of intensely

colored molecules all sharing a macrocycle of twenty carbon atoms and four nitrogen atoms. The porphyrins are aromatic molecules where four pyrrole rings forming a square, are connected by unsaturated methine bridges to complete a macrocycle [5] (Figure 1). They are aromatic macrocycles containing a total of 22 conjugated π electrons, 18 of which are incorporated into the delocalized pathway in agree with Huckel's [4n + 2] rule for aromaticity (n = 4). The porphyrin macrocycles are quite flexible and easy for being π-delocalized system furthermore by introducing substituents selectively at the β- or *meso*-positions, adding the central metal or extending the macrocycle. In general, metalloporphyrins have the central part of the ring occupied by a metal ion linked to two pyrrole rings to yield the necessary structural stability [5-7]. The central cavity of the porphyrin is sufficiently large to coordinate most metal ions such as Fe^{2+}, Zn^{2+}, Cu^{2+}, Ni^{2+}, Mg^{2+}, Ag^{2+}, and Co^{2+}. The porphyrin is a nearly flat molecule (x-ray crystallographic data). Although previous reported X-ray structures of simple porphyrins showed the ring to be planar, recently, there have been huge numbers of nonplanar porphyrins reported in the literatures [8] and [9]. Nonplanar porphyrins have interested inphysical and biological properties due to the distortion of the porphyrin ring. Many different factors such as metalation, peripheral substitutions, alkylation of the pyrrolenine nitrogen atoms, and even protonation, can distort the nominally planar structure of the porphyrin macrocyle.

1.2 Porphyrin in biological processes

Heme, vitamin B12 and chlorophyll are all biologically important compounds that are composed of an organic molecule bound to a metal ion. They are examples of metal complexes, which consist of a metal ion surrounded by one or more ligands. A ligand is an ion or molecule that contains at least one atom, such as oxygen or nitrogen that has the ability to bind to a metal ion through its lone electron pairs.

All of the compounds are known as metallated porphyrins or corrins. All porphyrins contain the porphine functional group as a core (see Figure 2), but they have various substituents attached around the outside of the ring.

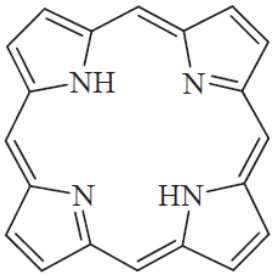

(a) Porphine

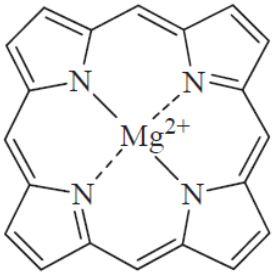

(b) Metallated porphine

Figure 2. Structure: (a)Porphine; (b) Metallated porphine

1.2.1 Heme

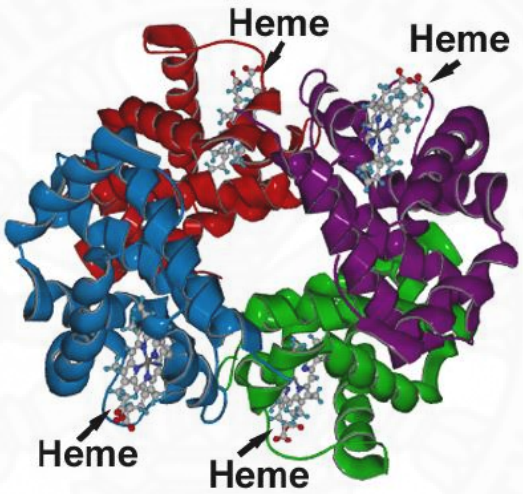

Figure 3. A molecular model of hemoglobin [2]

In hemoglobin, each subunit contains a heme group, which is displayed using the ball-and-stick representation in figure 3. Hemoglobin is the protein that transports oxygen (O_2) in human blood from the lungs to the tissues of the body. Each heme group contains an iron atom that is able to bind to one oxygen (O_2) molecule. Because hemoglobin contains four heme groups, each hemoglobin protein can bind four oxygen molecules.

A heme or haem is a chemical compound of a type known as a prosthetic group consisting of Fe^{2+} (ferrous) ion contained in the center of a large heterocyclic organic ring called a porphyrin (figure 4). Hemes are most commonly recognized as components of hemoglobin, the red pigment in blood, but are also

found in a number of other biologically important hemoproteins such as myoglobin, cytochrome, catalase, and endothelial nitric oxide synthase.

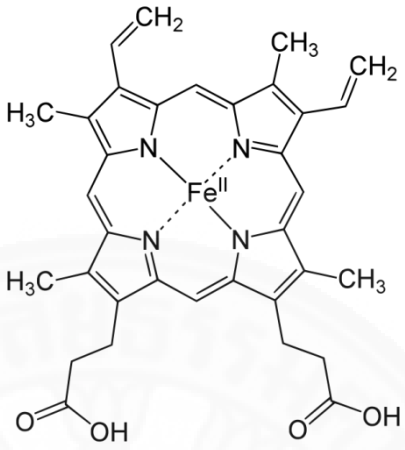

Figure 4. Structure of heme [2]

1.2.2 Vitamin B12

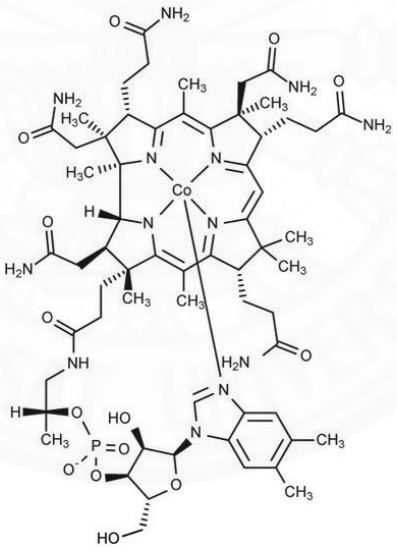

Figure 5. Structure of vitamin B12 [3]

Vitamin B12 that the structure as shown in figure 5 exists in several forms and contains the mineral cobalt, so compounds with vitamin B12 activity are collectively called “cobalamins”. Methylcobalamin and 5-deoxyadenosylcobalamin are the forms of vitamin B12 that are active in human metabolism. Vitamin B12 is an

essential water-soluble vitamin that is commonly found in a variety of foods such as fish, shellfish, meat, and dairy products [3].

1.2.3 Chlorophyll

Chlorophyll is the green photosynthetic pigment in the cells of plants. It also founds in many organisms such as algae and some species of bacteria. Chlorophyll enables plants and other chlorophyll-containing organisms to perform photosynthesis. Chlorophyll A is the most form of chlorophyll and gives plants their green color.

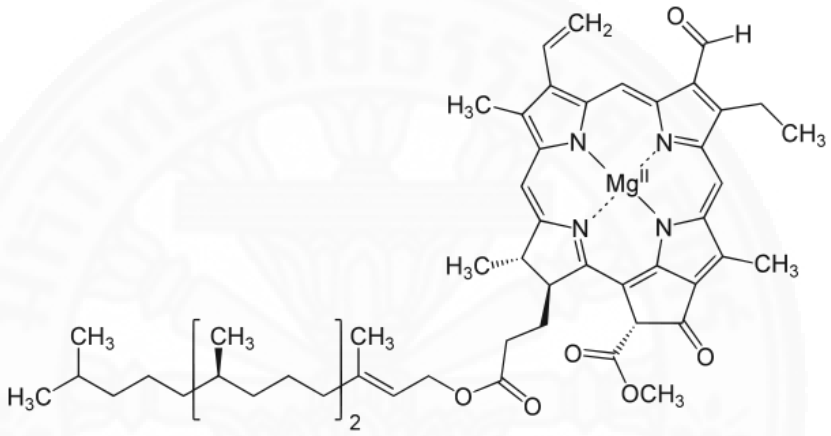

Figure 6. Structure of chlorophyll [4]

The structure as shown in figure 6, chlorophyll is a magnesium-porphyrins. The magnesium ion bonded within porphyrins ring is thought to be responsible for electron transfer during photosynthesis [10].

1.3 Porphyrin synthesis

Porphyrins have been the subject of intense interest since the early 19th century. A large variety of synthetic porphyrins and their metalloderivatives were made over the years to study the porphyrin based natural systems. In the past 100 years, porphyrin syntheses have been developed dramatically [11]. Today, almost any porphyrin can be synthesized from known synthetic methodology. For example, tetramerization of pyrroles, [3 + 1] condensation and [2 + 2] condensation are common methodologies [12]. Tetraarylporphyrins are synthetic porphyrins and have

various applications. A series of symmetrical and unsymmetrical porphyrins have been synthesized and have found applications in many fields.

A simple way to obtain symmetrical porphyrins is the condensation of pyrrole with aldehyde in acid catalyst, further is oxidation reaction. This procedure is originally developed by Rothemund and Menotti [13] and has been refined by Adler and Longo [14]. It generally gives around 20% yields for tetraarylporphyrins. Despite the modest yields, the relative simplicity of this method has made it well suited for preparation of large amounts of tetraarylporphyrins. Later, the Lindsey [15] group developed higher yielding and milder reaction conditions by using a Lewis acid (TFA or BF_3) as the catalyst. Subsequently, Lindsey's group also developed higher concentration conditions. Despite the slightly lower yields, this improved synthesis is more practical for larger scale preparations of tetraarylporpyrins. Also, the Lindsey method has the advantage that it can be used to prepare porphyrins that required the use of acid-unstable aldehydes not generally employed under Adler-Longo conditions.

It is possible to synthesize unsymmetrical substituted porphyrins via mixed aldehyde condensations. By using a mixture of two different aldehydes as starting materials in the Adler or Lindsey syntheses, a statistical mixture of products is obtained. The desired porphyrin is then separated by extensive chromatography (to achieve easy separation, polarity difference of the two aldehydes are often required). Mixed aldehyde condensation is a simple practical way to prepare unsymmetrical porphyrins. These unsymmetrical porphyrins are useful precursors for building biocojugates and porphyrin arrays. Another way to prepare this type of molecule is through direct regioselective functionalization of a symmetrical porphyrin.

1.3.1 Rothemund Method

Preparing specific porphyrin motifs requires the synthesis of porphyrin derivatives which possess functional groups at the periphery of the macrocycle. In 1936, Rothemund and Menotti were the first to synthesize such a porphyrin, known as tetraphenylporphyrin (TPP) (Scheme 1). The compound was obtained by reacting pyrrole and benzaldehyde in pyridine, while in a sealed tube at 150 °C for 24 hours, followed by oxidation of the resulting porphyrinogen. This method produced relatively low yields (~10%) and due to the harsh reaction

conditions, the range of feasible substituted benzaldehydes was very limited. When the reaction was performed in the presence of Zn $(OAc)_2$ at high pressure, an improved yield was observed [13].

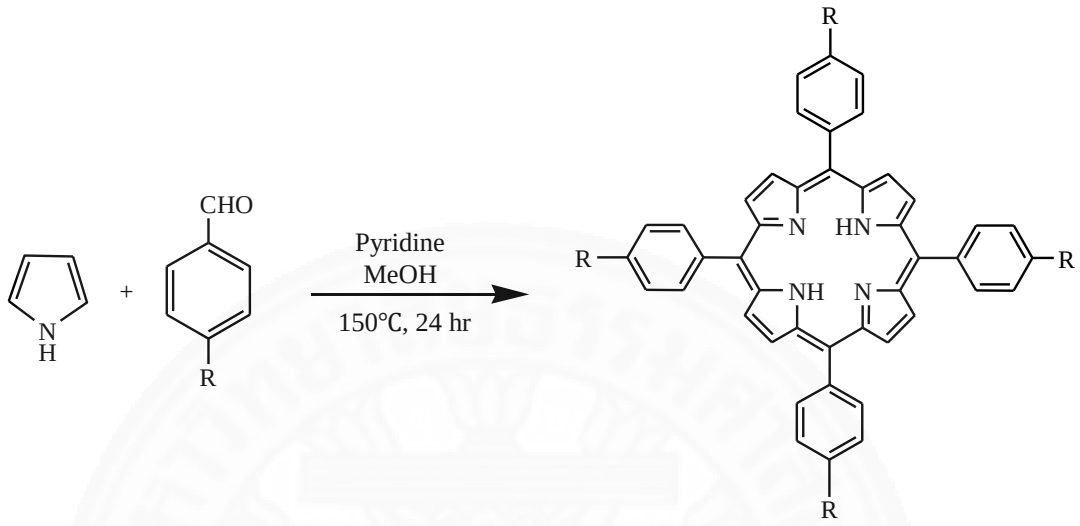

Scheme 1. Synthesis of TPP via Rothemund method

1.3.2 Alder-Longo Method

The Rothemund method was later modified by Adler and Longo under relatively milder reaction conditions. A wider range of substituents became attainable as a result of the conditions being less harsh. This new method of synthesizing TPP was also simpler than the original method. In fact, reaction rates were faster and the resulting yields were higher (20 ± 3 %). (Scheme 2)

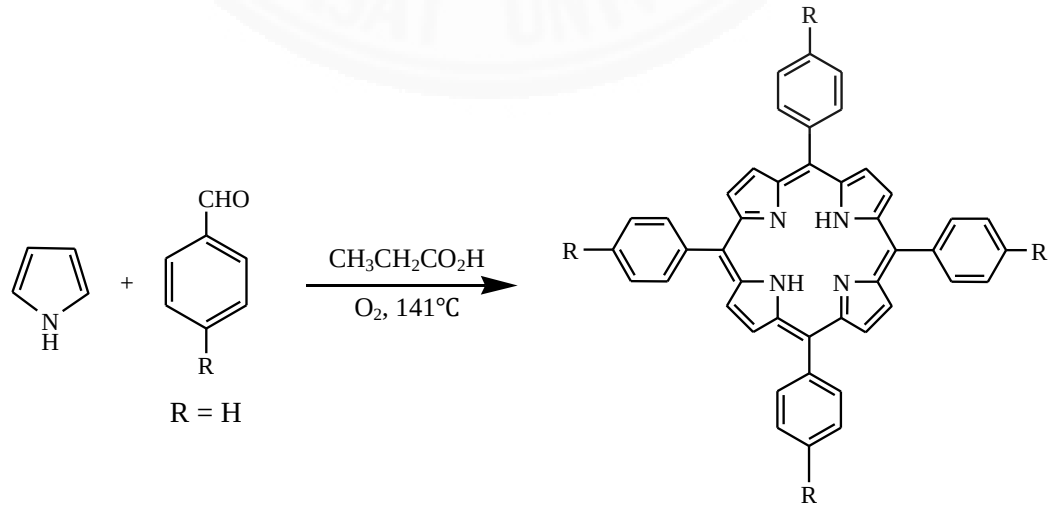

Scheme 2. Synthesis of TPP via Adler-Longo method

The reaction modifications involved refluxing pyrrole and benzaldehyde in propionic acid for 30 minutes at 141℃. Although the Adler–Longo method provides a higher yield of TPP under comparatively milder reaction conditions, there are still some associated drawbacks. For instance, a high degree of tar is produced during the reaction which makes purification very difficult. Regardless of this issue, the Adler-Longo method is still one of the most efficient in the synthesis of TPP, assuming the target porphyrin can be easily isolated [14].

1.3.3 Lindsey Method

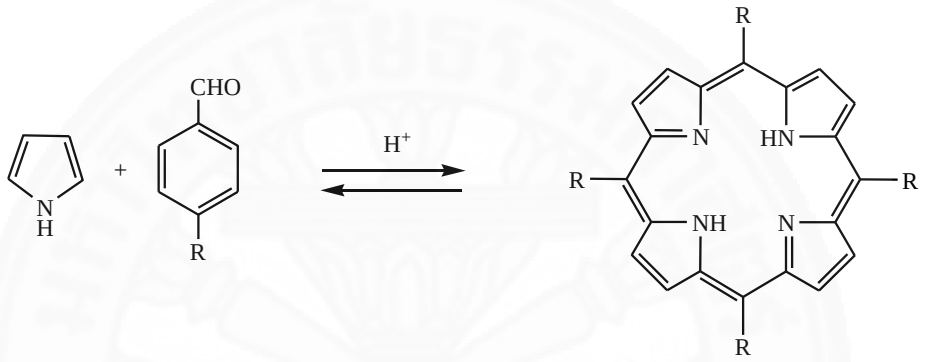

Scheme 3. Synthesis of tetraphenylporphyrinogen at room temperature

In 1987, Lindsey *et al.* determined that TPP could actually be produced under equilibrium conditions. This synthetic strategy permits the formation of substituted porphyrins which were once unattainable using alternate routes. The Lindsey method generates a colorless porphyrinogen product, and these intermediates are converted irreversibly to aromatic porphyrins upon oxidation. The procedure was developed based on pyrrole and benzaldehyde reacting to form tetraphenylporphyrinogen, in a dilute solution of dichloromethane (Scheme 3).

The Lindsey method has several factors that contribute to improved porphyrin yields. For instance, the selection of acid catalyst and oxidant, starting material concentrations, reaction time, and presence of water in the solvent can all influence the reaction. The synthesis involved reacting pyrrole, benzaldehyde, and triethyl orthoacetate in a dilute solution of anhydrous DCM at equimolar concentrations. An aliquot of a Lewis acid catalyst, such as BF_3, Et_2O or TFA, is added to the reaction mixture and allowed to sit at room temperature for ~1 h. Once the reaction has reached equilibrium, the oxidant can then be added to convert the

porphyrinogen intermediate to porphyrin. DDQ and *p*-chloranil are both useful oxidants for this conversion. Adding DDQ yields an immediate conversion of the intermediate, whereas, *p*-chloranil is a milder oxidant and requires at least an hour to completely react. Though the reaction time when using *p*-chloranil is longer, it produces a higher yield of porphyrin than DDQ. Also, similar to benzene chemistry, the nucleophilicity of the pyrrole group depends on the attached functional group. For instance, if the pyrrole ring has an electron-donating group (e.g. alkyl group) present, it will more readily participate in electrophilic substitution reactions. In the case of an electron-withdrawing group (e.g. ester group) being attached to the pyrrole ring, a decrease in the reactivity will occur. Being mindful of the aforementioned factors, Lindsey strategically optimized the reaction conditions by monitoring the yields of product at various reaction times via UV-Vis spectroscopy. As a result, the final TPP product can be obtained in much higher yields (50-55%) and more substituents are tolerated, which is a major improvement with respect to previous methods [15].

1.3.4 Asymmetrical Porphyrins from Symmetrical Porphyrins

Asymmetrical porphyrins can be prepared via mixed aldehyde condensation or selective functionalization of symmetrical porphyrins. The work described in this dissertation utilizes the latter method and will be the topic of discussion in this section. One of the earliest demonstrations of this procedure occurred in 1989, when Kruper *et al.* [16] synthesized mono-nitroporphyrin using fuming nitric acid to directly nitrate TPP (see figure 7). The yields obtained using this method were moderate (46~56%), yet a vast improvement compared to previously reported studies. Meng *et al*. [17] later reported a method for obtaining relatively higher yields (~74%) under milder reaction conditions. Luguya *et al*. [18] devised a synthetic route using sodium nitrite in TFA, which enhanced the yield, as well as regioselectivity. The concentration of sodium nitrate and permitted reaction time are key factors which determined the major products among various potential mixtures (e.g. mono-, di-, tri-, tetra-substituted TPP) in this reaction. Due to the absence of other tetrapyrrole byproducts, the mixtures are easily separated [19].

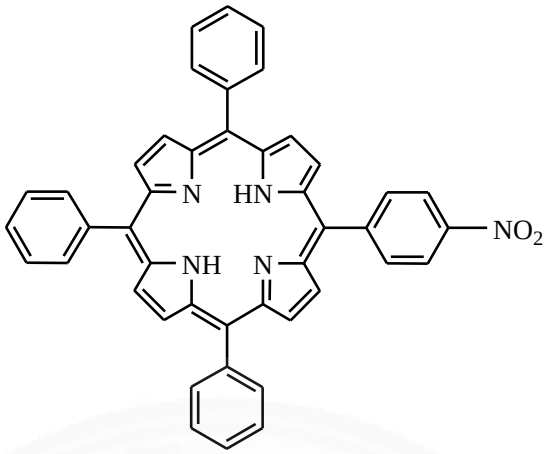

Figure 7. Molecular structure of mono-nitrophenylporphyrin

1.4 Applications of Porphyrins

Porphyrins and metalloporphyrins are found in many natural systems, where they play an essential role as photoactive, redox, guest-binding, and catalytic entities. They are immense biological importance and fascinating physical, chemical, and spectroscopic properties. The various properties of porphyrins, they have wide applications in many fields such as catalyst, light havesting system [20], photodynamic therapy [21], sensors [22, 23], dye sensitized solar cells (DSSCs) [24], and others. They are also important in biomimetic model; in fact they are widely used as models to study oxygen transport [25]. In particular, dye-sensitized solar cells have gained widespread attention in recent years because of their low production costs, ease of fabrication and tunable optical properties, such as color and transparency.

1.5 Research objectives

The aims of this research mainly focus on two different topics:

(a) The synthesis of unsymmetrical porphyrin

(b) The characterization and the chemical properties of synthesized porphyrins and their complexes

The first objective of this work consisted with the synthesis unsymmetrical phenylporphyrins that containing hydroxyl, alkoxy, alkyl, or carboxyl functional group on the *para* position of the phenyl rings. Then, the free base

porphyrins were attempted to add metal ions in the center hole. The second objective was characterization of all synthesized porphyrins and their complexes and studied the properties of theirs such as electronic absorption, electronic emission and thermal stability for further application.

1.6 Scope and limitations of the study

1. The metal-free tetrasubstituted phenylporphyrins containing hydroxyl or alkoxy or alkyl or carboxyl functional group on the *para* position of one of the phenyl rings were synthesized from condense a mixture of pyrrole, benzaldehyde, and the appropriately substituted benzaldehyde in a 4:3:1 ratio by modified Adler-Longo method.

2. The various aldehydes, precursors of this research, are including benzaldehyde, 4-hydroxybenzaldehyde, 4-methoxybenzaldehyde, 4-octyloxy benzaldehyde, 4-methylbenzaldehyde and 4-carboxybenzaldehyde.

3. The metalloporphyrins with various porphyrin were prepared by adding metal ion, Zn^{2+}, in each free base ligand.

4. The structure of synthesized porphyrins was examined by using infrared spectroscopy (that use as a tool for main functional group characterization), ^{1}H nuclear magnetic resonance spectroscopy (to confirm the synthesized structure) and mass spectrometry (to analyze molecular mass and fragmentation patterns of the synthesized samples).

5. The effects of macrocyclic structures with different peripheral substitutions were characterized by using UV-Vis, fluorescence spectroscopy and thermal gravimetric analysis (TGA).

1.7 Expected results

The tetrasubstituted phenylporphyrins containing different peripheral substitutions by functional group on the *para* position of one of the phenyl rings can be synthesized according to modified Adler-Longo with simple and pot reaction

method. Moreover, the synthesized porphyrins will be developed to use in dye-sensitized solar cells (DSSCs) [24] and other fields.

CHAPTER 2
REVIEW OF LITERATURE

The review of literature mentioned work done by previous researchers on the preparation, characterization and application of *meso*-substituted porphyrins bearing three identical substituents, B and one different A (AB_3 porphyrins).

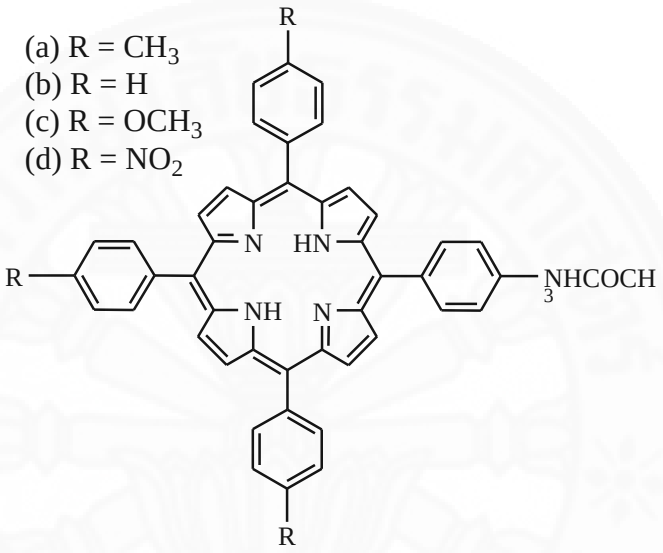

Figure 8. The structure of 5-(4-acetamidophenyl)-10,15,20 -tris(4-substituted phenyl) porphyrins

A convenient procedure for the synthesis of 5-(4-acetamidophenyl)-10,15,20-tris(4-substituted phenyl) porphyrins in the figure 8 from dipyrrolomethane is reported by Milanesio *et al.* (2000). The tetraphenylporphyrins (AB_3-porphyrins) were synthesized by the condensation of the appropriated benzaldehydes and *meso*-substituted dipyrrolomethanes that synthesized by the condensation of the corresponding benzaldehydes and excess pyrrole in catalyzed by acids. The reaction requires catalytic amount of boron trifluoride diethyl etherate in chloroform. This condensation produces porphyrin in its reduced form, therefore the reaction mixture was oxidized with 2,3-dichloro-5,6-dicyano-1,4-benzoquinone (DDQ). This reaction yielded a mixture of three porphyrins, which were separated with high purity by flash chromatography (yields 15-17%) [26].

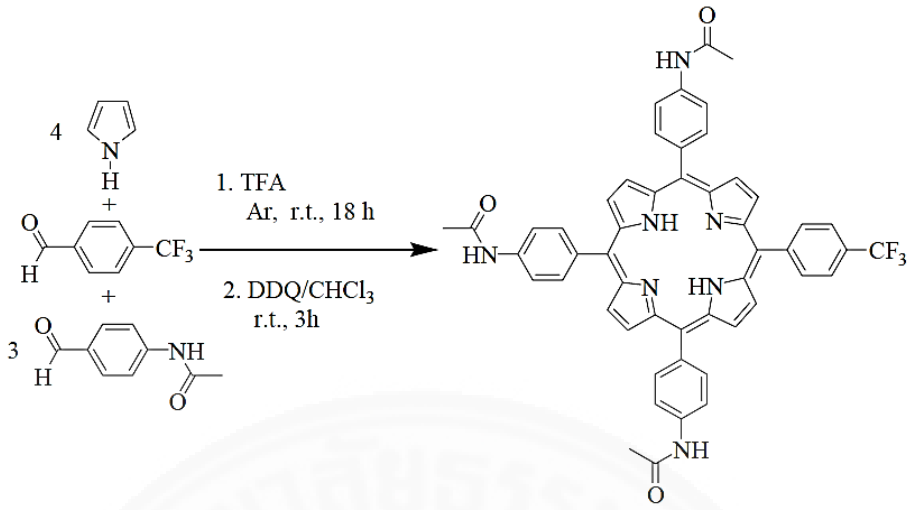

A

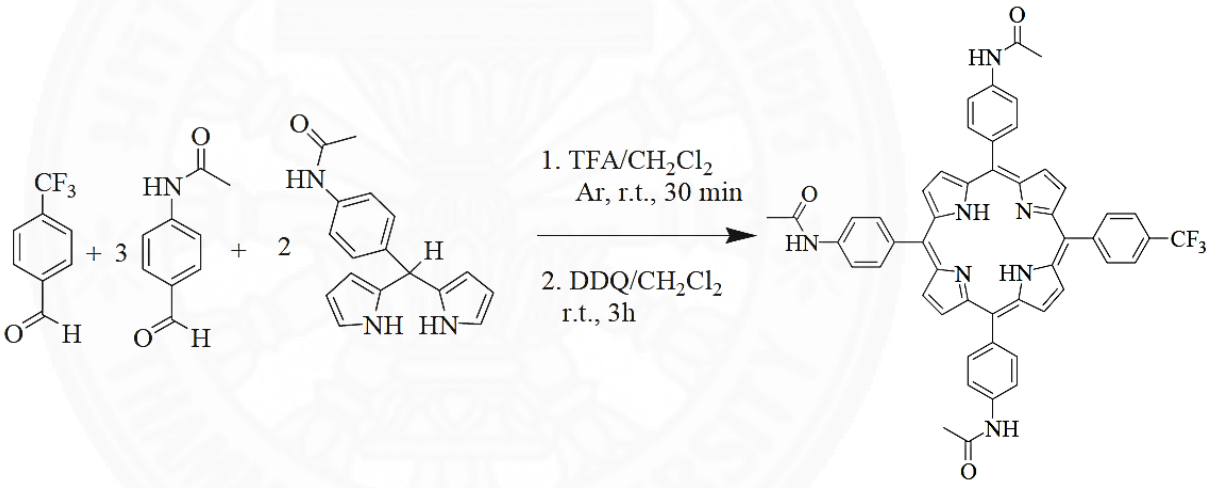

B

Scheme 4. The synthesis of 5-(4-Trifluoromethylphenyl)-10,15,20-tris(4-acetamidophenyl) porphyrin by two different methods: (A) Condensation of a binary mixture of aldehydes and pyrrole; (B) Condensation of dipyrromethane with the appropriate benzaldehyde mixture

Débora and Edgardo (2003) reported the synthesis of novel asymmetrically *meso*-substituted cationic porphyrins with AB_3-porphyrin symmetry pattern. 5-(4-Trifluoromethylphenyl)-10,15,20-tris(4-acetamidophenyl) porphyrin was synthesized by two different methods. In one case, the AB_3-porphyrin was obtained by a condensation of a binary mixture of aldehydes and pyrrole catalyzed by

trifluoroacetic acid, TFA, at room temperature (Scheme 4, A). After treatment with DDQ, the mixture produced porphyrin, which was separated by column chromatographic with a yield of 3.6 %. The alternative method to synthesize porphyrin involved two steps: 1) formation of *meso*-(4-acetamidophenyl)dipyrromethane and 2) condensation of dipyrromethane with the appropriate benzaldehyde mixture (Scheme 4, B). Thus, dipyrromethane was obtained from the condensation of 4-acetamidobenzaldehyde with a large excess of pyrrole (1:38 aldehyde/pyrrole mol ratio) catalyzed by TFA. The reaction mixture was stirred for 20 min at room temperature resulting in the complete disappearance of aldehyde. In these reaction conditions, pyrrole serves as the reactant in excess and as the solvent for the reaction, giving direct formation of dipyrromethane. The brown crude solution was washed with dilute aqueous NaOH. The dipyrromethane was isolated (70 %) by flash chromatography on silica gel in a mildly basic medium, using ethyl acetate/triethylamine (100:1) as eluent. Then, dipyrromethane was condensed with 4-acetamidobenzaldehyde and 4-trifluoromethylbenzaldehyde under catalysis by TFA and at room temperature to form a mixture of porphyrins. The reaction was catalyzed by TFA at room temperature. After oxidation with DDQ, the desired amido porphyrin 2 (15 %) was separated by flash chromatography [27].

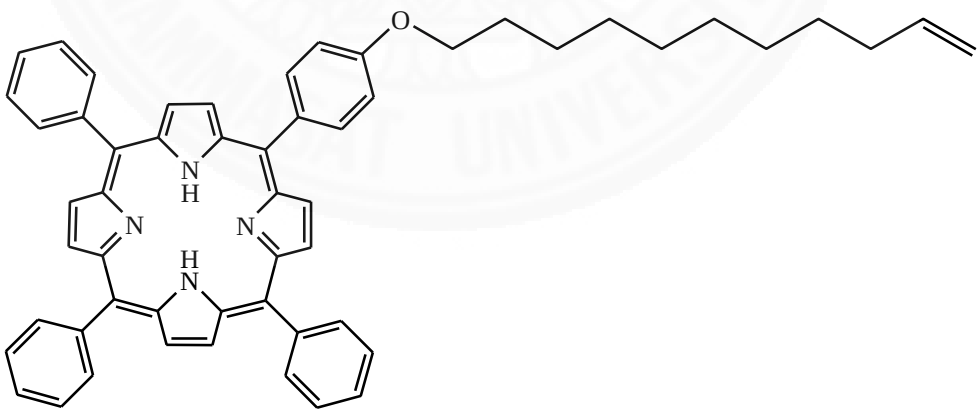

Figure 9. The structure of 5-(4-undecenyloxyphenyl)-10,15,20-triphenylporphyrin

Koiry *et al.* (2008) synthesized a specifically designed organic molecule and these molecules were electrografted on highly doped n-Si substrates. A specially designed molecule, 5-(4-undecenyloxyphenyl)-10,15,20-triphenylporphyrin was

synthesized and its structure as shown in figure 9. It is a purple color solid with a melting point of ~ 95 ℃. The main feature of this molecule consists of a vinyl (C=C) terminated 11-carbon atom alkyl-chain attached to the conjugated porphyrin ring. The vinyl group is essential for electrografting this molecule to H-terminated Si surface. They also demonstrate that such electrical bistability can be utilized for the molecular memory effect [28].

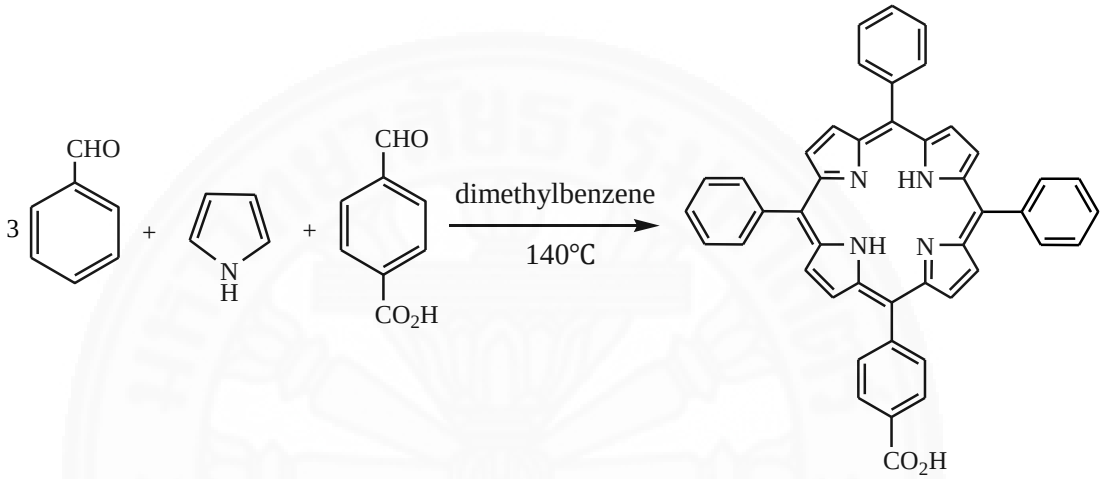

Scheme 5. Reaction formula about the preparation of 5-(4-carboxyphenyl)-10,15,20-triphenylporphyrin ($TCPPH_2$)

Preparation of 5-(4-carboxyphenyl)-10,15,20-triphenylporphyrin ($TCPPH_2$) was reported by Wang *et al.* (2013). In this report, a manganese(III) 5-(4-carboxyphenyl)-10,15,20-triphenylporphyrin chloride (Mn(TCPP)Cl) was designed to be grafted on NH_2-mPGMA which were cross-linked by DVB. Thus obtained catalyst (Mn-NH-mPGMA) leaded to a heterogeneous epoxidation of alkenes, showing high conversion and selectivity, easy recovery and steady reuse. 5-(4-carboxyphenyl)-10,15,20-triphenylporphyrin ($TCPPH_2$) was prepared by condensation of salicylic acid, benzaldehyde, 4-carboxy benzaldehyde, pyrrole in dimethylbenzene (Scheme 5). After refluxing for 0.5 h, the solution was cooled to room temperature and was added in absolute ethanol. After a hot water wash, the resulting purple crystals were air dried, and finally dried in vacuum. The product was purified by silica gel column chromatography using $CHCl_3$, 80% $CHCl_3$ and 20% methanol as the eluting solvents [29].

Marcin *et al.* (2013) synthesized the compounds that usefulness as potential photosensitizers in anticancer photodynamic therapy. Three hydroxyl groups in *meta* position and long alkyl chain in *para* position (this is shown schematically in figure 10). 5-(4-Hexadecyloxyphenyl)-10,15,20-tris(3-hydroxyphenyl) porphyrin was synthesized by condensation of appropriate aldehydes with pyrrole in propionic acid in typical Adler-Longo procedure. 3-Hydroxybenzaldehyde and 4-hexadecyloxybenzaldehyde were dissolved in propionic acid and heated to reflux. Pyrrole was added and the resulting mixture was heated under reflux for 1.5 h. A half of propionic acid was removed by distillation. The water was added to the rest of cooled mixture. Propionic acid was neutralized by solid sodium carbonate. Precipitated organic compounds were dissolved in dichloromethane, washed with water and dried with anhydrous Na_2SO_4. Dichloromethane was evaporated and the residue was chromatographed on silica gel with chloroform and ethyl acetate (3:1, v/v) mixture as eluent. Yield: 4% [30].

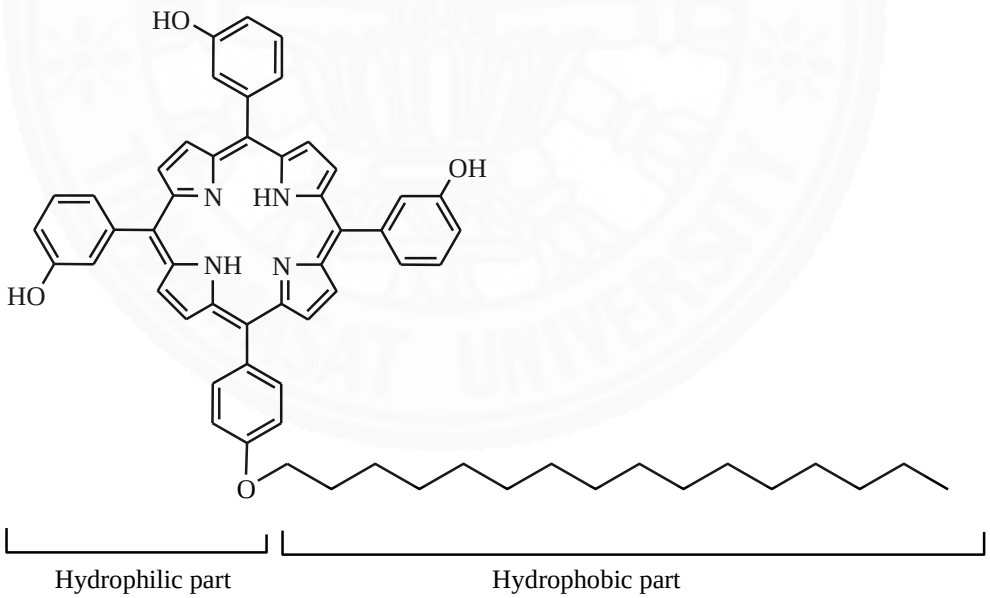

Figure 10. The structure of 5-(4-Hexadecyloxyphenyl)-10,15,20-tris(3-hydroxyphenyl) porphyrin

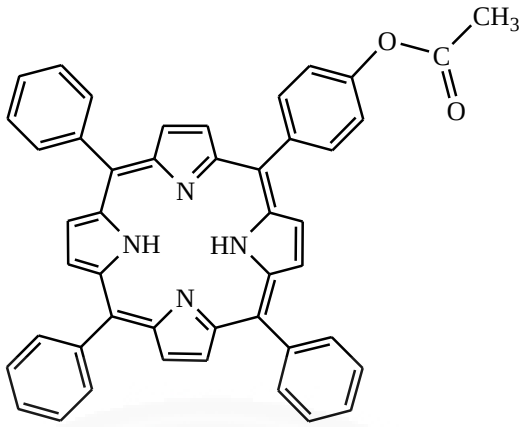

Figure 11. The structure of 5-(4-acetoxyphenyl)-10,15,20-triphenylporphyrin

Furuta *et al.* (2014) were prepared the compound that is stable linker for porphyrin monolayer on silicate glass. The preparation was 4-Acetoxybenzaldehyde and benzaldehyde were dissolved in propionic acid and the solution was refluxed. Pyrrole was slowly added to the refluxed solution and the mixture was refluxed for 30 min in dark. After the reaction mixture was cooled to room temperature, the solvent was evaporated under reduced pressure. The synthesized porphyrins were separated by silica gel column chromatography eluted with dichloromethane: hexane (3:1). Further purification by silica gel column chromatography using dichloromethane: hexane (2:1) yielded 5.4% of 5-(4-acetoxyphenyl)-10,15,20-triphenylporphyrin (figure 11) followed by silica gel chromatography using dichloromethane: hexane (3:1) gave 3.6% of 5,10-Bis(4-acetoxyphenyl)-15,20-diphenylporphyrin and 3.0% of 5,15-bis(4-acetoxyphenyl)-10,20-diphenylporphyrin [31].

Skrzypek *et al.* (2007) were prepared 5-(4-carboxyphenyl)-10,15,20-tritolylporphyrin by refluxing 4-methylbenzaldehyde, 4-carboxybenzaldehyde and pyrrole in propionic acid. Then, traces of propionic and partially formed tars were removed by washing with hot water. The desired product was obtained by column chromatography. The cobalt-porphyrin was synthesized by refluxing free base porphyrin and cobalt acetate in dimethylformamide for 1 hour. The successful metal insertion was checked by infrared spectroscopy, mass spectroscopy, UV-vis spectroscopy and thin layer chromatography (TLC) [32].

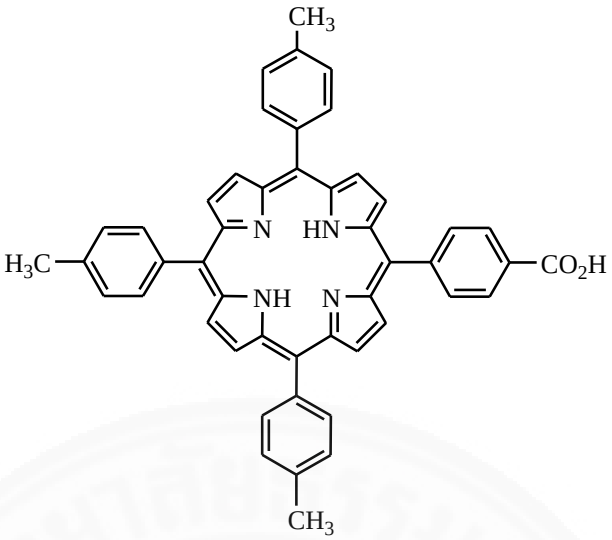

Figure 12. The structure of 5-(4-carboxyphenyl)-10,15,20-tritolylporphyrin

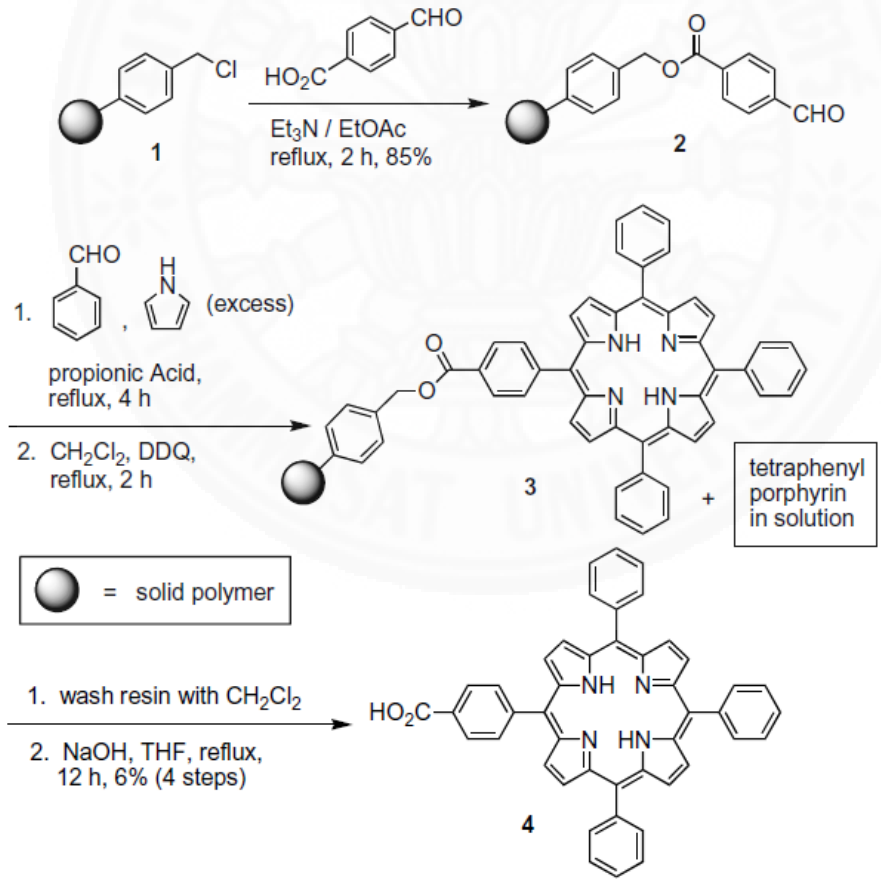

Scheme 6. Synthesis of mono-substituted porphyrins on insoluble polystyrene/divinyl benzene cross-linked polymer [33]

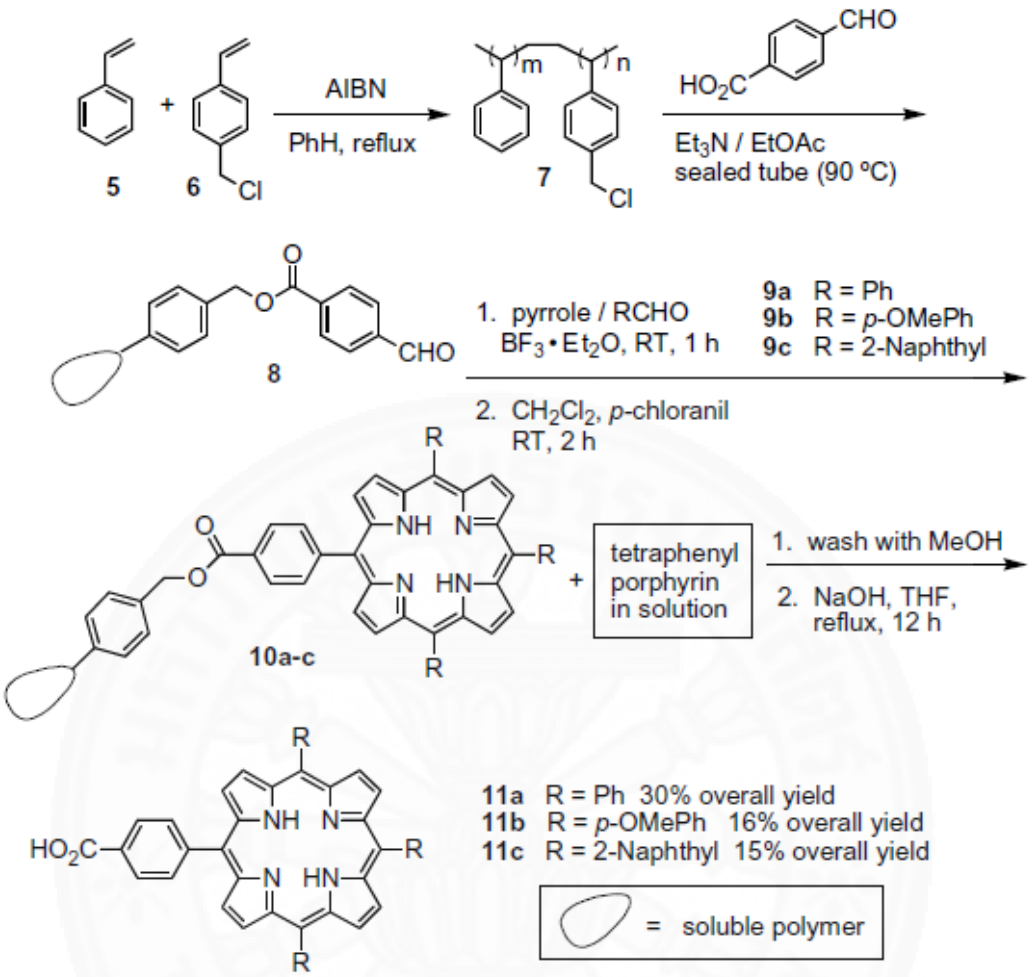

Scheme 7. Synthesis of mono-substituted porphyrins on soluble polystyrene polymer [33]

Yang *et al.* (2005) synthesized anchoring of substituted benzaldehydes to soluble and insoluble polymers allow for the synthesis of mono-substituted tetraarylporphyrins without the production of di-, tri-, and tetra-substituted porphyrin side products. The exclusion of the aforementioned side products during the synthesis of mono-substituted tetraarylporphyrin acids greatly reduced the complexity during purification of the product. The Synthesis of mono-substituted porphyrins on insoluble polystyrene/divinyl benzene cross-linked polymer is presented in Scheme 6 and synthesis of mono-substituted porphyrins on soluble polystyrene polymer is presented in Scheme 7. Limitations in the use of solid polymers in synthetic chemistry are pronounced by the difficulty in using NMR to characterize intermediates, and the

heterogeneous nature of the chemistry that could result in low yields. However, soluble polymers can be used as an alternate matrix for organic synthesis [33].

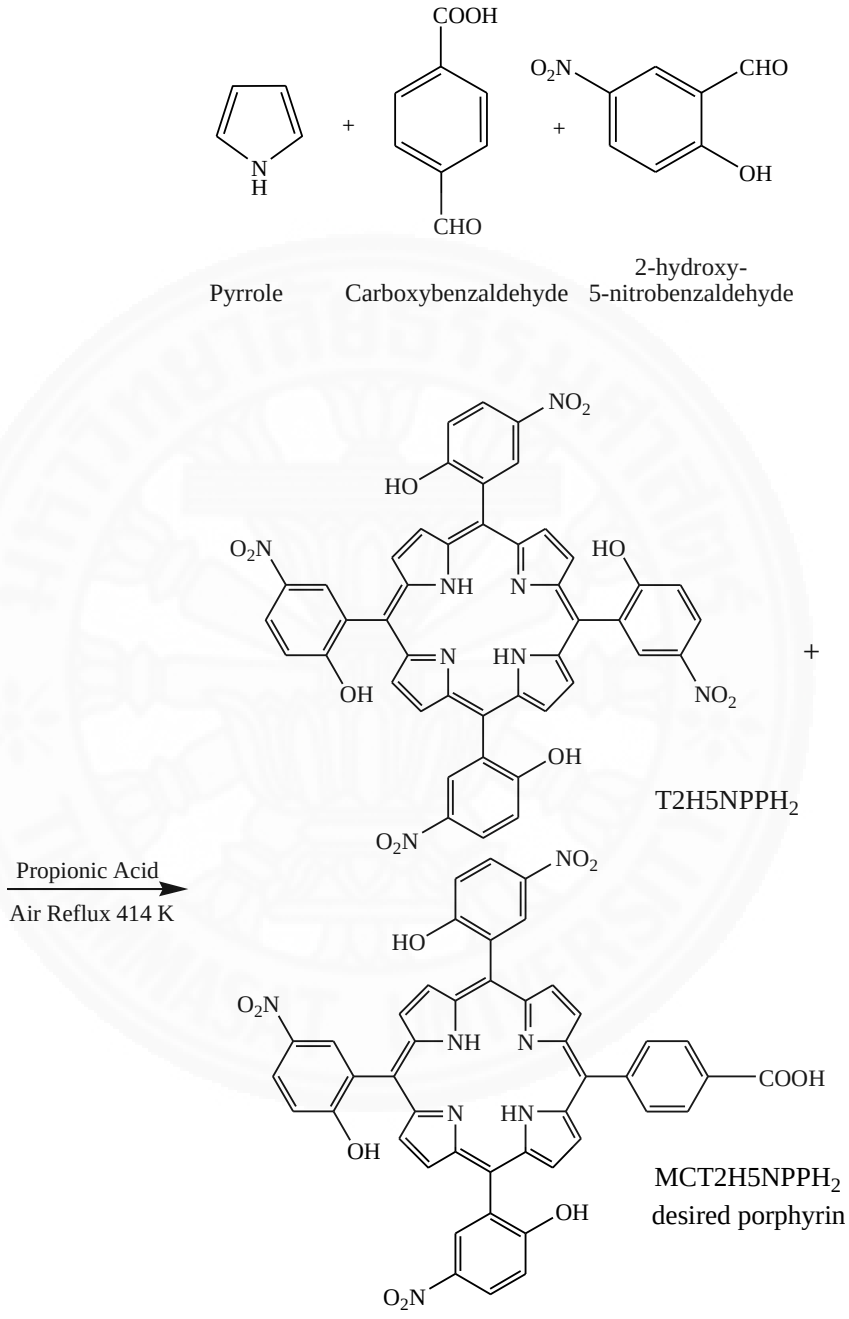

Scheme 8. Synthesis of 5-mono(carboxyphenyl)-10,15,20-tris(2-hydroxy-5-nitrophenyl)porphyrin

The goal of Ana *et al.* (2004) is to find an innovative formulation for new photosensitizers based on hydroxyphenyl systems. In this paper they report the synthesis, photophysical characterizations and photodynamic properties of 5,10,15,20-tetrakis(2-hydroxy-5-nitrophenyl)porphyrin and 5-mono(carboxyphenyl)-10,15,20-tris(2-hydroxy-5-nitrophenyl)porphyrin. The preparation of 5-mono(carboxyphenyl)-10,15,20-tris(2-hydroxy-5-nitrophenyl)porphyrin was carried out through the method of involving Adler et al, the condensation of pyrrole, 2-hydroxy-5-nitrobenzaldehyde and carboxybenzaldehyde in propionic acid, at 141 ºC (Scheme 8). Propionic acid was removed under reduced pressure. The crude product was initially purified by silica gel chromatography using dichloromethane as eluent. The porphyrins formed during the synthesis were separated by aluminum oxide chromatography using ethanol: acetic acid (1:100) as eluent, and later silica gel chromatography using acetonitrile: acetic acid (1:100). The yield was 30% [34].

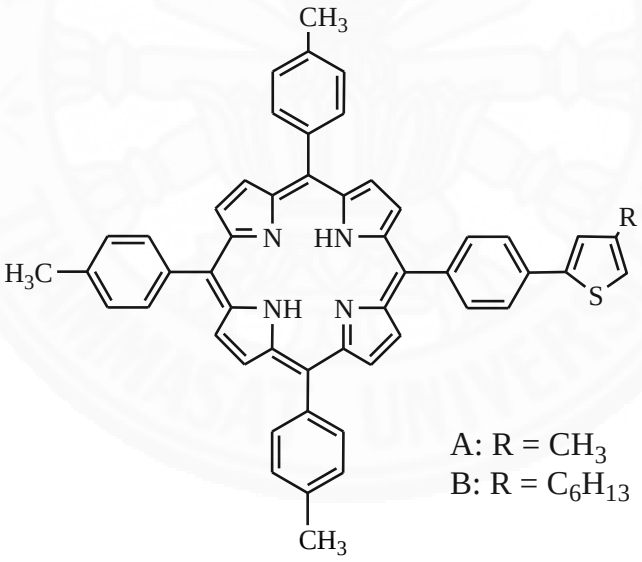

Figure 13. The structure of A) 5-(4-(4-Methyl) thienyl) phenyl-10,15,20-tris(4-methylphenyl) porphyrin and B) 5-(4-(4-Hexyl) thienyl)phenyl-10,15,20 -tris(4-methylphenyl)porphyrin

Xiang *et al.* (2011) were synthesized three donor (π-spacer)-acceptor porphyrin dyes that use in dye-sensitized solar cells. The dyes comprised the same donor (porphyrin derivative) and acceptor/anchoring group (2-cyanoacrylic acid) but varying π-spacer consisting of a combination of 4-methylthiophene, 4-hexylthiophene or 3,4-ethylenedioxythiophene groups. The dyes displayed different adsorption behavior and coverage of the TiO_2 surface. 5-(4-(4-Methyl) thienyl) phenyl-10,15,20-tris(4-methylphenyl) porphyrin (Figure 13, A) was synthesis by dissolved 4-methylbenzaldehyde and 4-(4-methyl)thienyl benzaldehyde in propionic acid. The solution was heated to reflux at 140℃. Then, pyrrole was added dropwise and the mixture stirred for another 30 min. After cooling to room temperature, half of the solvent was evaporated and methanol was added. The mixture was cooled overnight and filtered under vacuum. The crude product was purified using column chromatography (petroleum ether: dichloromethane = 2:3 as an eluent). After recrystallization from the mixture of $CHCl_3$ and CH_3OH (1:5), a desired purple solid of compound was obtained. The synthetic procedure for 5-(4-(4-Hexyl) thienyl) phenyl-10,15,20-tris(4-methylphenyl)porphyrin (Figure 13, B) was similar to A in figure 13, except that use only 4-methylbenzaldehyde. The crude product was purified using silica chromatograph with dichloromethane to give a purple solid (24%) [35].

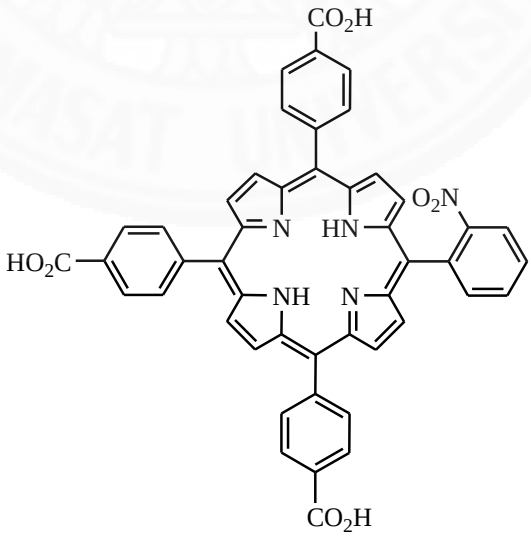

Figure 14. The structure of 5,10,15-tris(4-carboxyphenyl), 20-mono(2-nitrophenyl) porphyrin

The anionic 5,10,15-tris(4-carboxyphenyl), 20-mono(2-nitrophenyl) porphyrin, 5,10(or 15)-bis(4-carboxyphenyl),15(or10),20-bis(2-nitrophenyl)porphyrin and 5-mono(4-carboxyphenyl)-10,15,20-tris(2-nitrophenyl)porphyrin were synthesized directly by reaction of pyrrole with substituted benzaldehydes in nitrobenzene/propionic acid media by Marco *et al.* (2000). The benzaldehydes molar ratio was controlled to optimize the synthesis and purification of the desired porphyrins. The percentage yield of 5,10,15-tris(4-carboxyphenyl), 20-mono(2-nitrophenyl) porphyrin as shown in figure 14 is 5 % yield. The new series of porphyrins was characterized by TLC, mass spectrometry (FAB MS), ^{1}H NMR, UV/Vis, IR and electrochemistry. Iron(III) porphyrins were prepared by refluxing the free base porphyrins with iron(II) chloride tetrahydrate in *N*,*N*-dimethylformamide under nitrogen by the method of Adler *et al*. The reaction was monitored by UV/Vis spectroscopy and TLC. The iron porphyrins were washed with HCl and purified by silica column chromatography. The electrochemical reduction was investigated for the free base and corresponding iron(III) porphyrins on glassy carbon and mercury electrodes. The reduction potentials showed the expected dependence on the number of electron-withdrawing nitro groups present on the porphyrin ring providing additional evidences for the characterization of the synthesized compounds [36].

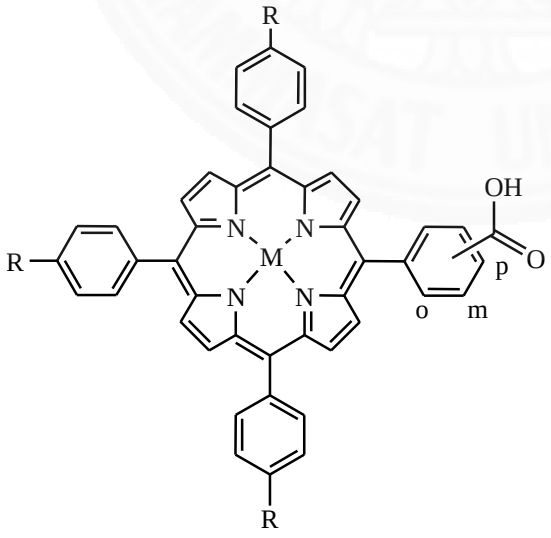

R = CH_3;M= 2H; para **1p**
R = CH_3;M= 2H; meta **1m**
R = CH_3;M= 2H; ortho **1o**
R = CH_3;M= Zn; para **1p-Zn**
R = CH_3;M= Zn; meta **1m-Zn**
R = CH_3;M= Zn; ortho **1o-Zn**
R = $(OCH_2CH_2)_3OCH_3$;M= 2H; para **2p**
R = $(OCH_2CH_2)_3OCH_3$;M= 2H; meta **2m**
R = $(OCH_2CH_2)_3OCH_3$;M= Zn; para **2p-Zn**
R = $(OCH_2CH_2)_3OCH_3$;M= Zn; meta **2m-Zn**
R = $CH_2CH_2CH_3$;M= 2H; meta **3m**
R = $CH_2CH_2CH_3$;M= Zn; para **3p-Zn**
R = $CH_2CH_2CH_3$;M= Zn; meta **3m-Zn**

Figure 15. The structures of porphyrin derivatives with the anchoring carboxyl group

Aaron *et al.* (2013) were synthesized porphyrin derivatives with the anchoring carboxyl group located either at the *para, meta,* or *ortho* position of one of the phenyl rings as shown in figure 15. The free based porphyrins have been synthesized according to Adler-Longo method. The stoichiometric amounts of pyrrole and aldehydes were refluxed in propionic acid and purified by column chromatography over silica gel. The metalation step, free based porphyrins and zinc acetate were refluxed in chloroform/methanol solution, monitoring the complete reaction by UV-vis spectroscopy. The thirteen porphyrin derivatives were synthesized and investigated for their cell performance, as shown in figure 16. As a result of bidentate carboxyl group on TiO_2, the position of *para*-derivatives was orthogonal to the TiO_2 surface. The position of *meta*-derivatives was at an angle (50−80°), whereas *ortho*-derivatives was even closer to the TiO2 surface. Therefore, the minor modification of carboxyl group on porphyrin ring affect to the relative orientation of the porphyrin to TiO_2 surface [37].

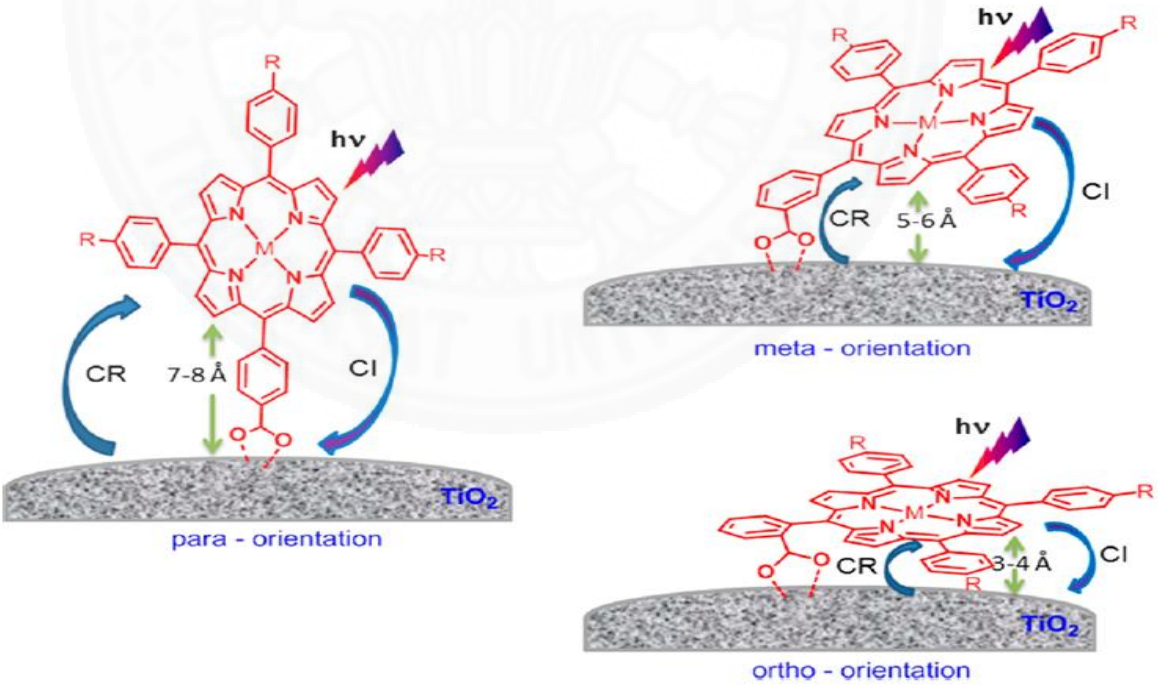

Figure 16. Relative orientation of *para, meta*, and *ortho* carboxyphenyl functionalized porphyrin adsorbed on TiO_2 surface. Key photochemical events responsible for cell performance are also shown (CI, chargeinjection; CR, charge recombination) [37]

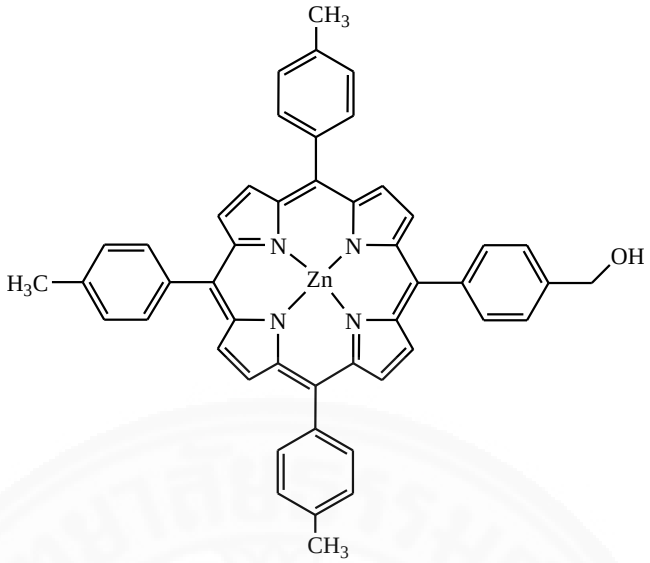

Figure 17. The structures of A_3B-porphyrin 5-(4-hydroxymethylphenyl) -10,15,20-tri-*p*-tolylporphinatozinc(II)

The metal free 5-(4-Hydroxymethylphenyl)-10,15,20-tri-p-tolylporphyrin and 5-(4-Hydroxymethylphenyl)-10,15,20-tri-p-tolylporphinatozinc(II) were synthesized by Syeda *et al.* (2006). The A_3B-porphyrin 5-(4-hydroxymethylphenyl)-10,15,20-tri-*p*-tolylporphinatozinc(II) (as shown in figure 17) is required in multigram quantities for possible commercial use in information storage applications. This compound has been carried out by reaction of 5-(4-hydroxymethylphenyl) dipyrromethane and the dicarbinol derived from 1,9-di-*p*-toluoyl-5-*p*-tolyldipyrromethane. Four improvements have been made to the steps leading to the dipyrromethane and dipyrromethane-dicarbinol: (i) use of 50 equiv of pyrrole in the condensation of an aldehyde to give the dipyrromethane (versus 100 equiv previously), (ii) 1,9-diacylation of a dipyrromethane using the hindered Grignard reagent 2,6-dimethylphenylmagnesium bromide and *p*-toluoyl chloride to give the 1,9-diacyl versus 1-acyl products in >10:1 ratio (versus 4:1 using EtMgBr), (iii) isolation of the dibutyltin complex of the 1,9-diacyldipyrromethane from the crude reaction mixture by direct crystallization using methanol/methyl *tert*-butyl ether (MTBE) (versus silica chromatography), and (iv) reduction of the dibutyltin complex of the 1,9-diacyldipyrromethane with 10-15 mol equiv of $NaBH_4$. The procedures have been carried out with no chromatography at large scale, affording the

dipyrromethane, the dibutyltin complex of a 1, 9-diacyldipyrromethane, and reduction of the latter. The reaction has been performed in a two-step process of condensation and oxidation to give the free base porphyrin. Metalation with zinc acetate afforded 5-(4-Hydroxymethylphenyl)-10,15,20-tri-p-tolylporphinatozinc(II), which was isolated by direct crystallization. Taken together, the various improvements facilitate synthesis of the target porphyrin and may have broad applicability [38].

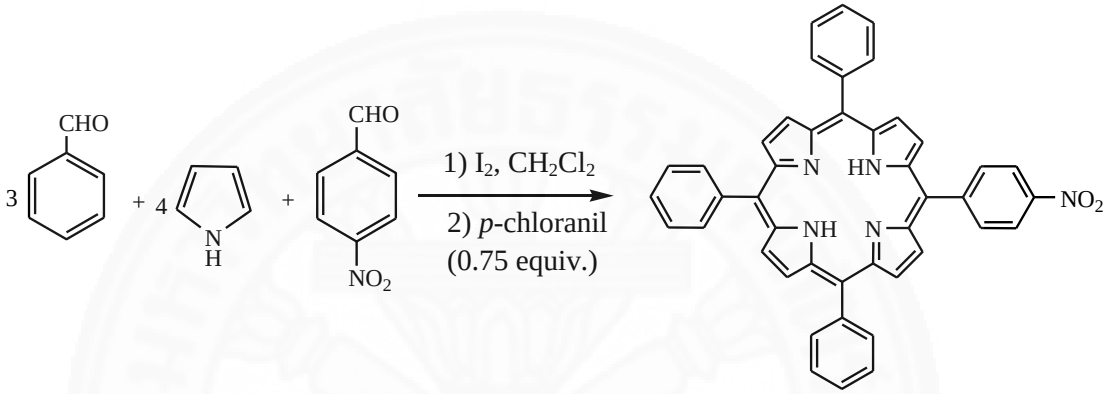

Scheme 9. Synthesis of 5-(4-nitrophenyl)-10,15,20-triphenylporphyrin

Benjamin *et al.* (2010) reported one-pot synthesis of unsymmetrical meso-substituted porphyrins that have iodine-catalyzed and the study of influence of electronic effects of functional groups (donor or acceptor). Unsymmetrical mono functionalized porphyrins with various functional groups have also been obtained to validate this method. The synthesis of 5-(4-nitrophenyl)-10,15,20-triphenylporphyrin is shown in the scheme 9. The comparation the synthesis with the classical mononitration of meso-tetraphenylporphyrin (which requires prior synthesis of tetraphenylporphyrin) show that addition of molecular iodine at room temperature instead of another acid system led to the final product with a sensible yield (12%). Furthermore, taking into account a previous work, activation by microwave irradiation resulted in a significant yield increase (22%). These two results confirm that iodine act as Lewis acid catalyzes the synthesis of 5-(4-nitrophenyl)-10,15,20-triphenylporphyrin in good yield after purification, and show the possible effect of microwave on the selectivity of this reaction [39].

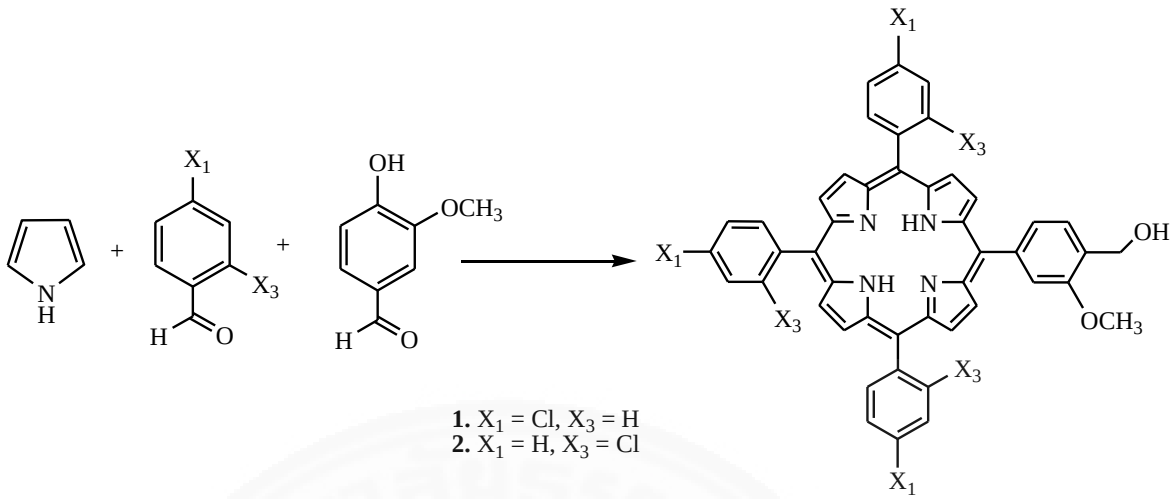

Scheme 10. Synthesis of 5-[(4-Hydroxy-3-methoxy) phenyl]-10, 15, 20 -tris(4-chlorophenyl)porphyrin and 5-[(4-hydroxy-3-methoxy)phenyl] -10, 15, 20-tris(2-chlorophenyl)porphyrin

The synthesis and characterization of new meso-substituted unsymmetrical metalloporphyrins has been reported by Bandgar *et al.* (2008). A new modified Adler method was used for the synthesis of two unsymmetrical free base porphyrins as shown in scheme 10. Reactions of these unsymmetrical porphyrins with metal acetates afforded the corresponding metalloporphyrins in high yields with excellent purity. The synthesis of metalloporphyrins, a mixture of free base porphyrin in $CHCl_3$ and $Ni(OAC)_2 \cdot 4H_2O$ in methanol was stirred at 50℃ for 3 h. After completion of reaction as indicated by TLC, the solvent was removed under reduced pressure. Then crude product was purified by column chromatography (silica gel. These porphyrins and their metal derivatives were characterized by spectroscopic methods. However, the copper complexes were further studied by ESR spectra and zinc complex by fluorescence spectrum [40].

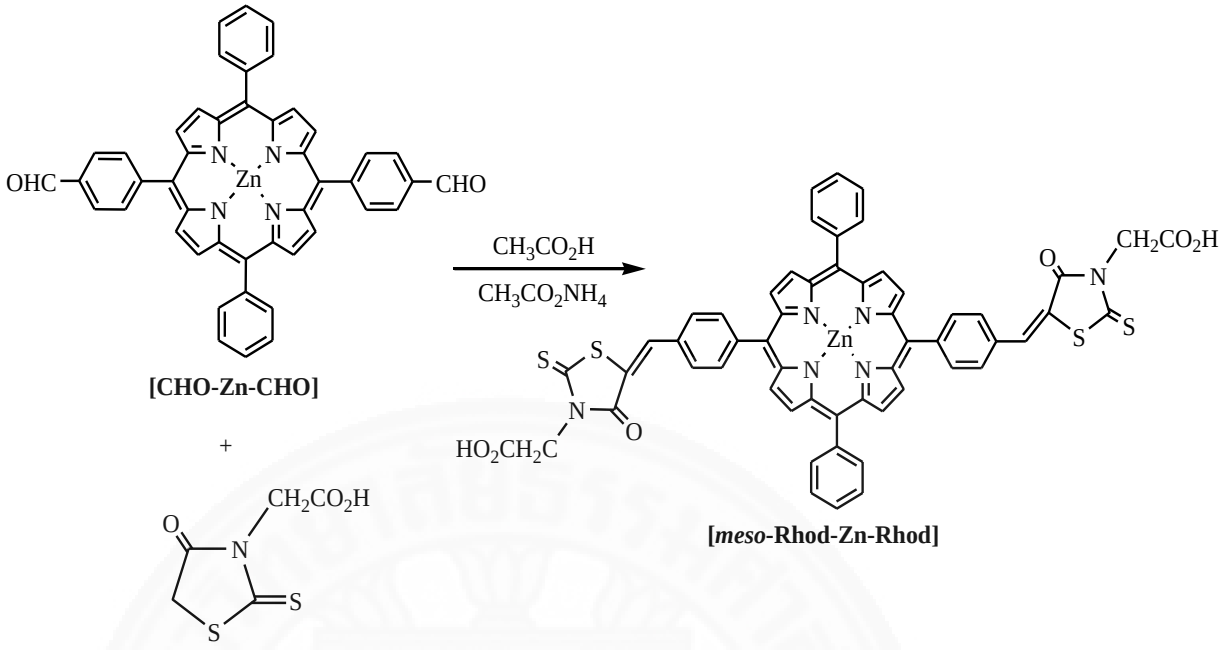

Scheme 11. Synthesis of a new photosensitizer having two rhodanine acetic acid groups at meso-positions of a zinc porphyrin [meso-Rhod-Zn-Rhod]

Giribabu *et al.* (2008) synthesized a new photosensitizer having two rhodanine acetic acid groups at meso-positions of a zinc porphyrin [*meso*-Rhod-Zn-Rhod] (Scheme 11) and characterized by UV-Visible, ^{1}H NMR, MALDI-MS, fluorescence spectroscopies and cyclic voltammetry. The [*meso*-Rhod-Zn-Rhod] was synthesized by condensation of 5,10-bis-(4-formyl phenyl)-15,20-bisphenyl porphyrinato zinc(II) [CHO-Zn-CHO], rhodanine acetic acid and ammonium acetate for 24 h. The new sensitizer was tested in DSSC by using three different liquid redox electrolytes and compared with dyad. In order to overcome the liquid redox electrolyte problems, both dyad and triad were tested in DSSC by using polymer gel electrolyte (quasi-solid-state DSSC). The DSSC with polymer gel electrolyte is found to be more durable than liquid redox electrolyte [41].

CHAPTER 3
RESEARCH METHODOLOGY

3.1 Reagent

The chemical reagents were purchased and used without further purification. The organic solvents were distilled at their boiling point ranges prior to use for synthesis, purification and characterization.

- 4-Carboxybenzaldehyde ($C_8H_7O_2$, Assay 97%, Sigma-Aldrich)
- 4-Hydroxybenzaldehyde ($C_7H_6O_2$, Assay 97%, Sigma-Aldrich)
- 4-Methoxybenzaldehyde ($C_8H_8O_2$, Assay 99%, Sigma-Aldrich)
- 4-Methylbenzaldehyde (C_8H_8O, Assay 97%, Sigma-Aldrich)
- Acetone (C_3H_6O, Assay 98%, RCI Labscan)
- Benzaldehyde (C_7H_6O, Assay 99%, Sigma-Aldrich)
- Chloroform ($CHCl_3$, Assay 98%, RCI Labscan)
- Chloroform-*d* ($CDCl_3$-*d*, A.R. grade, Cambridge Isotope)
- Dichloromethane (CH_2Cl_2, Assay 98%, RCI Labscan)
- Dichloromethane (CH_2Cl_2, HPLC grade, Merck)
- Distilled water (H_2O)
- Ethyl acetate ($C_4H_8O_2$, Assay 98%, RCI Labscan)
- Hexane (C_6H_{14}, Assay 98%, RCI Labscan)
- Methanol (CH_3OH, Assay 98%, RCI Labscan)
- Methanol (CH_3OH, HPLC grade, Merck)
- *N*,*N*-dimethylformamide(C_3H_7NO, Analytical grade, MAY&BAKER)
- Propionic acid ($C_3H_6O_2$, Assay 95%, Poison)
- Pyrrole (C_4H_5N, A.R. grade, Aldrich, Steinheim)
- Thin layer chromatography (Macherey-Nagel)
- Zinc acetate dihydrate ($Zn(CH_3COO)_2 \cdot 2H_2O$, Assay 98%, Sigma-Aldrich)

3.2 General techniques

3.2.1 Thin Layer Chromatography (TLC)

Techniques: One way, ascending

Adsorbent: Silica gel 60 GF_{254} pre-coated on aluminum plate, layer thickness 0.20 mm

Detection: UV light at 254 nm

3.2.2 Column Chromatography

Adsorbent: Silica gel 60 with particle size 0.063-0.200 mm (70-230 mesh ASTM)

Packing: Slurry packing

Loading: The sample was dissolved in a small amount of suitable organic solvent, mixed with a small quantity of silica gel, dried under reduce pressure and added gently onto the top of column.

Elution: After loading of the sample, the column was eluted with suitable solvent system using gradient technique.

3.2.3 Recrystallization

Each impure solid sample is dissolved in an appropriate solvent. Then, the solution was allowed to slowly crystallize out as the solution cools. The compound crystallizes to from the solution of solvent in solid crystals.

3.2.4 Infrared (IR) Spectroscopy

Infrared spectroscopy spectra (4000-600 cm^{-1}) were performed using a spectrum GX FT-IR spectrometer (Perkin Elmer). Spectra of solid sample were recorded as potassium bromide (KBr) pellets.

3.2.5 Nuclear Magnetic Resonance (NMR) Spectroscopy

The high resolution 400 MHz ^{1}H-NMR awas performed on a BRUKER-NMR 400 MHz spectrometer. Spectra were recorded by using deuterochloroform ($CDCl_3$) and recorded as chemical shift (δ) value in ppm.

3.2.6 Mass Spectrometry (MS)

The high resolution mass spectra were performed on a Thermo Finnigan mass spectrometer.

3.2.7 UV-Visible Spectroscopy

Electronic absorption spectra of free base porphyrin and their metal complexes were carried out on a SHIMADSU UV-Vis spectrophotometer (UV-1700) using a pair of quartz cells of 10 mm path length at room temperature.

3.2.8 Fluorescence Spectroscopy

Emission spectra of porphyrins were measured by a Jasco FP-6200 spectrofluorometer at room temperature.

3.2.9 Elemental analysis

Elemental analysis of the samples was performed on a Perkin Elmer CHNO/S analyzer model 2400 series.

3.2.10 Thermogravimetric Analysis (TGA)

The thermal analysis was performed by Perkin Elmer TGA-7. The dye of samples about 10 mg were used and heated in range 25℃ to 700℃ under nitrogen flow with scan rate of 20℃ per minute.

3.2.11 X-ray crystallography

The crystallization of porphyrins was prepared in the mixture solvent (dichloromethane: methanol, 1:1). A single crystal was selected and fixed with epoxy cement on a fine glass fibre which was mounted on a Bruker Porphyrin SMART APEX diffraction with graphite-monochromated Mo Kα (λ = 0.71073 A˚) for cell determination and data collection.

3.3 Free base porphyrins Synthesis

Adler-Longo method is one of the most common methods for the synthesis of porphyrins. In this work, the free base porphyrins synthesis was carried out under anhydrous condition using modified conventional Adler-Longo method.

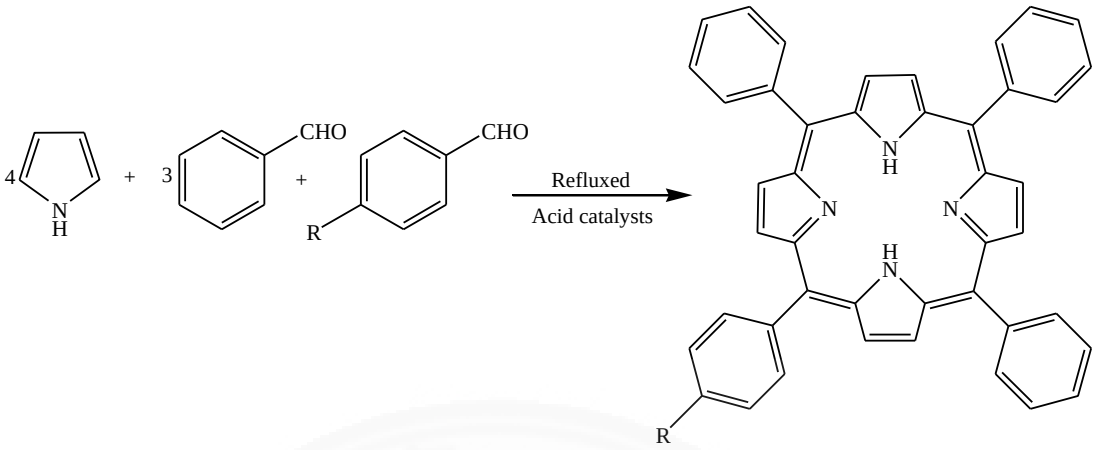

Scheme 12. The reaction for free base porphyrins synthesis

Before the complexes of porphyrins can be synthesized, the free base porphyrins must be generated. The free base porphyrins that containing hydroxyl, alkoxy, alkyl or carboxyl functional group on the *para* position of one of the phenyl rings was synthesized by following the development of Adler-Longo method. The reaction is carried out in one pot reaction. In Scheme 12, a mixture of pyrrole, benzaldehyde, and each substituted benzaldehyde (as shown in Figure 18) with a 4:3:1 ratio was refluxed in the acid catalysts (propionic acid). Then, the compounds were purified by using silica gel column chromatography and recrystallization. The expected structures of free base porphyrins were shown in the Figure 19.

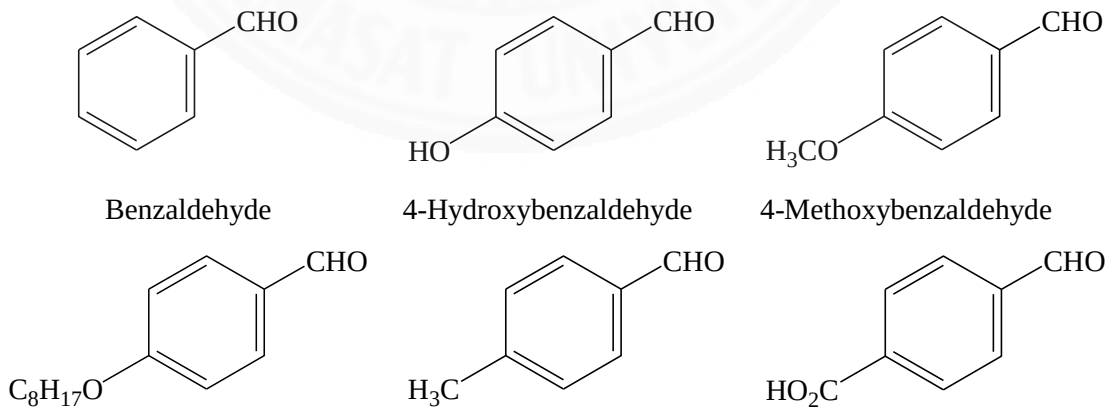

Figure 18. The structures of aldehydes

***Synthesis of 5-(4-Methoxyphenyl)-10,15,20-triphenylporphyrin* (MeTrPP)**

MeTrPP, the free-based porphyrins that containing methoxy group on the *para* position of the phenyl rings was synthesized by a condensation reaction between pyrrole, benzaldehyde and 4-methoxybenzaldehyde in propionic acid (scheme 12). Benzaldehyde (1.5 mL, 14.7 mmol) and 4-methoxybenzaldehyde (1.5 mL, 12.4 mmol) were heated with refluxed in propionic acid (50 mL) for 15 minutes. Then, pyrrole (1.0 mL, 14.3 mmol) was added dropwise. The mole ratio of pyrrole to benzaldehyde to 4-methoxybenzaldehyde was controlled at 4:3:1, respectively.

The solution quickly changed from colorless to vary dark brown, and then turned to opaque. Color change was clearly noticeable after about 5 minutes. Once the solution was homogeneous, the reaction mixture was then further refluxed and stirred for 1.5 hours at 110˚C. After cooling, the dark brown solution was filtered under reduce pressure. The deep-purple powders were collected as mixed residues. The residue mixture was purified by using silica gel column chromatography.

Table 1. The concentration of precursors that use for free base porphyrins synthesis

Compounds	Propionic acid (mL)	Pyrrole (mL, mmol)	Benzaldehyde (mL, mmol)	Substituted Benzaldehyde (mL, mmol)
MeTrPP	50	2.8, 40.1	3.0, 29.7	1.2, 9.9
CTrPP	50	2.8, 40.1	3.0, 29.7	1.5 (g*), 12.5
MTrPP	50	2.8, 40.1	3.0, 29.7	1.2, 10.2
OTrPP	50	2.8, 40.1	3.0, 29.7	2.3, 10.0
HTrPP	50	2.8, 40.1	3.0, 29.7	1.2 (g*), 10.0

* 4-Carboxybenzaldehyde and 4-hydroxybenzaldehyde were used in solid form.

The other free base porphyrins, they were synthesized under the same experimental conditions as MeTrPP. The concentrations of precursors that use for synthesis were shown in Table 1. The substituted benzaldehydes, precursors of MeTrPP, CTrPP, MTrPP, OTrPP and HTrPP synthesis were 4-methoxybenzaldehyde, 4-carboxybenzaldehyde, 4-methylbenzaldehyde, 4-octyloxybenzaldehyde and 4-hydroxybenzaldehyde, respectively.

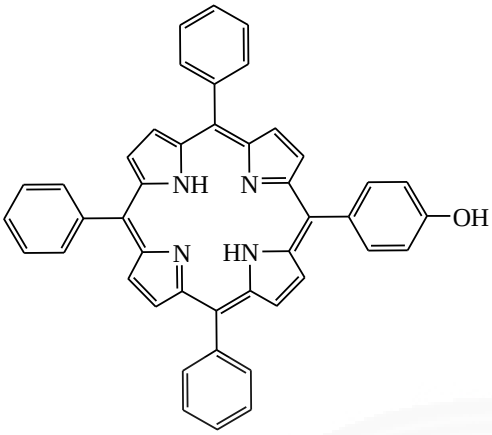

5-(4-Hydroxyphenyl)-10,15,20-triphenylporphyrin (HTrPP)

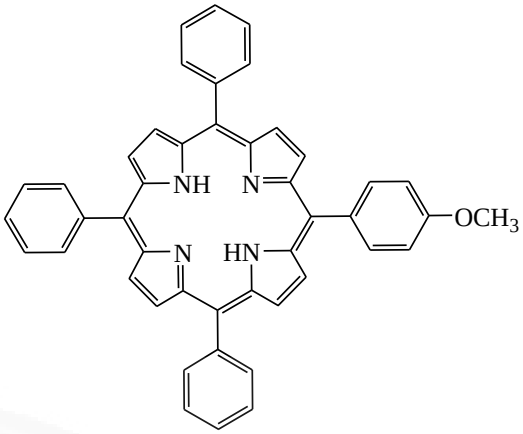

5-(4-Methoxyphenyl)-10,15,20-triphenylporphyrin (MeTrPP)

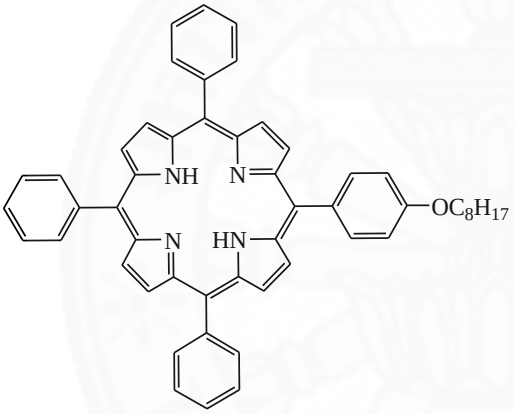

5-(4-Octyloxyphenyl)-10,15,20-triphenylporphyrin (OTrPP)

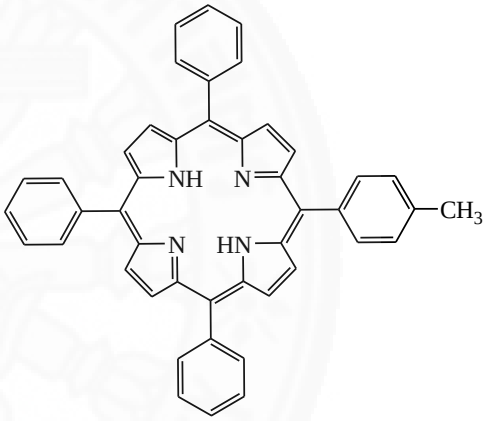

5-(4-Methylphenyl)-10,15,20-triphenylporphyrin (MTrPP)

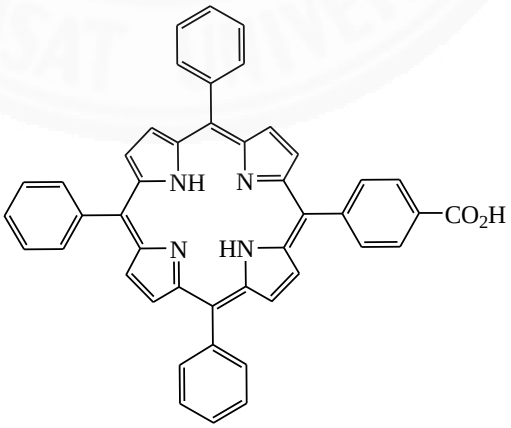

5-(4-Carboxyphenyl)-10,15,20-triphenylporphyrin (CTrPP)

Figure 19. The expected structures of free base porphyrins

3.4 Synthesis of metalloporphyrins

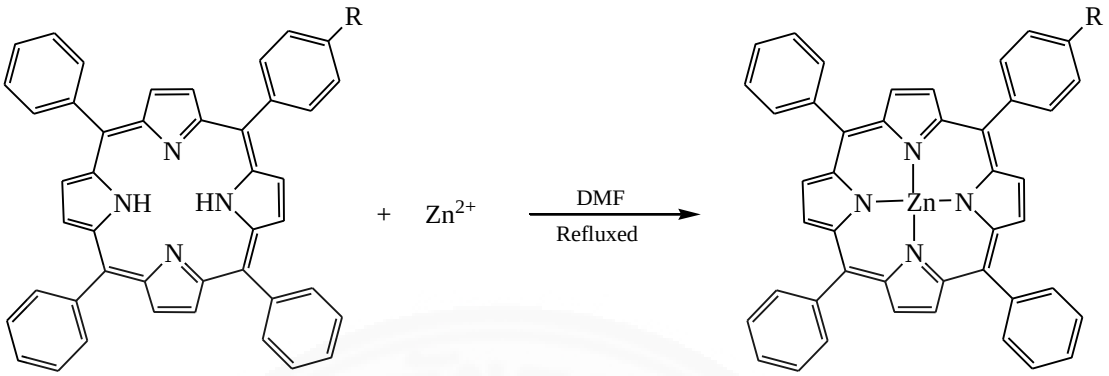

Scheme 13. The reaction for Zn metalloporphyrins synthesis

The metallation process of free base porphyrin with zinc (II) ion was synthesized (Scheme 13). The free base porphyrin was taken in DMF. Then, zinc acetate was added into the refluxed and continues stirring. The reaction mixture was further refluxed and stirred for 6 hours at 90˚C. Each reaction mixture was frequency monitored by TLC, until the reaction completed (No band of starting materials). After cooling to room temperature 30 mL dichloromethane was added, and the solution was extracted with water (4×50 mL). The organic layers were collected. Then the solvent was removed under reduce pressure. The resultant crystals were appeared. The further purification by silica gel column chromatography was required. The expected structures of zinc metalloporphyrins were shown in the Figure 20.

3.5 Characterization

The UV-Vis absorption spectra of the synthesized compounds were studied by recording between 200 and 800 nm, the fluorescence spectra were measured in range 530-700 nm. ^{1}H–NMR spectroscopy, the infrared spectroscopy, elemental analysis and mass spectrometry were performed to study their chemical properties and to confirm the structure. Thermogravimetry was measured to study the thermal stability of the expected complexes.

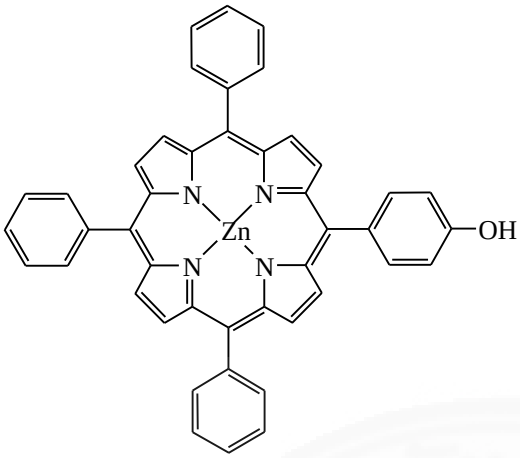

Zinc 5-(4-hydroxyphenyl)-10,15,20-triphenylporphyrin (ZnHTrPP)

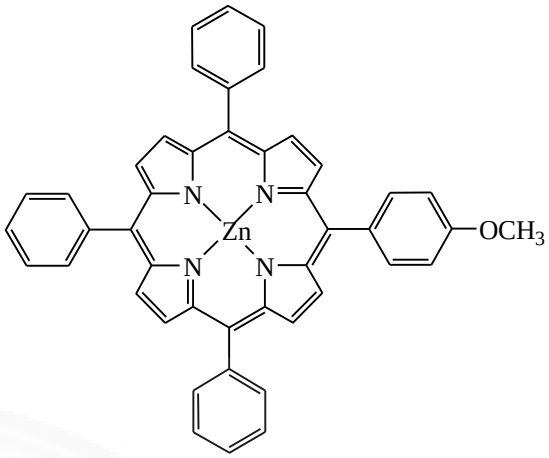

Zinc 5-(4-methoxyphenyl)-10,15,20-triphenylporphyrin (ZnMeTrPP)

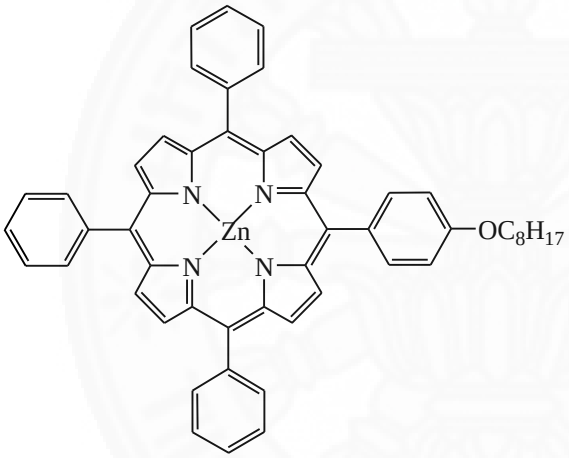

Zinc 5-(4-octyloxyphenyl)-10,15,20-triphenylporphyrin (ZnOTrPP)

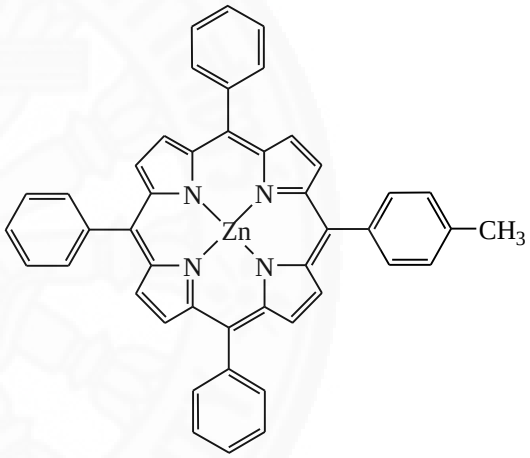

Zinc 5-(4-methylphenyl)-10,15,20-triphenylporphyrin (ZnMTrPP)

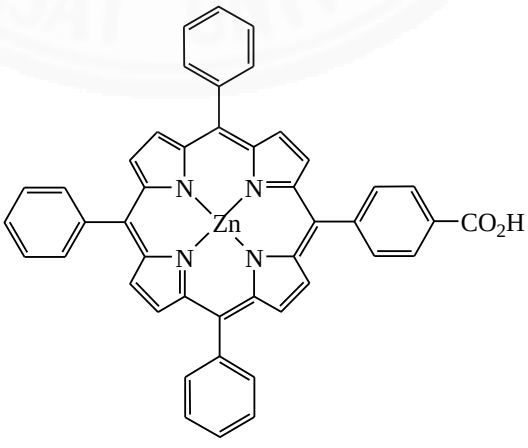

Zinc 5-(4-carboxyphenyl)-10,15,20-triphenylporphyrin (ZnCTrPP)

Figure 20. The expected structures of zinc metalloporphyrins

3.6 Spectral data of synthesized compounds

3.6.1 5,10,15,20-Tetraphenylporphyrin (TPP)

Molecular formular: $C_{44}H_{30}N_4$

Molecular weight: 615

ESI-MS m/z: 614

^{1}H-NMR ($CDCl_3$, 400 MHz):

δ = 8.84 (8H, s, *β*-pyrrole), 8.22 (8H, d, *J* = 6.1 Hz, *ortho*-phenyl), 7.76 (12H, q, *J* = 6.6 Hz, *meta* and *para*-phenyl)

FTIR (KBr), (υ, cm^{-1}): 3315, 1595, 1472, 1350, 965, 800

UV-Visible (λ_{max}, nm): 416, 514, 549, 590, 647

Fluorescence (nm): 650, 711

3.6.2 5-(4-Methoxyphenyl)-10,15,20-triphenylporphyrin (MeTrPP)

Percentage yield (%): 11.5 (purple solid)

Molecular formular: $C_{45}H_{32}N_4O$

Molecular weight: 645

ESI-MS m/z: 644, 1305 (may related to di-molecular)

^{1}H-NMR ($CDCl_3$, 400 MHz):

δ = 8.88 (2H, d, *J* = 5.0 Hz, *β*-pyrrole near methoxy phenyl), 8.84 (6H, d, *J* = 2.7 Hz, *β*-pyrrole near phenyl), 8.21 (6H, d, *J* = 7.7 Hz, *ortho*-phenyl), 8.13 (2H, d, *J* = 8.6 Hz, *ortho*-methoxy phenyl), 7.76 (9H, m, *J* = 6.2, 5.7 Hz, *meta* and *para*-phenyl), 7.29 (2H, d, *J* = 8.6 Hz, *meta*-methoxy phenyl), 4.10 (3H, s, OCH_3)

FTIR (KBr), (υ, cm^{-1}): 3314, 1596, 1471, 1349, 1249, 966, 798

UV-Visible (λ_{max}, nm): 416, 515, 551, 591, 646

Fluorescence (nm): 650, 713

3.6.3 5- (4-carboxyphenyl)-10,15,20-triphenylporphyrin (CTrPP)

Percentage yield (%): 3.7 (purple solid)

Molecular formular: $C_{45}H_{30}N_4O_2$

Molecular weight: 659

ESI-MS m/z: 659, 1325 (may related to di-molecular)

^{1}H-NMR ($CDCl_3$, 400 MHz):

δ = 8.79 (2H, *β*-pyrrole near carboxy phenyl), 8.87-8.85 (6H, m, *β*-pyrrole near phenyl), 8.21 (6H, d, *ortho*-phenyl), 8.34 (2H, d, *ortho*-carboxy phenyl), 7.76 (9H, m, *meta* and *para*-phenyl), 8.47 (2H, d, *meta*-carboxy phenyl), 11.95 (1H, s, CO_2H)

FTIR (KBr), (υ, cm^{-1}): 3450-3100, 3311, 1695, 1600, 1492, 1352, 1275, 965, 799

UV-Visible (λ_{max}, nm): 416, 510, 548, 586

Fluorescence (nm): 650, 712

3.6.4 5,10,15,20-Tetraphenylporphyrin Zinc(II) (ZnTPP)

Molecular formular: $ZnC_{44}H_{28}N_4$

Molecular weight: 678

ESI-MS m/z: 676

^{1}H-NMR ($CDCl_3$, 400 MHz):

δ = 8.94 (8H, s, *β*-pyrrole), 8.22 (8H, d, *J* = 6.1 Hz, *ortho*-phenyl), 7.76 (12H, q, *J* = 6.6 Hz, *meta* and *para*-phenyl)

FTIR (KBr), (υ, cm^{-1}): 1596, 1488, 1340, 1003, 799

UV-Visible (λ_{max}, nm): 416, 548, 585

Fluorescence (nm): 593, 640

3.6.5 5-(4-Methoxyphenyl)-10,15,20-triphenylporphyrin Zinc(II) (ZnMeTrPP)

Percentage yield (%): 29.8 (purple solid)

Molecular formular: $ZnC_{45}H_{30}N_4O$

Molecular weight: 708

ESI-MS m/z: 708, 1417 (may related to di-molecular)

^{1}H-NMR ($CDCl_3$, 400 MHz):

δ = 8.98 (2H, d, *β*-pyrrole near methoxy phenyl), 8.94 (6H, d, *β*-pyrrole near phenyl), 8.22 (6H, *ortho*-phenyl), 8.13 (2H, d, *ortho*-methoxy phenyl), 7.76 (9H, m, *meta* and *para*-phenyl), 7.30 (2H, d, *meta*-methoxy phenyl), 4.11 (3H, s, OCH_3)

FTIR (KBr), (υ, cm^{-1}): 1607, 1442, 1341, 1250, 996, 799

UV-Visible (λ_{max}, nm): 420, 549, 588

Fluorescence (nm): 595, 640

3.6.6 5- (4-carboxyphenyl)-10,15,20-triphenylporphyrin Zinc(II) (ZnCTrPP)

Percentage yield (%): 14.6 (purple solid)

Molecular formular: $ZnC_{45}H_{28}N_4O_2$

Molecular weight: 722

ESI-MS m/z: 720, 1465 (may related to di-molecular)

^{1}H-NMR ($CDCl_3$, 400 MHz):

δ = 8.91 (2H, *β*-pyrrole near carboxy phenyl), 9.01-8.98 (6H, m, *β*-pyrrole near phenyl), 8.25 (6H, d, *ortho*-phenyl), 8.37 (2H, d, *ortho*-carboxy phenyl), 7.79 (9H, m, *meta* and *para*-phenyl), 8.52 (2H, d, *meta*-carboxy phenyl), 11.98 (1H, s, CO_2H)

FTIR (KBr), (υ, cm^{-1}): 3419, 1675, 1607, 1420, 1339, 1270, 995, 798

UV-Visible (λ_{max}, nm): 415, 548, 586

Fluorescence (nm): 597, 641

CHAPTER 4
RESULTS AND DISCUSSION

4.1 Synthesis of free base porphyrins and characterization

The target of this research is to synthesis the asymmetric-*meso*-substituted porphyrin that contains hydroxyl, alkoxy, alkyl, or carboxyl functional group on the *para* position of one of the phenyl rings. Asymmetric free base porphyrins (A_3B) have previously been prepared by the condensation of pyrrole and two types of aldehydes, affording a mixture of asymmetrical substituted products [26-35]. Generally, Adler-Longo method is commonly used to obtain symmetrical porphyrins. The reaction conditions were relatively mild and provided the fast reaction rate. The attempts has been tried to synthesize asymmetrical substituted porphyrins via simple methodology using pyrrole and a mixture of two different aldehydes in the Adler-Longo method. Thus, this research was attempted to develop the synthetic methods to gain asymmetric porphyrins by using a modified conventional Adler-Longo method.

The synthesis methodology of the free base porphyrins with Adler-Longo method have been widely explored in the literature. In this work used the different controlled parameters. The molar ratio of starting materials, temperature of condensation reaction, concentration of propionic acid and time of reaction were changed from the reported Adler-Longo method. The free base porphyrins MeTrPP, CTrPP, MTrPP crude products were synthesized using the same molar ratio of starting materials (pyrrole: benzaldehyde: appropriately substituted benzaldehyde) in 4:3:1 ratio. However, this molar ratio was inappropriate for porphyrins HTrPP and OTrPP. Then, the reaction was changed to 4:2:2 ratio. The resultant residue from both reactions yielded a sticky dark crude oil, after condensation in propionic acid. Moreover, the crude oil was examined by mass spectrometry techniques. There were not shown the expected molecular ion peaks. Therefore, HTrPP and OTrPP are unsuccessful prepared via the current method.

The general for Adler-Longo synthesis, the temperature is about 140℃. The condensation at this temperature was relatively violent reaction because of the propionic acid's boiling. Thus the reaction temperature was performed at lower temperature, 110℃. The product yields were still the same.

The use of propionic acid as catalyst is an important and efficient requirement for the synthesis of *meso*-substituted porphyrins. The acid catalyst is responsible for the protonation of the carbonyl group of the aldehydes, which are then attacked by pyrrole in an aromatic electrophilic substitution, leading to the formation of the tetrapyrrolic chain [42]. In the typical procedure, 100 mL of propionic acid was used as solvent and catalyst. It was removed at the filtration step. The crude product was filtered and washed with methanol to remove the acid catalyst and the tarry impurity. In this asymmetric porphyrins synthesis, propionic acid was not successfully separated from crude products with the mentioned process. However, the separation by simple distillation or water extraction may require. The attempts have been tried but the purification is unsuccessful. Thus, the amount of acid catalyst was decreased and allows the reaction time was taken longer. The reaction was monitored by TLC as shown in Figure 21.

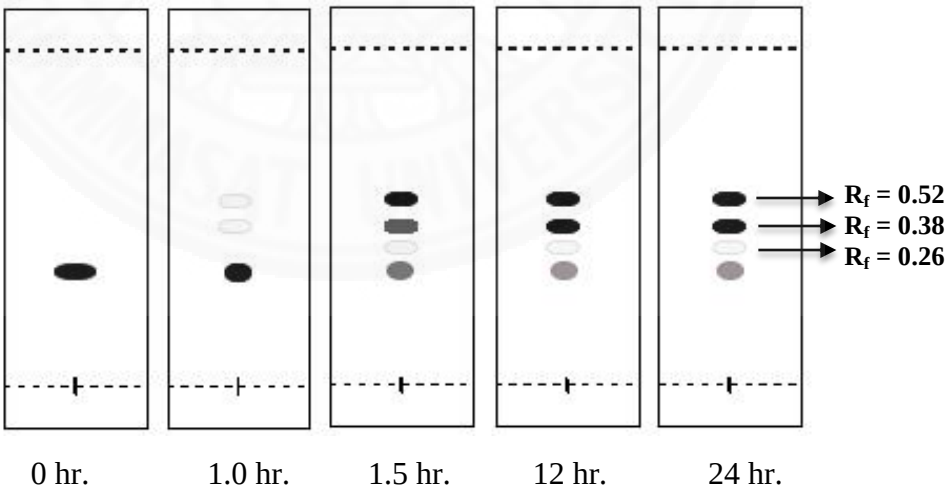

Figure 21. The TLC plate at during a reaction of MeTrPP crude synthesis

The TLC method was used to determine the optimum time reaction required to obtain the expected porphyrins. The samples of the reaction mixture were subjected to TLC analysis and TLC plates at various reaction times were shown in

Figure 21. At the start of the reaction, only the mixture of reactants was found on the TLC plate. As the reaction progresses, 1 hour, the product spots started to form with the R_f =0.52, 0.38 but the starting mixture spot was shown a very strong intensity. It was found that the intensity of starting material band was decreasing while the intensity of products band were more intense with the reaction time. In the previous work, the reaction time was 0.5 hr. The current work selected the 1.5 hr. as an optimal reaction time due to no significant change for longer reaction time.

It can be summarized the suitable controlled conditions for the synthesis of asymmetric free base porphyrins.

(a) The molar ratio of starting materials (pyrrole: benzaldehyde: appropriately substituted benzaldehyde) was 4:3:1.

(b) The selected temperature of condensation reaction was 110℃.

(c) The concentration of propionic acid was 50 mL.

(d) The time of reaction was 1.5 hours.

The modified conventional Adler-Longo method is suitable for MeTrPP, CTrPP and MTrPP. However, this condition could not give the product of HTrPP and OTrPP.

4.1.1 Synthesis of 5-(4-Methoxyphenyl)-10,15,20-triphenylporphyrin (MeTrPP)

MeTrPP was synthesized by condensation of pyrrole, benzaldehyde and 4-methoxybenzaldehyde in propionic acid, Scheme 14. TLC analysis (50 % dichloromethane in hexane) of the crude products revealed a mixture of three components with spots at R_f = 0.52, 0.38 and 0.26. This purification process was very challenging because the components showed very close retention factors. After the reaction, the mixture was purified by a column chromatography separation with an optimal condition checked by TLC. Mass spectrometry of the crude revealed the expected molecular ion peak of MeTrPP at m/z 644 with further fragments ion peak at m/z 613, 674 and 704, related to TPP, MeTrPP-2 and MeTrPP-3 respectively.

This compound was applied as wet method prior separation by a silica gel column chromatography with an increasing gradient of eluent from 10%

dichloromethane to polar solvent. A crude purple solution was eluted from column, monitored by TLC and collected into three fractions.

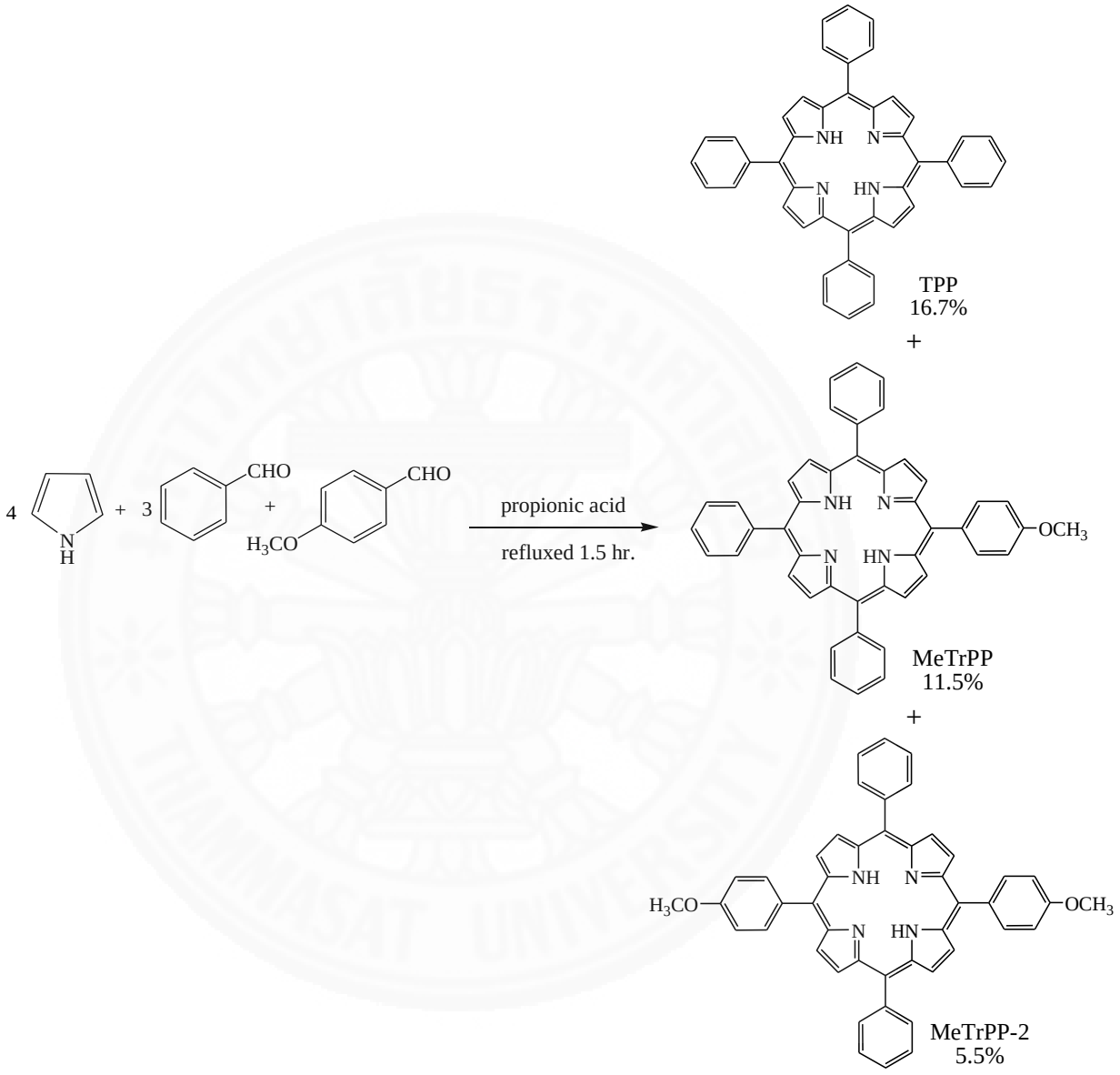

Scheme 14. The synthesis of 5-(4-Methoxyphenyl)-10,15,20-triphenylporphyrin (MeTrPP)

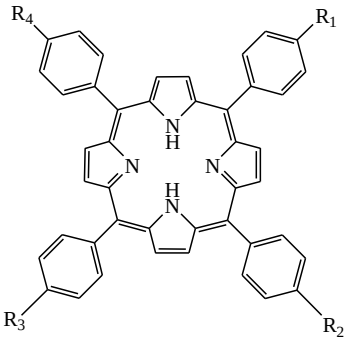

	R_1	R_2	R_3	R_4	MW
TPP	H	H	H	H	615
MeTrPP	$-OCH_3$	H	H	H	645
MeTrPP-2	$-OCH_3$	H	$-OCH_3$	H	675
MeTrPP-3	$-OCH_3$	$-OCH_3$	$-OCH_3$	H	705
TMePP	$-OCH_3$	$-OCH_3$	$-OCH_3$	$-OCH_3$	735

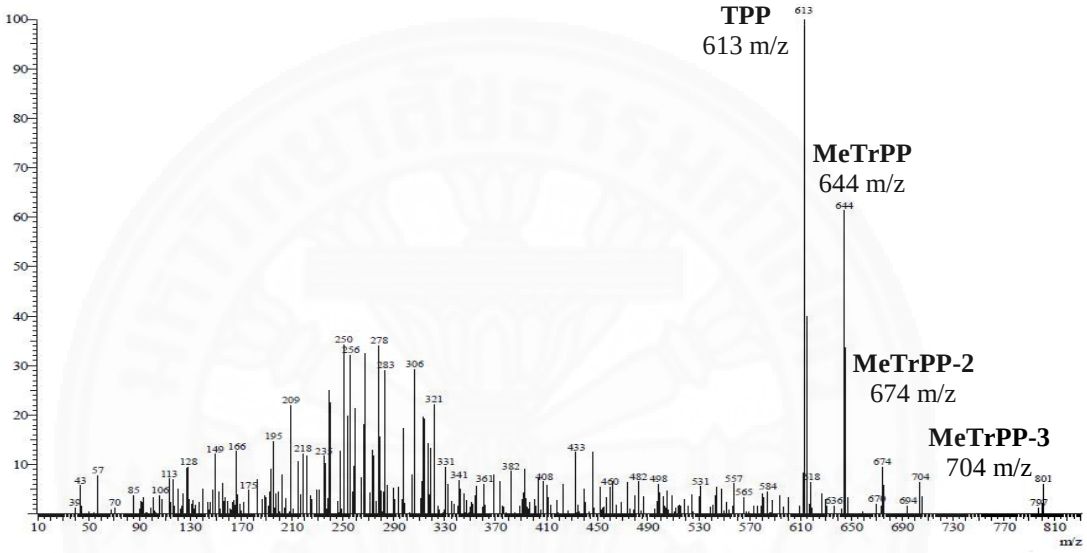

Figure 22. Mass spectra of MeTrPP crude

Table 2. Characteristic data for the composition of **MeTrPP** mixture

Fractions	**Compounds**	**Yield (%)**	**Elemental analysis ([a]), %**			**Formula weight**	**MS (m/z) $[M-H]^+$**
			C	H	N		
1	TPP ($C_{44}H_{30}N_4$)	16.7	86.00 (85.97)	4.88 (4.92)	9.35 (9.11)	615	614, 1274 [b]
2	MeTrPP ($C_{45}H_{32}N_4O$)	11.5	83.80 (83.83)	5.00 (5.00)	8.83 (8.69)	645	644, 1305 [b]
3	MeTrPP-2 ($C_{46}H_{34}N_4O_2$)	5.5	81.89 (81.88)	5.24 (5.08)	8.16 (8.30)	675	674, 1335 [b]

[a] Theoretical values are given in parentheses.

[b] The product ions may be formed in di-molecular.

From Table 2, the yield and characteristic data including elemental analysis and mass spectrometry of MeTrPP and its derivatives were shown. This procedure gave successful 11.5% of MeTrPP. Further recrystallization from dichloromethane and methanol mixture solvent yielded a purple microcrystalline solid of the desired product. The synthesized MeTrPP porphyrin has been characterized by spectroscopy to confirm the structure of the expected compound. The mass spectrometry and elemental analysis are in agreement with the proposed molecular formula as shown in Table 2 and spectrum is shown in Appendix B. However, the mass spectrum of MeTrPP was found the ion peak at m/z 1305, may relate to dimolecular compound.

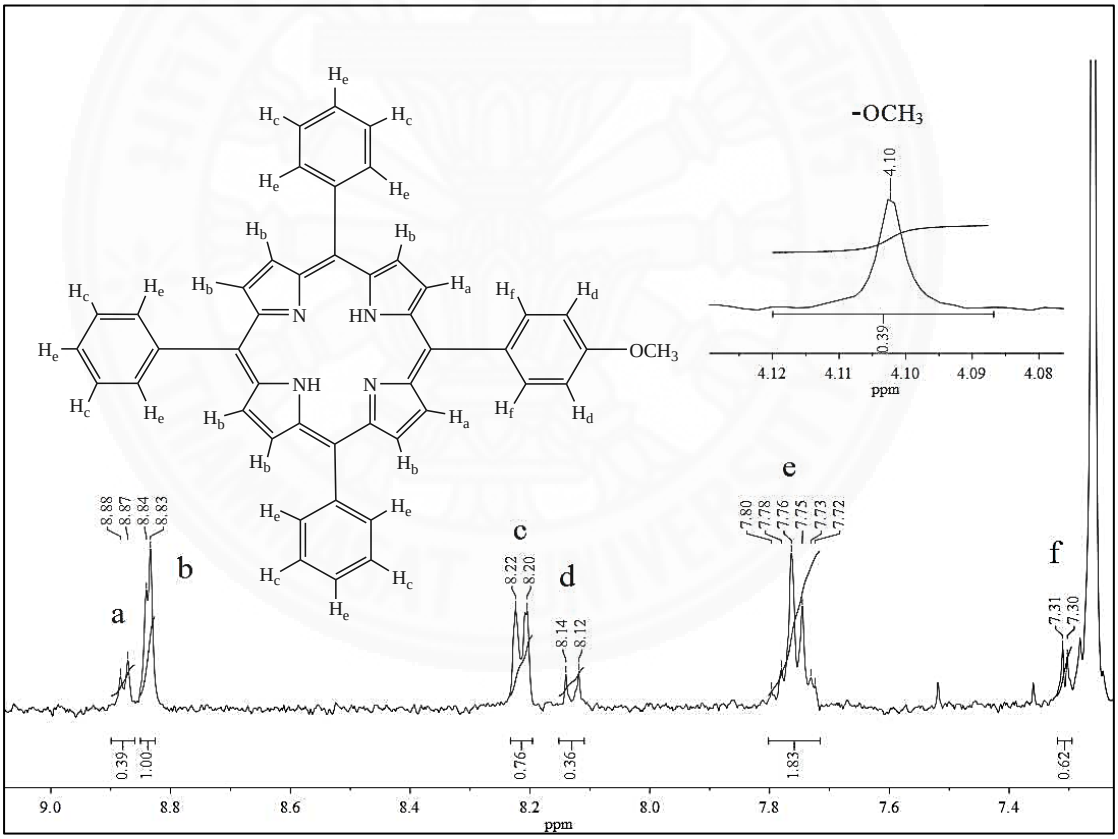

Figure 23. ^{1}H NMR spectra of MeTrPP in $CDCl_3$ solution

Figure 23 is the ^{1}H NMR spectrum of a purified MeTrPP. The result was revealed the protons of β-pyrrole, aromatic porphyrins and methoxy group. The eight protons of β-pyrrole were separated into two groups due to the different

environment. The first group was near the methoxy phenyl group found (H_a) at 8.87 ppm because of the electron donating effect from the methoxy group. The second group was closer to the phenyl ring (H_b), found the chemical shift at 8.83 ppm as a doublet. The *ortho* phenyl protons gave doublet of six protons at 8.21 ppm. A doublet corresponding to the two *ortho*-methoxy phenyl protons, appearing at 8.13 ppm due to electronic effect. Moreover, the *meta*- and *para*-phenyl protons gave multiplet signals of nine protons at 7.76 ppm. The doublet signal at 7.29 ppm represented the two *meta*-methoxy phenyl protons. The chemical shift of the protons at 4.10 ppm, corresponding to methoxy group protons, was found in agreement with TMePP. The NMR spectroscopy confirmed the expected MeTrPP structure.

IR spectroscopy was carried out for identifying functional groups of MeTrPP molecule. IR spectrum of MeTrPP was collected in Apendix D. The presence of N–H stretching was found at 3314 cm^{-1} in the aromatic secondary amine of four pyrrole rings. The band near 1249 and 1031 cm^{-1} were interpreted as C–O vibration of methoxy group. The other bands i.e. 3022–2866 cm^{-1} (sp^2 C– H stretching of the phenyl ring), 1596 cm^{-1} (C=C stretching of pyrrole ring), 1471 cm^{-1} (C=C vibration modes of the phenyl rings), 1349 cm^{-1} (C–N stretching of pyrrole), 1177 cm^{-1} (C–H phenyl), 982 cm^{-1} (=C–H out of plane bending), 966 cm^{-1} (=C–H pyrrole out of plane bending), 846 cm^{-1} (C–H pyrrole in plane bending), 798 cm^{-1} (C–H pyrrole), 725 cm^{-1} (C–H phenyl) and 702 cm^{-1} (C–H phenyl).

4.1.2 Synthesis of 5-(4-carboxyphenyl)-l0,15,20-triphenylporphyrin (CTrPP)

Scheme 15, a mixture of 4-carboxybenzaldehyde (1.5 g, 12.5 mmol) in propionic acid (50 mL) was heated with refluxed stirring at 110℃. To this solution were slowly added benzaldehyde (1 mL, 29.7 mmol) and pyrrole (2.8 mL, 40.1 mmol). This mixture was allowed to react for 1.5 h. After cool down over night at 5℃, the violet pellet were filtered and washed with methanol. The crude material was redissolved in CH_2Cl_2.

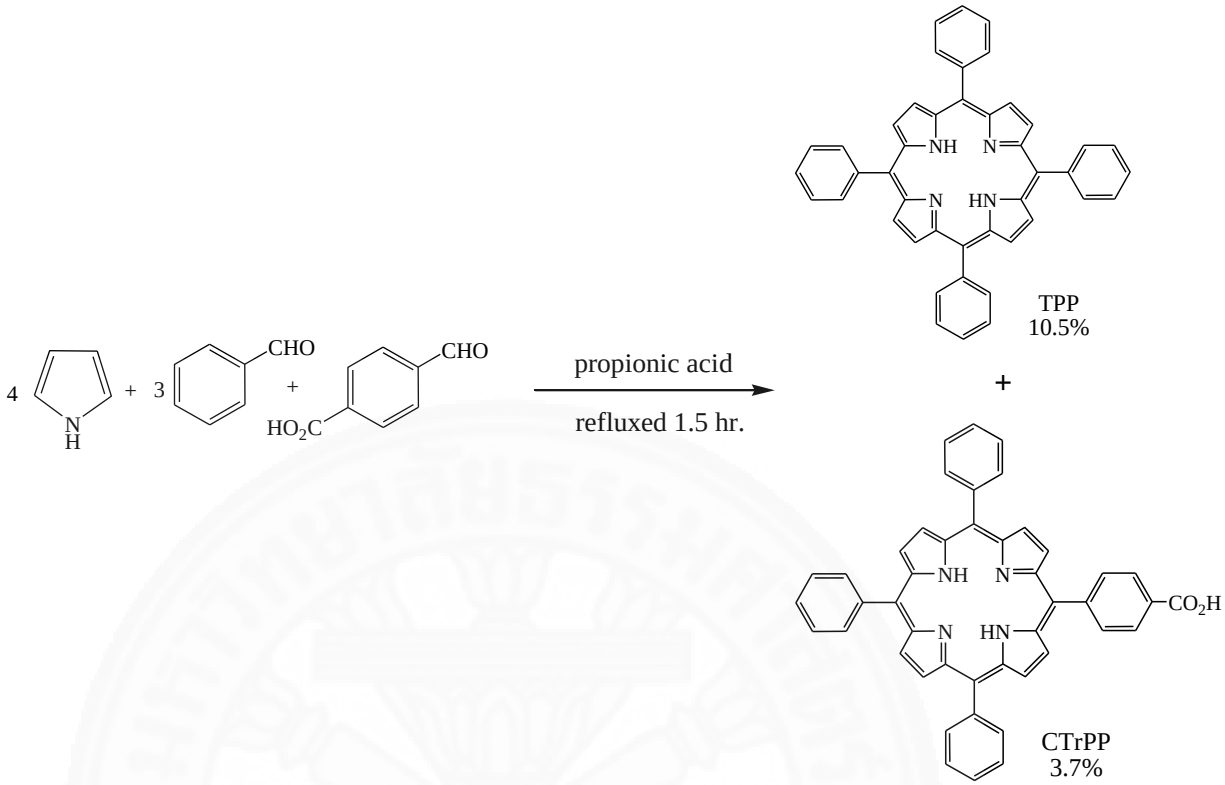

Scheme 15. The synthesis of 5-(4-Carboxyphenyl)-10,15,20-triphenylporphyrin (MeTrPP)

The reaction was monitored by mass spectrometry. The crude products yield an expected CTrPP compound with the molecular ion peak at m/z 660. However, the TPP, CTrPP-2 and TCPP were also observed at m/z 614, 700 and 790, respectively (Figure 24). The results are different from previous reports where the pure CTrPP was obtained after the extreme reaction condition [31, 41]. The mass spectrum of CTrPP was found the ion peak at m/z 1325, may relate to dimolecular compound.

After purification by column chromatography (silica gel), the purified product was successfully separated into two fractions, TPP and CTrPP. The rest of mentioned compound were stuck in the column. Further characterization on elemental analysis was illustrated in Table 3.

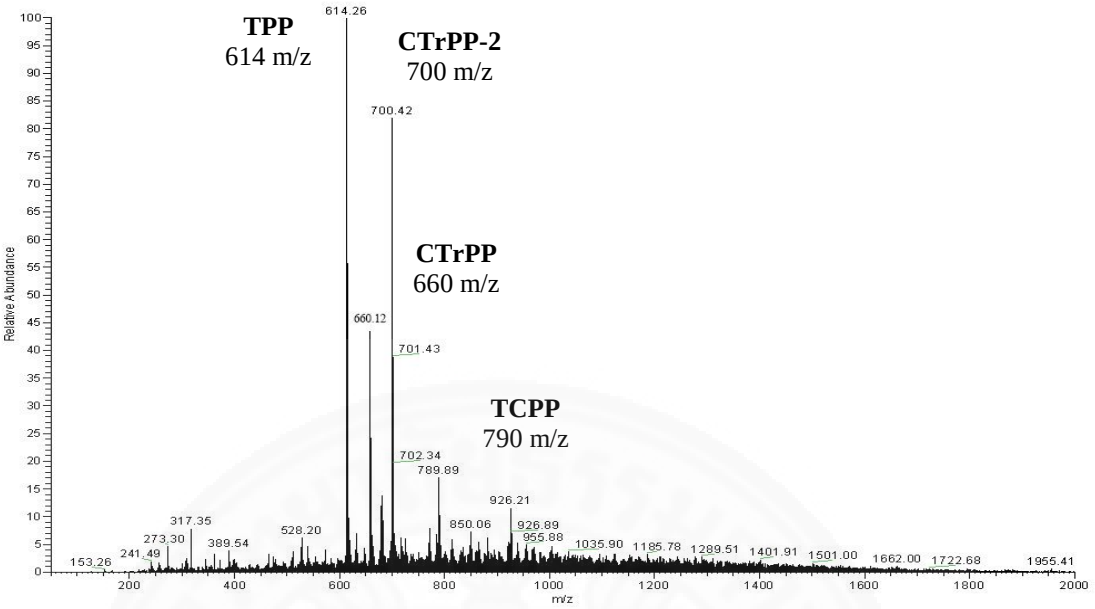

Figure 24. Mass spectra of CTrPP crude

Table 3. Characteristic data for the composition of **CTrPP** mixture

Fractions	**Compounds**	**Yield (%)**	**Elemental analysis ([a]), %**			**Formula weight**	**MS (m/z) $[M-H]^+$**
			C	H	N		
1	TPP ($C_{44}H_{30}N_4$)	10.5	86.00 (85.97)	4.88 (4.92)	9.35 (9.11)	615	614
2	CTrPP ($C_{45}H_{30}N_4O_2$)	3.7	84.42 [c] (82.05)	4.48 [c] (4.59)	7.79 [c] (8.51)	659	659, 1325 [b]

[a] Theoretical values are given in parentheses. [b] The product ions may be formed in dimolecular compound. [c] Mixed hexane in compound.

The symmetric porphyrins, TPP and TCPP references, were also characterized for the comparative analysis with the synthesized porphyrins. TLC of the first fraction matched with the TPP reference. The ^{1}H-NMR spectrum for fraction 2 was revealed the protons of *β*-pyrrole, aromatic porphyrins and carboxylic acid group. The eight protons of *β*-pyrrole and the *o*-phenyl protons were found similar to MeTrPP compound. However, the two *ortho*-carboxy phenyl protons appeared at 8.34 ppm due to electron effect. The signal at 8.47 ppm was assigned to the two *meta*-

carboxy phenyl protons. The chemical shift of the protons of the carboxylic acid group was found at 11.95 ppm. The NMR spectroscopy confirmed that the purified compound from fraction 2 was the expected CTrPP structure.

IR spectroscopy was carried out for identifying functional group of CTrPP. The carboxylic acid O–H stretch appeared as a very broad band in the region 3500-2500 cm^{-1}. The carbonyl stretch C=O of a carboxylic acid appeared as an intense band at 1695 cm^{-1}. It showed the presence of N–H stretching at 3311 cm^{-1} in the aromatic secondary amine of four pyrrole rings. The band near 1421 cm^{-1} and 1274 cm^{-1} were interpreted as O–H bending and C–O stretching of carboxylic acid group. The assignment peaks are related with the reported compound of TCPP [42].

4.1.3 Synthesis of 5-(4-methylphenyl)-10,15,20-triphenylporphyrin (MTrPP)

A mixture of benzaldehyde and 4-methylbenzaldehyde in a 4:3:1 ratio was dissolved in 50 mL of propionic acid with 10–20 mL CH_2Cl_2 and heated to reflux. Pyrrole (40.1 mmol) was added into the heating mixture. The reaction was further refluxed for 1.5 hour. The reaction product was put in refrigerator (5℃) for overnight before the purple crystals would appear. The products were filtered by vacuum filtration with a Buchner funnel. The purple crystals were washed with a little portion of cold methanol before air-dried on the Buchner funnel.

The synthesized was compared with TPP and TMPP references by TLC. TLC analysis revealed the only one spot of TPP. Mass spectrometry of the crude reaction revealed four molecular ion peaks there were 614, 628, 642 and 656 m/z (Figure 25). The analysis fitted in a mixture of TPP, MTrPP, MTrPP-2 and MTrPP-3, respectively. This purification process was unsuccessful.

However, the modified conventional Adler-Longo method was not suitable for the synthesis of 5-(4-octyloxyphenyl)-10,15,20-triphenylporphyrin (OTrPP) and 5-(4-hydroxyphenyl)-10,15,20-triphenylporphyrin (HTrPP). After condensation in propionic acid, the resultant residue was a sticky dark crude oil. Moreover, the crude oil was examined by mass spectrometry techniques. The synthesis is unsuccessful with the current method.

The unpurified MTrPP was applied into the further reaction with Zn, in the expectation that Zn-MTrPP would be able to purify. From the attempts, the

modified Adler-Longo method can be applied in the preparation of ZnMeTrPP and ZnCTrPP. However, It's not suitable for the synthesis of 5-(4-methylphenyl)-l0-10,15,20-triphenylporphyrin (MTrPP).

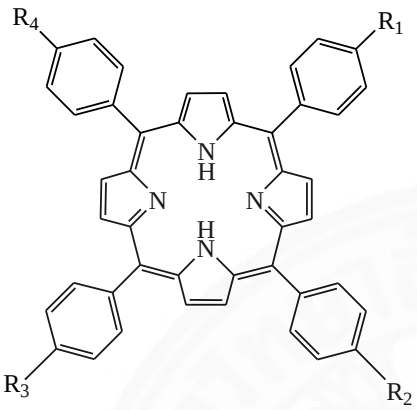

	R_1	R_2	R_3	R_4	MW
TPP	H	H	H	H	615
MTrPP	$-CH_3$	H	H	H	629
MTrPP-2	$-CH_3$	H	$-CH_3$	H	643
MTrPP-3	$-CH_3$	$-CH_3$	$-CH_3$	H	657
TMPP	$-CH_3$	$-CH_3$	$-CH_3$	$-CH_3$	671

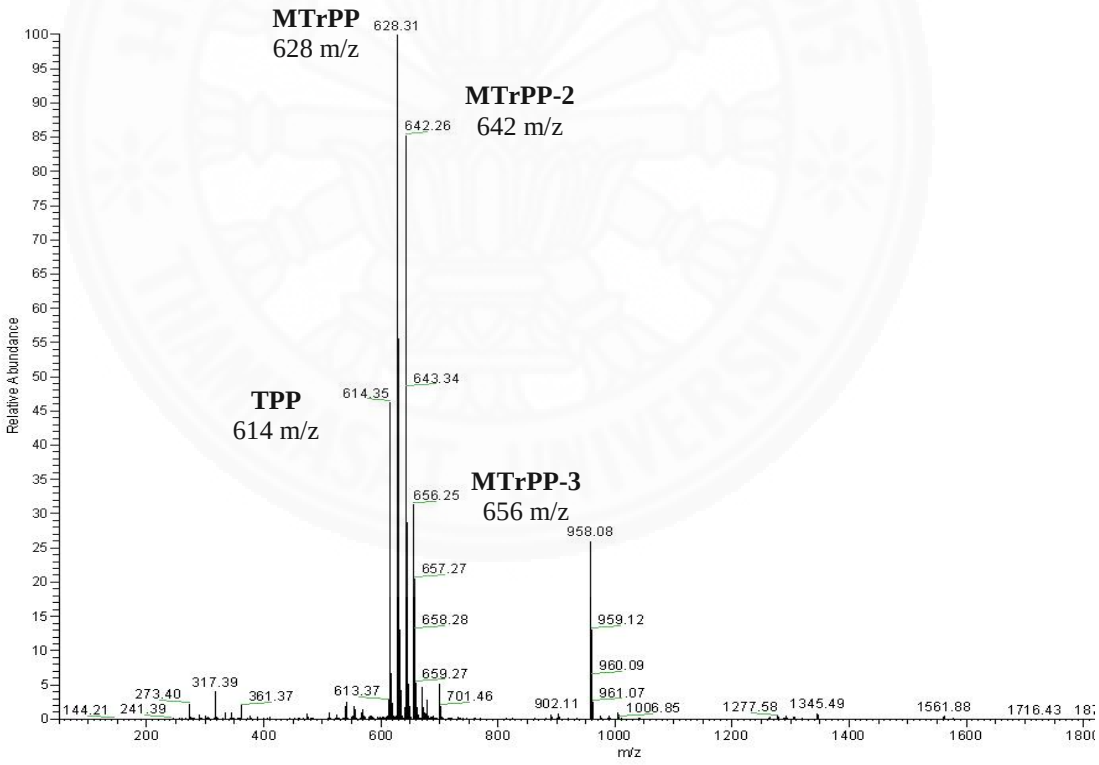

Figure 25. Mass spectra of MTrPP crude

4.2 Synthesis of Zinc porphyrins

The preparation of zinc asymmetric porphyrin complex is a two-step process, which includes synthesis of a ligand and the reaction of a ligand with appropriate metal salts. In the metallation step, the free base porphyrin was used without purification. The metallated was refluxed with zinc in DMF in the presence of an equivalent Zn(II) acetate for six hours. The reaction was monitored by TLC. The further purification by silica gel column chromatography is required.

4.2.1 Synthesis of ZnMeTrPP

Zinc acetate (0.22 g, 0.99 mmol) was added to a solution of MeTrPP crude (0.51 g, 0.79 mmol) in the mix of 10 mL DMF and 10 mL dichloromethane. This mixture was refluxed at 90℃ for 6 hours or when the TLC show the completely change. Then the solution was extracted with water. The resulting crude product was a purple solid.

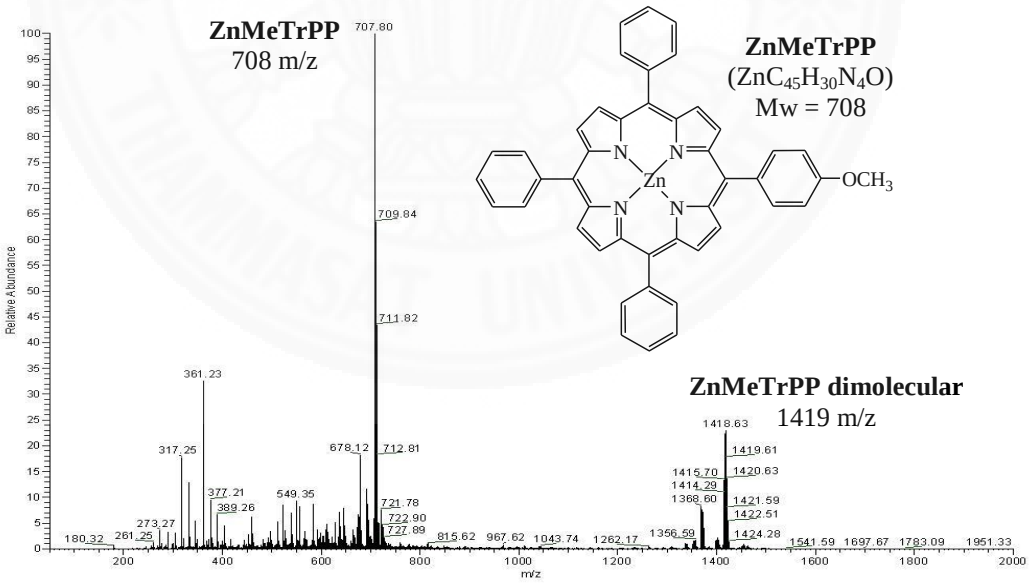

Figure 26. Mass spectrum of ZnMeTrPP in dichloromethane

Table 4. Characteristic data for the ZnMeTrPP compositions

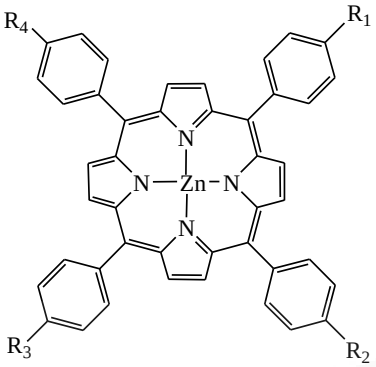

	R_1	R_2	R_3	R_4
ZnTPP	H	H	H	H
ZnMeTrPP	$-OCH_3$	H	H	H
ZnMeTrPP-2	$-OCH_3$	H	$-OCH_3$	H
ZnMeTrPP-3	$-OCH_3$	$-OCH_3$	$-OCH_3$	H
ZnTMePP	$-OCH_3$	$-OCH_3$	$-OCH_3$	$-OCH_3$

Fractions	**Compounds**	**Yield (%)**	**Elemental analysis ([a]), %**			**Formula weight**	**MS (m/z) $[M-H]^+$**
			C	**H**	**N**		
1	ZnTPP ($ZnC_{44}H_{28}N_4$)	20.5	75.38 (77.93)	4.13 (4.16)	8.21 (8.26)	678	678, 1357 [b]
2	ZnMeTrPP ($ZnC_{45}H_{30}N_4O$)	29.8	76.26 (76.33)	4.11 (4.27)	7.92 (7.91)	708	708, 1417 [b]
3	ZnMeTrPP-2 ($ZnC_{46}H_{32}N_4O_2$)	9.8	75.07 (74.85)	4.27 (4.37)	7.58 (7.59)	738	738, 1479 [b]
4	ZnMeTrPP-3 ($ZnC_{47}H_{34}N_4O_3$)	0.7	74.50 (73.49)	4.42 (4.46)	7.22 (7.29)	768	768, 1538 [b]
5	ZnTMePP ($ZnC_{48}H_{36}N_4O_4$)	*least*	72.44 (72.23)	4.41 (4.55)	7.02 (7.02)	798	798, 1596 [b]

[a] Theoretical values are given in parentheses.

[b] The product ions may be formed in dimolecular complex.

The column chromatography of ZnMeTrPP with various polarity solvent yielded five different fractions. The R_f of each fraction are 0.53, 0.37, 0.24 and 0.11. Then each fraction was analyzed, respectively by mass spectrometry. Those five fractions are related to ZnTPP, ZnMeTrPP, ZnMeTrPP-2, ZnMeTrPP-3 and ZnTMePP. The further characterization by elemental analysis, NMR and IR spectroscopy are also confirmed.

The percentage yield and characteristic data from elemental analysis and mass spectrometry for the composition of ZnMeTrPP mixture were shown in

Table 4. The purple solid of ZnMeTrPP yielded 29.8%. The mass spectrum of ZnMeTrPP was illustrated in Figure 26. The mass spectrum was shown the parent peak of the ZnMeTrPP compound at m/z 708, confirmed the occurrences of the expected metalloporphyrins. The ion peak was found at m/z 1419, may relate to a dimolecular complex. The elemental analysis data for all metalloporphyrins are in agreement with theoretical value as shown in Table 4. The NMR spectroscopy show the absent of the N-H proton. The other's protons found similar to free base ligand. IR spectroscopy was carried out for identifying functional group of ZnMeTrPP. The band near 1248 cm^{-1} was interpreted as C–O vibration of methoxy group. The other bands i.e. 3051–2833 cm-1 (sp^2 C–H stretching of the phenyl ring), 1597 cm^{-1} (C=C stretching of pyrrole ring), 1486 cm^{-1} (C=C vibration modes of the phenyl rings), 1339 cm^{-1} (C–N stretching of pyrrole), 1175 cm^{-1} (C–H phenyl), 797 cm^{-1} (C–H pyrrole) and 701 cm^{-1} (C–H phenyl). The absence of N–H stretching was confirmed the Zn^{2+} sit into the central hole. Similar evidence found in ZnTPP [43].

4.2.2 Synthesis of ZnCTrPP

In the case of the preparation of zinc porphyrins from CTrPP, zinc acetate (0.22 g, 0.98 mmol) was reacted with CTrPP crude (0.44 g, 0.67 mmol) in the solution of 10 mL dimethylformamide and 10 mL dichloromethane. After purification, ZnCTrPP crude provided three major fractions, including ZnTPP, ZnCTrPP and ZnCTrPP-3.

The desired reaction product (ZnCTrPP) eluted in fraction 2 with 70% dichloromethane in hexane. It was further purified by recrystallization to yield ZnCTrPP, zinc unsymmetrical porphyrins. The compound recovery in these fractions was 0.1420 g, or 17.6% reaction yield. Mass spectrometry of this fraction revealed the expected molecular ion peak that was 720 m/z (Table 5) and found the ion peak at m/z 1466, may relate to di-molecular complex. However, the elemental analysis data of ZnCTrPP was afforded to difference theoretical value, due to the trace of hexane solvents in the molecule, which was observed the hexane peaks in ^{1}H-NMR spectroscopy. The NMR spectroscopy show the absent of the N-H proton. The other's protons found similar to free base ligand. IR spectroscopy was carried out for identifying functional group of CTrPP. The carboxylic acid O–H stretch appeared as a very broad band in the region 3500 – 3000 cm^{-1}. The carbonyl stretch C=O of a

carboxylic acid appeared as an intense band at 1675 cm^{-1}. The band near 1420 cm^{-1} and 1270 cm^{-1} were interpreted as O–H bending and C–O stretching of carboxylic acid group.

Table 5. Characteristic data for the ZnCTrPP compositions

Fractions	Compounds	Yield (%)	Elemental analysis ([a]), %			Formula weight	MS (m/z) $[M-H]^+$
			C	H	N		
1	ZnTPP ($ZnC_{44}H_{28}N_4$)	17.6	75.38 (77.93)	4.13 (4.16)	8.21 (8.26)	678	676
2	ZnCTrPP ($ZnC_{45}H_{28}N_4O_2$)	14.6	77.06 (74.85)	4.15 (3.91)	7.94 (7.76)	722	720, 1465 [b]
3	ZnCTrPP-3 ($ZnC_{47}H_{28}N_4O_6$)	0.9	71.06 [c] (69.68)	4.73 [c] (348)	6.32 [c] (6.92)	810	814

[a] Theoretical values are given in parentheses. [b] The product ions may be formed in dimolecular complex. [c] Mixed hexane in compound.

The yield of fraction 1 was 17.6%. This fraction eluted with 40% dichloromethane in hexane gave the similar R_f value with ZnTPP. Further the fraction was analyzed and confirmed that fraction 1 is ZnTPP. The characteristic data of fraction 1 was shown in Table 5. The mass spectrum, NMR spectra and IR spectrum were shown in appendix B, C and D, respectively. The analyses are in agreement with previous report [43].

Furthermore, the preparation of zinc porphyrins from zinc acetate and CTrPP crude gave the last fraction that eluted with 20% ethyl acetate in dichloromethane. This fraction only yielded 0.9%. Although the mass spectrum shows the parent peak of the ZnCTrPP-3 compound at m/z 813.55, the elemental analysis disagrees with theoretical value of ZnCTrPP-3.

4.3 Characterization of synthesized porphyrins

4.3.1 NMR spectroscopy

The ^{1}H-NMR spectrum was recorded at 400 MHz in $CDCl_3$. The ^{1}H–NMR of all purified free base porphyrins (MeTrPP and their derivatives, CTrPP and their derivatives) have been assigned by a comparison with reported data of TPP, TMePP and TCPP. Furthermore, the synthesized zinc porphyrins were also compared with the ZnTPP, ZnTMePP and ZnTCPP [28, 30, 43, 44]. The data were obtained in $CDCl_3$ solvent at room temperature.

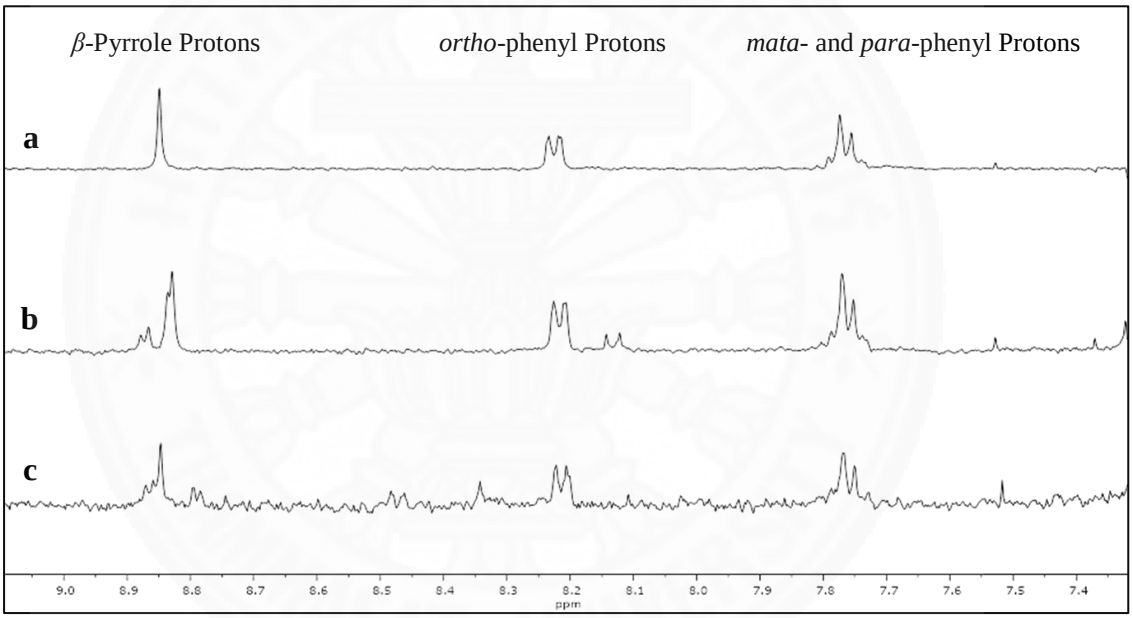

Figure 27. ^{1}H-NMR overlay of the aromatic regions. Solvent peak of $CDCl_3$ at 7.25 ppm. Spectrum: (a) TPP; (b) MeTrPP; (c) CTrPP

The completed ^{1}H-NMR spectra of all synthesized porphyrins is shown in Appendix C, and the overlay of free base porphyrins spectra in the aromatic region is presented in Figure 27. The aromatic protons on the phenyl rings are identified with respect to their positions relative to the porphyrin ring system. The ^{1}H-NMR chemical shifts of all porphyrins are listed in Table 6. The peak appeared in weak field (8.6 - 9.0 ppm) can be generally attributed to the *β*-pyrrole protons as reported in previous work [28, 30].

The two doublet peaks ranges from 7.5-8.5 ppm were found (Figure 27). These peaks are related to the aromatic protons which attached to the phenyl ring. Because of the differences in the chemical environment with substituents on phenyl ring, these peaks appear in two different fields in unsymmetrical porphyrins. The effects due to electron-donating (MeTrPP) and electron-withdrawing (CTrPP) groups are readily apparent within the set of *para*-substituted porphyrins. The electron-donating groups in MeTrPP (substituents on phenyl ring is $-OCH_3$) cause the protons in the substituted phenyl ring to be more shielded (upfield chemical shifts), whereas electron electron-withdrawing groups at the *para* site (substituents on phenyl ring is CO_2H) result in decreased shielding (downfield chemical shifts) [45].

Moreover, the chemical shift of *para*-substituted on phenyl of MeTrPP ($-OCH_3$) and CTrPP ($-CO_2H$) were assigned at 4.10 and 11.98 ppm. The singlet N–H peaks are found at very high field (-2.76 ppm), since they are located within the shielding central hole of the porphyrin ring. The results are in agreement with the previous reported by Wang *et al.* [28] and Furuta *et al*. [30]. For the metalloporphyrins, the ^{1}H-NMR spectroscopy show the absent of the N-H proton. The others protons found similar to free base ligand.

Table 6. ^{1}H−NMR spectral data of synthesized porphyrins

Compound	chemical shift/ppm							
	***β*−pyrrole near substituted phenyl**	***β*−pyrrole near phenyl**	***ortho*-phenyl**	***ortho*-substituted phenyl**	***meta* and *para*-phenyl**	***meta*-substituted phenyl**	**−OCH_3**	**−CO_2H**
TPP	-	8.84	8.22	-	7.76	-	-	-
MeTrPP	8.88	8.84	8.21	8.13	7.76	7.29	4.10	-
MeTrPP−2	8.88 – 8.86	8.83 – 8.82	8.21	8.13	7.76	7.29	4.10	-
TMePP	8.86	-	-	8.12	-	7.29	4.10	-
CTrPP	8.79	8.87 – 8.85	8.21	8.34	7.76	8.47	-	11.98
ZnTPP	-	8.94	8.22	-	7.76	-	-	-
ZnMeTrPP	8.98	8.94	8.22	8.13	7.76	7.30	4.11	-
ZnMeTrPP-2	8.98	8.93	8.22	8.13	7.75	7.29	4.11	-
ZnMeTrPP-3	8.98	8.93	8.22	8.13	7.77-7.74	7.30	4.11	-
ZnCTrPP	8.91	9.01 – 8.98	8.25	8.37	7.79	8.52	-	11.98

4.3.2 UV-Vis spectroscopy

The UV–Vis absorption of free base porphyrins and their zinc complexes, which were recorded from 350 to 700 nm, are shown in Table 7. The intensity and color of porphyrins were derived from the highly conjugated π-electron systems. The UV-vis spectra of porphyrins patterns were consisted with two regions, in the near ultraviolet (Soret band) and in the visible regions (Q bands). The absorption bands in porphyrin systems arise from transitions between two HOMOs and two LUMOs of the ring [5].

The spectra of the free base porphyrins TPP, MeTrPP, MeTrPP-2 and TMePP showed the significant characteristics of an extreme intense Soret band and a set of four Q bands. The results of absorption for free base porphyrins are in agreement with the previous reported [39, 46]. The MeTrPP is the representative example for all free base ligand as shown in Figure 28.

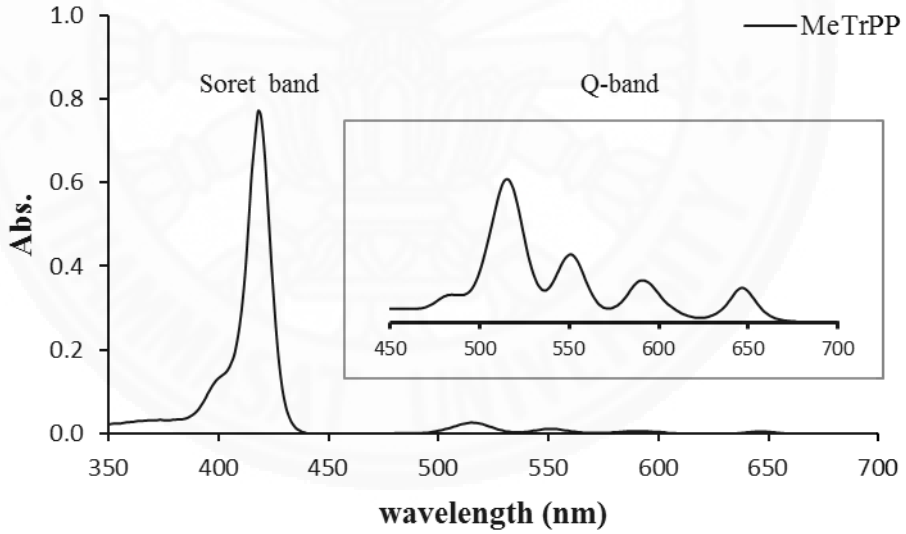

Figure 28. UV-vis spectrum of MeTrPP in dichloromethane

The absorption spectrum of CTrPP in the current work was obtained the maximum of the one Soret band at 417 nm and three Q-bands in the visible region 510, 548 and 586 nm, respectively. From the previous work by Fagadar *et al.* [41], the additional weak band at 647 nm was reported.

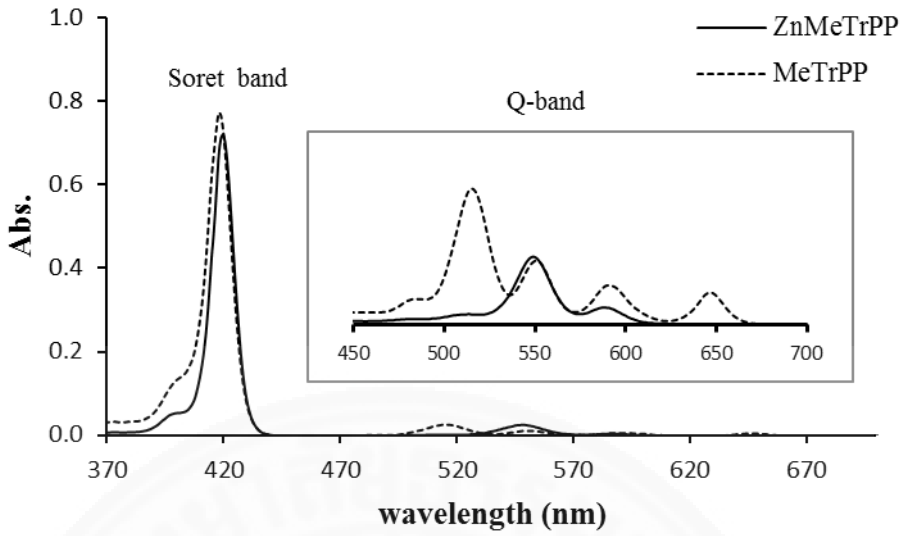

Figure 29. UV-vis spectra of MeTrPP in dichloromethane

The Figure 29 revealed the insertion of metal ion into the central macrocycle molecule. The UV-vis spectra showed different patterns depend on metal center. The zinc complexes showed one S-band and two Q-bands. Except for ZnTMePP, the complex was found one S-band and three Q-bands. When the zinc ion was inserted into the porphyrin ring and then coordinated with four N atoms, the zinc ion located in the center of the porphyrin ring to form the zinc porphyrin complexes. Then the number and intensity of the Q bands decreased and the Soret band occurred slightly red shift (e.g. MeTrPP to ZnMeTrPP, from 416 nm red shift to 420 nm), which is the characteristics pattern of zinc porphyrin compounds [47].

Table 7. UV-vis and fluorescence data of free base porphyrins and zinc porphyrins

Compounds	Absorption					Fluorescence	
	Soret band	Q band (nm)				Excitation	Emission
	(nm)	IV	III	II	I	(nm)	(nm)
TPP	417	514	549	590	647	530	650, 711
MeTrPP	418	515	551	591	646	530	650, 713
MeTTrPP-2	420	516	552	591	647	530	650, 713
TMePP	422	519	555	594	650	530	655, 715
CTrPP	417	510	548	586	-	530	650, 712
ZnTPP	419	-	548	585	-	570	593, 640
ZnMeTrPP	420	-	549	588	-	570	595, 640
ZnMeTrPP-2	421	-	548	586	-	570	596, 641
ZnTMePP	423	-	551	591	651	570	601, 651
ZnCTrPP	419	-	548	586	-	570	597, 641

* All solution were prepared in the concentration of $1x10^{-5}$ mol/L, (n=3, 5RSD≤1.6).

4.3.3 Fluorescence spectroscopy

Porphyrins are known for their interesting emission properties. Many special applications of these systems are based on such emission properties. The fluorescence spectroscopy was study by observing the emission spectra when excited in specific wavelength, related to the first Q-band of absorption spectra. The fluorescence emission data of free base porphyrins and zinc porphyrins as shown in Table 7 were recorded in dichloromethane.

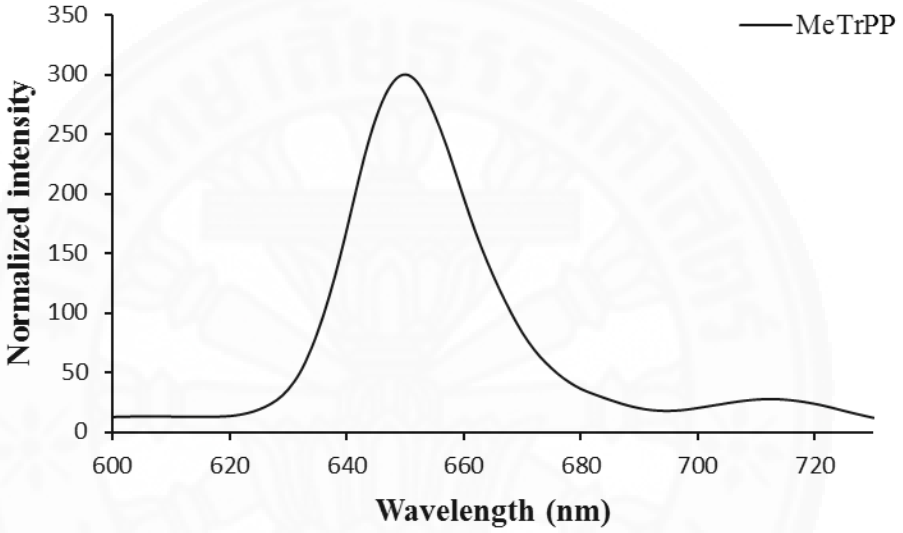

Figure 30. The emission spectrum of MeTrPP in dichloromethane

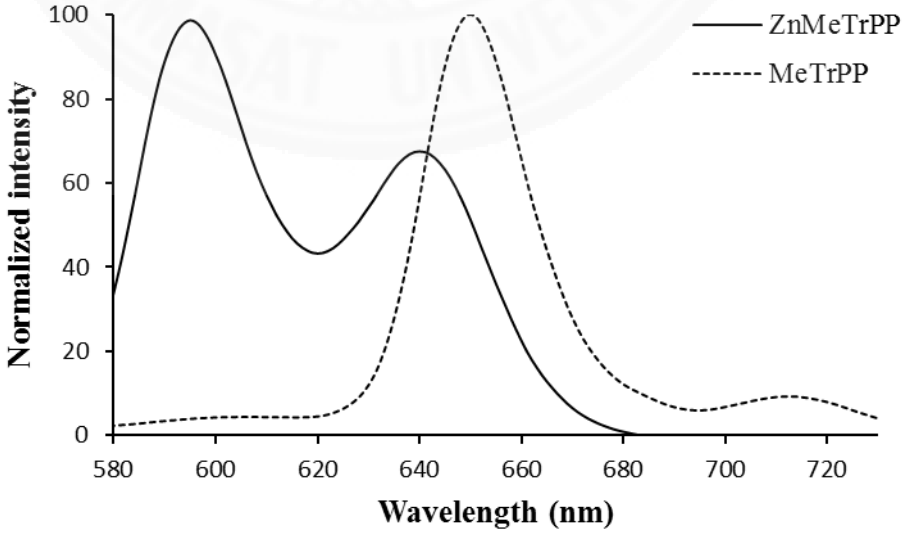

Figure 31. The blue shifted emission spectrum of ZnMeTrPP comparing with MeTrPP in dichloromethane

The emission of porphyrin shows two peaks, one strong peak at 650 – 655 nm and a weaker free base at 711 – 715 nm, similar to free base porphyrins in another work [42, 47]. The MeTrPP is the representative example for all free base ligand as shown in Figure 30. When adding the metal ion, the emission of zinc porphyrins had two emission wavelengths due to the transition state of the metal [48]. In ZnMeTrPP emission, there were two well defined emission bands at 595 nm and 640 nm. The emission wavelengths of zinc porphyrins were blue shifted from their free base ligands as shown in Figure 31.

The emission wavelength of the one peripheral substituent position porphyrins (MeTrPP and CTrPP) was similar as TPP, while TMePP was a little shift (5 nm) to the red and TCPP was a little shift (2 nm) to the blue when comparing with TPP. The peripheral substituent may influence the emission wavelength. The adding metal ion causes the shift of emission wavelength.

When comparing to previous reported work [50], they chose the Soret band as the excitation wavelength and revealed the strong fluorescence. However, the current work selects the first Q-band as the excitation wavelength, the spectra also showed strong fluorescence intensity. The results indicated that, the synthesized porphyrins have potential to develop in fluorescent sensor application.

4.3.4 Thermal gravimetric analysis (TGA)

The synthesized free base porphyrins and their zinc complexes were determined the decomposition temperature by the thermogravimetric measurements, TGA under a nitrogen flow, in range 30–700℃. The results of thermogravimetric analysis were shown in table 8 and the plotted graph of MeTrPP and CTrPP were shown in Figure 32. MeTrPP-2 shows two-step weight loss that may represent the elimination of small molecular impurity, which MeTrPP and CTrPP had one step curve. The weight loss of MeTrPP and CTrPP was detected at 445℃ and 450℃, respectively. The carboxylic group on CTrPP may slightly have H-bond to stabilize the molecule. The asymmetrical free base porphyrins, its steric hindrance may cause the less thermal stability, comparing with TPP (461℃). However, the decomposition temperatures for free base porphyrins were stable up to 400℃, in agreements with the literature [51].

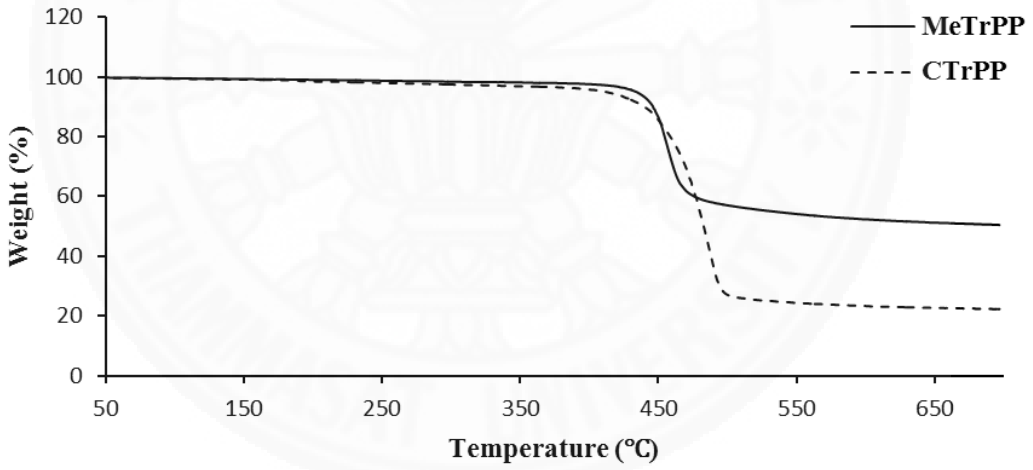

Figure 32. Thermogravimetric analysis (TGA) curves of MeTrPP and CTrPP

The higher thermal stability was found in ZnMeTrPP (465℃) and ZnCTrPP (485℃). ZnMeTrPP exhibited only one step similarly thermal decomposition process to the free base porphyrins. Whereas, the TGA curves of ZnCTrPP was showed two-step weight loss that may represent the elimination of small molecular impurity. The initial decomposition temperature (181℃) was revealed the 3.38% weight loss (expected to be trace of solvent) and observed the major stage decomposition temperature at 478℃.

Table 8. Temperatures of decomposition of porphyrins and their zinc complexes

Compound	Decomposition			
	I		II	
	T_d (℃)	Weigth loss (%)	T_d (℃)	Weigth loss (%)
TPP	-	-	461	54.70
MeTrPP	-	-	445	49.50
MeTrPP-2	175 [a]	4.80	432	50.70
CTrPP	-	-	450	77.63
ZnTPP	192 [a]	5.46	478	75.06
ZnMeTrPP	-	-	457	31.80
ZnMeTrPP-2	-	-	455	26.10
ZnCTrPP	181[a]	3.38	478	53.23

T_d: decomposition temperature; [a] expected to be trace of solvent.

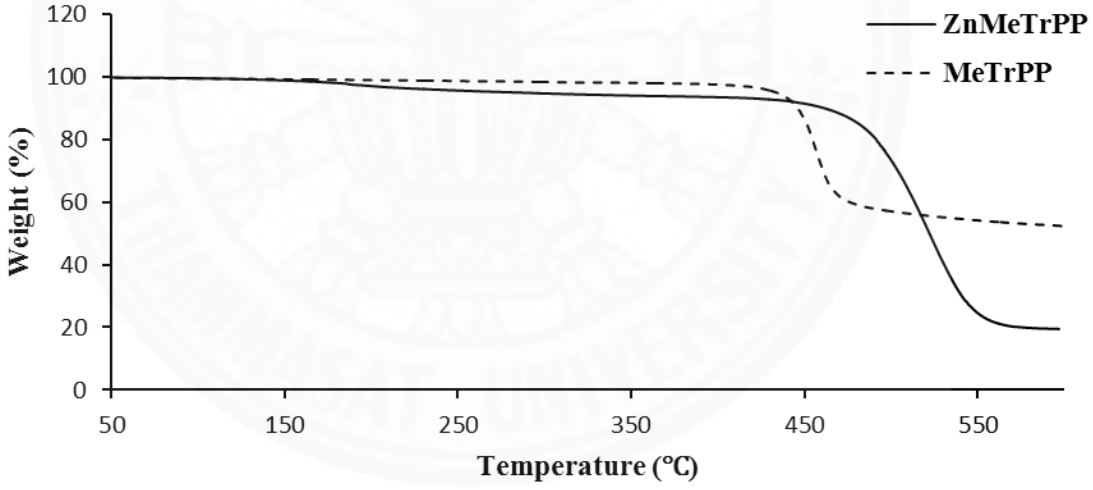

Figure 33. Thermogravimetric analysis (TGA) curves of MeTrPP and ZnMeTrPP

Moreover, thermogravimetric analyses found that the thermal stability of zinc complexes was higher than pure ligand as shown in the Figure 33. The greater the thermal stability may be related to the bond between metal ion and ligand in complexes. The TGA of compounds are confirm the stability in the chamber for the coating process in alternative energy section of solar cell and be a good choice in many applications.

4.3.5 X-ray crystal structure

The violet crystals of the ZnMeTrPP complex were obtained by liquid-liquid diffusion of dichloromethane solvent to a porphyrin solution in methanol. The molecular structure of ZnMeTrPP, with 50% probability displacement ellipsoids, is shown in figure 34. The refinement details and structural parameters are summarized in Table 9. The selected bond lengths and angles of ZnMeTrPP complex is also incorporated in Table 10.

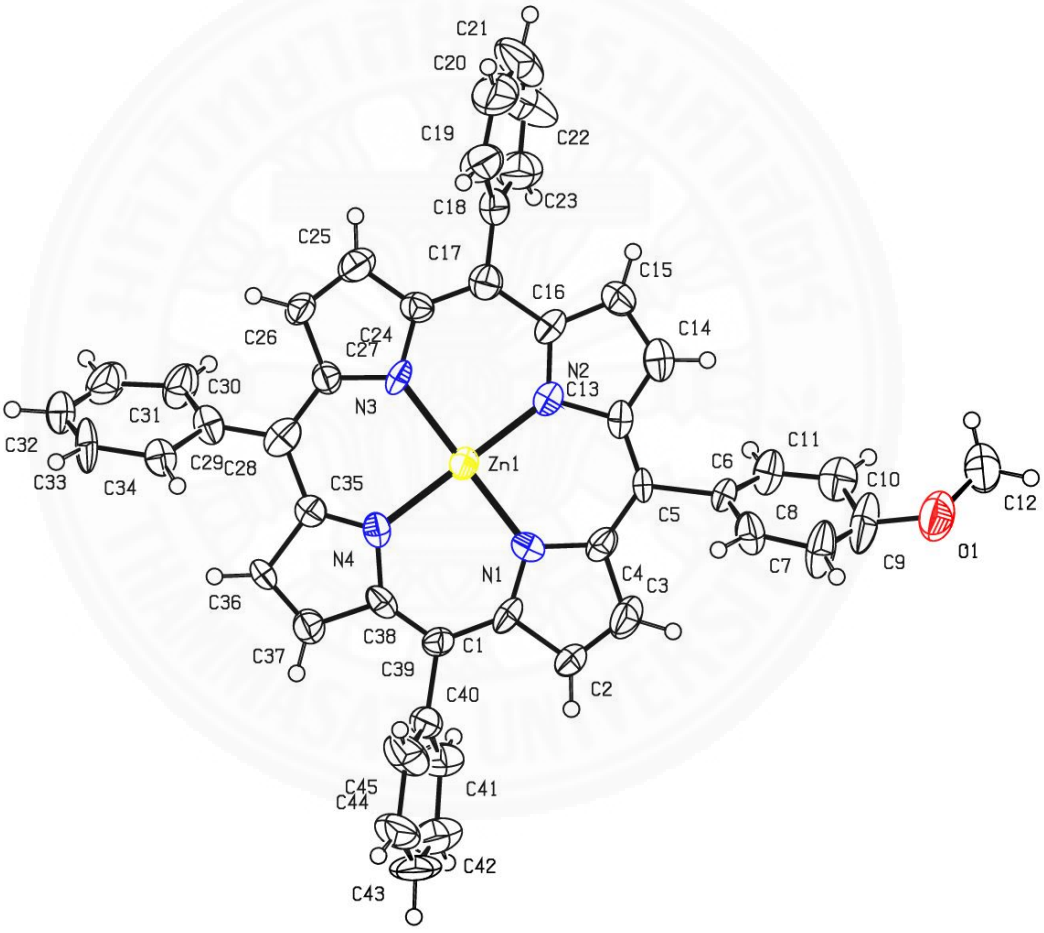

Figure 34. The molecular structure of ZnMeTrPP with 50% probability displacement ellipsoids

Table 9. Crystallographic data of ZnMeTrPP

Crystal data	
Empirical formula	$ZnC_{45}H_{30}N_4O$
Formula weight	708.10
Temperature/K	273 (2)
Crystal system	Triclinic
Space group	P1
a/Å	6.543 (2)
b/Å	10.451 (3)
c/Å	13.170 (4)
α/°	88.466(11)
β/°	77.366(10)
γ/°	8.913(11)
Volume/Å^3	862.2(5)
Z	1
$D_{(calc)}$	1.364
Radiation	Mo K_α (λ = 0.71073)
μ/mm^{-1}	0.755
F(0 0 0)	366
No. of reflections collected	16604
No. of independent reflections	7480 [R_{int} = 0.0240, R_{sigma} = 0.0355]
θ range for data collection	3.25 to 27.88
Goodness-of-fit on F^2	1.055
R indices [I > 2σ(I)]: R1	R_1 = 0.0504, ωR_2 = 0.1281
R indices (all data): R1	R_1 = 0.0655, ωR_2 = 0.1401

Table 10. The selected bond lengths and angles of the ZnMeTrPP complex

Bond lengths (*Å*)		Bond angles (°)	
Zn–N(1)	2.001 (7)	N(1)–Zn–N(2)	89.6 (3)
Zn–N(2)	2.023 (7)	N(2)–Zn–N(4)	178.8 (3)
Zn–N(3)	2.051 (6)	N(4)–Zn–N(3)	90.0 (2)
Zn–N(4)	2.080 (6)	N(3)–Zn–N(1)	179.6 (3)
Zn–C(5)	3.467 (9)	N(2)–Zn–N(3)	90.0 (3)
Zn–C(17)	3.467 (9)	N(1)–Zn–N(4)	90.4 (3)
Zn–C(39)	3.419 (8)		
Zn–C(28)	3.483 (8)		

The skeletal framework of the ZnMeTrPP molecule is illustrated in Figure 34. This complex was crystallized in the triclinic space group P1 with the following unit-cell parameters: a = 6.543 (2) Å, b = 10.451 (3) Å, c = 13.170 (4) Å, α = 88.466 (11) °, β = 77.366 (10) °, γ = 78.913 (11) °, V = 862.2 (5) $Å^3$ and Z = 1. It reveals the asymmetrical unit that contains one zinc atom and one porphyrin ligand. The coordination geometry of the zinc atom can be described as a square planar consisting of four nitrogen atoms from the porphyrin molecule. The zinc ion is situated 0.012 Å slightly above the basal plane defined by the four nitrogen atoms. The four different zinc–nitrogen bond lengths in the basal plane lie within a range of 2.001 to 2.080 Å. This difference has been reflected as a difference of the type of peripheral substituted, whereas the average zinc–nitrogen distance (2.039 Å) and N–Zn–N angles (90°, 179.2°) in ZnMeTrPP is similar to the privious reported for four coordinated ZnTPP (2.037 Å, 90° and) [54]. Upon examination, the phenyl rings are almost planar and are oriented almost perpendicular to the porphyrin core at an angle of 59.28°–71.55°. The peripheral methoxy groups may cause the deviation from the perpendicular of the porphyrin ring.

CHAPTER 5
CONCLUSIONS AND RECOMMENDATIONS

5.1 Conclusions

In this study, the unsymmetrical-*meso*-substituted porphyrins were attempted to synthesis via modified conventional Adler-Longo method by using pyrrole and a mixture of two different aldehydes with a fix molar ratio. The controlled conditions for this synthesis were including the molar ratio of pyrrole, benzaldehyde, and substituted aldehyde as 4:3:1, respectively, the condensation temperature (110℃), propionic acid catalyst (50 mL) and reaction time (1.5 hours). After purification, the reaction yield free base porphyrins, MeTrPP (11.5%) and CTrPP (3.7%). The attempts had tried on preparation of OTrPP and HTrPP, but gave unsuccessful products (tarry oil).

The molar ratio of pyrrole, benzaldehyde, and substituted aldehyde, 4:3:1 gave a mixture of mono-, di-, tri- and tetrasubstituted porphyrins, monitored by mass spectrometry. Further silica gel column chromatography was required for purification. The characterization confirmed the expected product with the present of a dimolecular compound.

The metallation of Zn^{2+} in the central hole porphyrins was performed under heating refluxed of free base porphyrins with Zinc acetate in DMF for 6 hours. The successful purified zinc complex yield ZnMeTrPPP and ZnCTrPP at 29.8 and 14.6%, respectively.

The structure of all compounds was confirmed by mass spectrum, the elemental analysis (CHN), ^{1}H-NMR, FT-IR spectroscopy and UV-vis spectroscopy, which in agreement with the expected value and the previous reports.

All free base porphyrins and complexes were attempted to grow the crystals in dichloromethane/hexane. However, the only ZnMeTrPP crystal was qualified for X-ray diffraction. The results confirmed the expected product (ZnMeTrPP) with four-coordination geometry of zinc and nitrogen atom in central hole of porphyrins. However, further refinement is required to gain more details.

The purple micro crystals of all synthesized compounds showed strong Soret band (S-band, 417-422 nm) and a set of weak four Q-bands, ranged from 510-650 nm, characteristic signature for free base porphyrins. The insertion of zinc ion (Zn^{2+}) into the central macrocycle molecule shows one S-band and two Q-bands.

The fluorescence spectra (excitation at 530 nm for free base ligands and 570 nm for zinc-porphyrins) show emission bands at 650-713 nm for free base ligand. When adding the metal ion, there were two well defined emission bands at 595-641 nm: The emission wavelengths of zinc-porphyrins were blue shifted from their free base; due to the electronic effect of substituent.

The weight loss of CTrPP and MeTrPP was detected at 450℃ and 445℃, respectively. The carboxylic group on CTrPP may slightly have H-bond to stabilize the molecule. However, the asymmetrical free base porphyrins and its steric hindrance may cause the less thermal stability, comparing with TPP (461℃). The higher thermal stability was found in ZnMeTrPP (465℃) and ZnCTrPP (485℃). The greater thermal stability may be related to the bond between metal ion and ligand in complexes. The TGA of compounds are confirm the stability in the chamber for the coating process in alternative energy section of solar cell and be a good choice in many applications.

5.2 Future work

In order to the present of mono and dimolecular compound,

1. The further purification technique may require.
2. The variation solvent system in column chromatography need for differentiate the solubility of the mono and dimolecular mixture.
3. The various metallation adding into the central hole may help separate the mixture.

In order to comparison of free base porphyrins and complexes,

1. The crystal growths for comparable compound are required.
2. The various special crystal growth techniques may worth to try on growing crystals.
3. The selection high quality crystal without impurity coating is needed prior X-ray diffraction analysis.

In order to understand the unsuccessful reaction,

1. The characterization of tarry oil may give more information.
2. The various extreme reaction conditions may need to apply on the unsuccessful reaction.

REFERENCES

1. Markham C, Manglik A, Castillo K, Mao K, Frey R. Hemoglobin and the Heme Group: Metal Complexes in the Blood for Oxygen Transport. Washington University. 2007.

2. Wikipedia [Internet]. Heme, [cited 2014 Sep 13]. Available from: http://en.wikipedia.org/wiki/Heme.

3. U.S. National library of medicine [Internet]. Vitamin B12, [cited 2014 Sep 13]. Available from: http://www.nlm.nih.gov/medlineplus/druginfo/natural/patient-vitaminb12.html.

4. Wikipedia [Internet]. Chlorophyll, [cited 2014 Sep 13]. Available from: https://en.wikipedia.org/wiki/Chlorophyll.

5. Gouterman M. Spectra of Porphyrins. Journal of Molecular Spectroscopy. 1961; 6: 138–163.

6. Gouterman M, Wagniere G, Snyder L. Spectra of Porphyrins part II: Four orbital model. Journal of Molecular Spectroscopy. 1963;11: 108–127.

7. Kalyanasundaram K. Photochemistry of Polypyridine and Porphyrin Complexes. Academic Press, San Diego, CA. 1992.

8. Song Y, Haddad R, Jia SL, Hok S, Olmstead M, Nurco D, Schore N, Zhang J, Ma J, Smith K, Gazeau S, Pécaut J, Marchon J, Medforth C, Shelnutt J. Energetics and Structural Consequences of Axial Ligand Coordination in Nonplanar Nickel Porphyrins. Journal of the American Chemical Society. 2005;127: 1179-1192.

9. Retsek J, Drain C, Kirmaier C, Nurco D, Medforth C, Smith K, Sazanovich I, Chirvony V, Fajer J, Holten D. Photoinduced Axial Ligation and Deligation Dynamics of Nonplanar Nickel Dodecaarylporphyrins. Journal of the American Chemical Society. 2003;125: 9787-9800.

10. A xylem brand [Internet]. Chlorophyll, [cited 2014 Sep 13]. Available from: https://www.ysi.com/parameters/more-parameters/chlorophyll?Chlorophyll-6.

11. Vicente M, Smith K. M. Porphyrins and Derivatives Synthetic Strategies and Reactivity Profiles. Current Organic Chemistry. 2000;4(36): 139-174.

12. Arsenault G.P, Bullock E, MacDonald S.F. Pyrromethanes and Porphyrins Therefrom. Journal of the American Chemical Society. 1960;82(16): 4384-4389.

13. Rothemund P. Formation of Porphyrins from Pyrrole and Aldehydes. Journal of the American Chemical Society. 1935;57(10): 2010-2011.

14. Adler A.D, Longo F.R, Finarelli J.D, Goldmacher J, Assour J, Korsakoff L. A simplified synthesis for meso-tetraphenylporphine. The Journal of Organic Chemistry. 1967;32(2): 476-476.

15. Lindsey J.S, Hsu H.C, Schreiman I.C. Synthesis of tetraphenylporphyrins under very mild conditions. Tetrahedron Lett. 1986;27(41): 4969-4970.

16. Kruper W.J, Chamberlin T.A, Kochanny M. Regiospecific aryl nitration of meso-substituted tetraarylporphyrins: a simple route to bifunctional porphyrins. The Journal of Organic Chemistry. 1989;54: 2753-2756.

17 Meng G.G, James B.R, Skov K.A. Porphyrin chemistry pertaining to the design of anticancer drugs; part 1, the synthesis of porphyrins containing meso-pyridyl and mesosubstituted phenyl functional groups. Canadian Journal of Chemistry. 1994;72(12): 2447-2457.

18. Luguyaa R, Jaquinoda L, Fronczek F.R, Vicente M.G.H, Smith K.M. Synthesis and reactions of meso-(*p*-nitrophenyl)porphyrins. Tetrahedron. 2004;60: 2757-2763.

19. Hollingsworth J.(2012) Synthesis, characterization, and self-assembly of porphyrins conjugated to superparamagnetic colloidal particles for enhanced photodynamic therapy. (Doctoral dissertation). Louisiana State University Department of Chemistry.

20. Gust D, Moore T.A, Moore A.L. Mimicking photosynthetic solar energy transduction. Accounts of Chemical Research. 2001;34: 40–48.

21. Ochsner M. Photophysical and photobiological processes in the photodynamic therapy of tumours. Journal of Photochemistry and Photobiology B: Biology. 1997;39: 1–18.

22. Chou J.H, Kosal M.E, Nalwa H.S, Rakow N.A, Suslick K.S. Applications of porphyrins and metalloporphyrins to materials chemistry, in: K. Kadish, K. Smith, R. Guillard (Eds.), The Porphyrin Handbook, Academic Press, New York. 2000: 43–141.

23. Pavinatto F.J, Gameiro A.F, Hidalgo A.A, Dinelli L.R, Romualdo L.L, Batista A.A, Barbosa Neto N.M, Ferreira M, Oliveira O.N. Langmuir and Langmuir–Blodgett

(LB) films of tetrapyridyl metalloporphyrins. Applied Surface Science. 2008; 254(18): 5946–5952.

24. O'Regan B, Grätzel M. A low-cost, high-efficiency solar cell based on dye-sensitized colloidal TiO_2 films. Nature. 1991;353: 737−740.

25. Cavaleiro J, Smith K.M. Porphyrin Synthesis. Revista portuguesa de química. 1989;31: 29-41.

26. Milanesio E, Chiacchiera S.M, Silber J.J, Durantini E.N. Synthesis of Asymmetrical Porphyrins Substituted in the meso-Position from Dipyrrolomethanes. Molecules. 2000;5: 531-532.

27. Débora L, Edgardo D. Synthesis of *meso*-substituted cationic porphyrins as potential photodynamic agents. Archive for Organic Chemistry. 2003:227-239.

28. Koiry S.P, Aswal D.K, Chauhan A.K, Saxena V, Nayak S.K, Gupta S.K, Yakhmi J.V. Electrical bistability in electrografted 5-(4-undecenyloxyphenyl)-10,15,20-triphenylporphyrin monolayer on Si. Chemical Physics Letters. 2008;453: 68–72.

29. Wang Y, Jiang P, Zhang W, Zheng J. 15-(4-Carboxyphenyl)-10,15,20-triphenylporphyrin manganese(III) chloride grafted on magnetic polyglycidyl methacrylate as biomimetic catalyst and their catalytic activity. Applied Surface Science. 2013;270: 531– 538.

30. Marcin R, Piotr K, Patrycja K, Marta K. The synthesis of new potential photosensitizers [1]. Part 2.Tetrakis-(hydroxyphenyl)porphyrins with long alkyl chain in the molecule. Dyes and Pigments. 2013;99: 627–635.

31. Furuta N, Mizutani T. Tris(3-hydroxypropyl)methyl as a stable linker for porphyrin monolayer on silicate glass. Thin Solid Films. 2014;556: 174–185.

32. Skrzypek D, Madejsk I, Habdas J. The characterization of cobalt(II) derivatives of selected substituted meso-tetraphenyl and tetrapyridyl porphyrins by EPR spectroscopic study. Solid State Sciences. 2007;9: 295–302.

33. Yang Q, Streb K.K, Borhan B. Polymer-supported synthesis of mono-substituted porphyrins. Tetrahedron Letters. 2005;46: 6737–6740.

34. Ana M, Antonio T, Cláudio R.N, Maria E.F.G, Osvaldo A.S, Yassuko I. Synthesis, Spectroscopy and Photosensitizing Properties of Hydroxynitrophenyl porphyrins. Journal of the Brazilian Chemical Society. 2004;15(5): 708-713.

35. Xiang N, Huang X, Feng X, Liu Y, Zhao B, Deng L, Shen P, Fei J, Tan S. The structural modification of thiophene-linked porphyrin sensitizers for dye-sensitized solar cells. Dyes and Pigments. 2011;88: 75-83.

36. Marco A.S, Lidia S.I, Antônio G.F, Yassuko I, Maria Z, Marilda D. Synthesis and Characterization of a Novel Series of Meso (Nitrophenyl) and Meso (CarboxyPhenyl) Substituted Porphyrins. Journal of the Brazilian Chemical Society. 2000;11(5) 458-466.

37. Aaron S.H, Chandra B.KC, Habtom B.G, Lindsey R.S, Francis D. Porphyrin-Sensitized Solar Cells: Effect of Carboxyl Anchor Group Orientation on the Cell Performance. ACS Applied Materials & Interfaces. 2013;5: 5314−5323.

38. Syeda Z, Robert S.L, Brad A.C, Marc J.J, Jonathan S.L. Nearly Chromatography-Free Synthesis of the A_3B-Porphyrin 5-(4-Hydroxymethylphenyl)-10,15,20-tri-p-tolylporphinatozinc(II) Organic Process Research & Development. 2006;10: 304-314.

39. Benjamin B, Faugeras P, Vergnaud J, Lucas R, Teste K, Zerrouki R. Iodine-catalyzed one-pot synthesis of unsymmetrical *meso*-substituted porphyrins. Tetrahedron. 2010;66: 1994–1996.

40. Bandgar B.P, Gujarathi P.B. Synthesis and characterization of new *meso*-substituted unsymmetrical metalloporphyrins. Journal of Chemical Sciences. 2008;120(2): 259–266.

41. Giribabu L, Kumar C, Raghavender M, Somaiah K, Reddya P, Venkateswara P. Functionalized zinc porphyrin as light harvester in dye sensitized solar cells. Journal of Chemical Sciences. 2008;120(5): 455-462.

42. Gomes A. Acid Catalysis in the Way to Porphyrins: Reaction of Pyrrole/Aldehydes in the Synthesis of *meso*-Substituted Porphyrins. Revista Virtual de Química. 2013;5(2): 312-317.

43. Jansaeng K. (2013). Synthesis and Characterization of Metalloporphyrin Derived from Co, Ni, Cu, Zn. Thammasat University, Faculty of science and technology, Department of chemistry.

44. Webb M, Bampos N. Electronic Supplementary Information Noncovalent interactions in acid-porphyrin complexes. Electronic Supplementary Material (ESI) for Chemical Science. 2012.

45. RaeAnne E.F, Larry M.M. Microscale Synthesis and ^{1}H NMR Analysis of Tetraphenylporphyrins. Journal of Chemical Education. 1999;76(2): 237-239.

46. Bruno H.V, Jader L.A, Paulo S.P, Silvia L.F, Katieli C, Adriana P.G, André L.T, Noboru H, Wilker C. Physico-Chemical Properties of *meso*-tetrakis(*p*-methoxyphenyl)porphyrin (TMPP) incorporated into pluronic™ P-123 and F-127 polymeric micelles. Quim. Nova. 2014;37(10): 1650-1656.

47. Zhang G, Chena Q, Zhang Y, Kong L, Tao X, Luc H, Tian Y, Yang J. Bulky group functionalized porphyrin and its Zn (II) complex with high emission in aggregation. Inorganic Chemistry Communications. 2014;46: 85–88.

48. Kang M.S, Oh J.B, Roh S.G, Kim M, Lee J.K, Jin S, Kim H.K. Novel Extended π -Conjugated Dendritic Zn(II)-porphyrin Derivatives for Dye-sensitized Solar Cell Based on Solid Polymeric Electrolyte: Synthesis and Characterization. Korean Chemical Society. 2007;28(1): 33-40.

49. Wu Y, Chen L, Yu J, Tong S, Yan Y. Synthesis and spectroscopic characterization of meso-tetra (Schiff-base substituted phenyl) porphyrins and their zinc complexes. Dyes and Pigments. 2013;97: 423-428.

50. Zabardasti A. (2012). Molecular interactions of some free base porphyrins with σ- and π-acceptor molecules, molecular interactions, Prof. Aurelia Meghea (Ed.), ISBN: 978-953-51-0079-9, In Tech, Available from: http://www.intechopen.com/books/molecular-interactions/molecular-interactions-of-some-free-basesporphyrins-with-sigma-and-pi-acceptor-molecules

51. Gamboa M, Campos M, Torres L.A. Study of the stability of 5,10,15,20-tetraphenylporphine (TPP) and metalloporphyrins NiTPP, CoTPP, CuTPP, and ZnTPP by differential scanning calorimetry and thermogravimetry. The Journal of Chemical Thermodynamics. 2010;42: 666–674.

52. McGill S, Nesterov V.N, Goulda S.L. [5,10,15,20-Tetrakis(4-methoxyphenyl)-porphyrinato]zinc dichloromethane disolvate. Acta Crystallographica Section E: Crystallographic Communications. 2013. E69.

53. Giovannetti R. (2012). The use of spectrophotometry UV-Vis for the study of porphyrins. Macro to Nano Spectroscopy. Available from: http://www.intechopen.com/books/macro-to-nano-spectroscopy/the-use-of-spectrophotometry-uv-vis-for-thestudy-of-porphyrins.

54. Scheidt W.R, Mondal J.U, Eigenbrot C.W, Adler A, Radonovich L.J, Hoard J.L. Crystal and Molecular Structure of the Silver(II) and Zinc(II) Derivatives of *meso* -Tetraphenylporphyrin. An Exploration of Crystal-Packing Effects on Bond Distance. Inorganic Chemistry. 1986;25: 795-799.

APPENDICES

APPENDIX A

General Techniques

Thin Layer Chromatography (TLC)

Thin Layer chromatography (TLC) is one of the most widely used types of chromatography. This technique uses to separate the components of a mixture using a thin stationary phase. The separation is carried out on a flat plate coated with a thin layer of an adsorbent such as silica gel or alumina. Moreover, TLC is important for quick qualitative analysis of mixtures. It may be performed on the analytical scale as a tool of monitoring the progress of the reaction. Furthermore, it is used to determine the operating conditions on the preparative scale column chromatography to purify the compound. TLC is an analytical tool widely used because of its simplicity, relative low cost, high sensitivity, and speed of separation.

Techniques: One way, ascending

Adsorbent: Silica gel 60 GF_{254} pre-coated on aluminum plate, layer thickness 0.20 mm

Detection: UV light at 254 nm

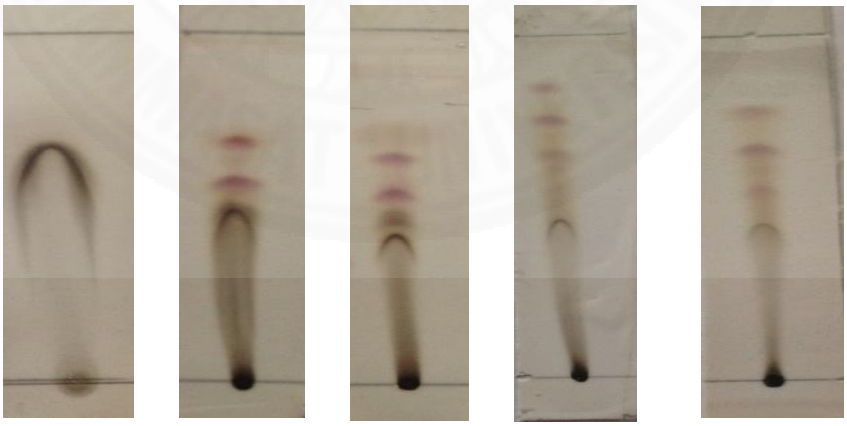

0 hr. 1.0 hr. 1.5 hr. 12 hr. 24 hr.

Figure A1. The TLC plate at during a reaction of porphyrins synthesis

Column Chromatography

Column chromatography is one of the most important chromatographic techniques because it can be used to determine the number of components of a mixture and as well as the separation and purification of the compounds. For the separation, components in the mixture that have different interactions with the stationary and mobile phases will be separated. While the mixture is adsorbed on the stationary phase, it does not move. The soluble component will be carried along with the mobile phase to varying degrees and a separation will be achieved. The mobile phase is a solvent that flows under the influence of gravity through the stationary phase, dissolving the molecules of the component to be separated some of the time. In this work, the wet method was used to prepare a column. The sample was prepared of within the small of silica gel powder which is stationary phase and dissolved in a small amount of appropriate solvent. The eluting solvent changed to a more polarity solvent during the elution process and the composition of each fraction is analyzed by TLC-silica.

Adsorbent:	Silica gel 60 with particle size 0.063-0.200 mm (70-230 mesh ASTM)
Packing:	Slurry packing
Loading:	The sample was dissolved in a small amount of suitable organic solvent, mixed with a small quantity of silica gel, dried under reduce pressure and added gently onto the top of column.
Elution:	After loading of the sample, the column was eluted with suitable solvent system using gradient technique.

Recrystallization

Recrystallization is the primary method for purifying compounds an impure compound in a solvent. The impurities may include some combination of insoluble, soluble, and colored impurities. To obtain a pure compound these impurities must be removed. The method of purification is based on the principle that the solubility of most solids increases with increased temperature. Crystallization is

not the same as precipitation of a solid. In crystallization, there is a slow, selective formation of the crystal framework resulting in a pure compound.

In this technique, an impure solid compound is dissolved in an appropriate solvent. After that, the solution was allowed to slowly crystallize out as the solution cools. The molecules of the other compounds dissolved in solution are excluded from the growing crystal lattice. The compound crystallizes from the solution giving a pure solid.

Infrared (IR) Spectroscopy

Infrared (IR) spectroscopy is one of the most common and widely used spectroscopic techniques because it is very useful in the identification and structure analysis of compounds. It can also be used for both qualitative and quantitative analysis of complex mixtures of similar compounds.IR is used to analyze the presence of functional groups (bond types) in the molecules. It can be very sensitive to determination of functional groups within a sample since different functional group absorbs different particular frequency of IR radiation. Also, each molecule has a characteristic spectrum often referred to as the fingerprint. A molecule can be identified by comparing its absorption peak to a data bank of spectra.

In this work, Infrared spectroscopy spectra (4000-600 cm^{-1}) were performed using a spectrum GX FT-IR spectrometer (Perkin Elmer). Spectra of solid sample were recorded as potassium bromide (KBr) pellets.

Nuclear Magnetic Resonance (NMR) Spectroscopy

NMR spectroscopy is a great tool for determining structures of organic compound. The high resolution 400 MHz ^{1}H-NMR was performed on a BRUKER-NMR 400 MHz spectrometer. Spectra were recorded by using deuterochloroform ($CDCl_3$) and recorded as chemical shift (δ) value in ppm. The following abbreviations are used for multiplicity: s = singlet, brs = broadsinglet, d = doublet, t = triplet, dt = doublet of triplet, dd = doublet of doublet and m = multiplet. Coupling constants (J) are recorded in Hertz (Hz).

For ^{1}H NMR, 5 mg of sample was used characterization. The sample was dissolved in $CDCl_3$ solvent. The solvent level should be about 4.0 cm from the bottom of the tube.

Mass Spectrometry (MS)

The high resolution mass spectra were performed on a Thermo Finnigan mass spectrometer. The mass spectrometer is an analytical chemistry instrument which can measure the masses for identify the amount and type of chemicals present in a sample. It determines the mass of a molecule by measuring the mass-to-charge ratio (m/z). The solution of samples were prepared by dissolved 10 mg of them in appropriate solvent (HPLC grade) and made up to 50 mL.

UV-Visible Spectroscopy

Molecules containing π-electrons or non-bonding electrons can absorb the energy in the form of ultraviolet or visible light to excite these electrons to higher anti-bonding molecular orbitals. Electronic absorption spectra of free base porphyrin and their metal complexes were carried out on a SHIMADSU UV-Vis spectrophotometer using a pair of quartz cells of 10 mm path length at room temperature. For the preparation of 0.1 mM solution, 10 mg of free base porphyrins and metalloporphyrins were dissolved and made up to 100 mL by appropriate solvent in volumetric flask.

Fluorescence Spectroscopy

Fluorescence spectroscopy measures the intensity of photons emitted from a sample after it has absorbed photons. In this technique, a sample is probed using an excitation of a specific wavelength and the fluorescence emission is detected. The same prepared sample from UV-Visible spectroscopy was used to analyze for fluorescence spectroscopy. Emission spectra of porphyrins were measured by a Jasco FP-6200 spectrofluorometer at room temperature.

Elemental analysis

Elemental analysis is a useful qualitative analysis technique. This technique is an experiment that determines the amount (typically a weight percent) of an element in a compound. The common type of elemental analysis is for carbon, hydrogen, and nitrogen (CHN analysis). This type of analysis is especially useful for organic compounds (compounds containing carbon-carbon bonds). The elemental analysis of a compound enables one to determine the empirical formula of the compound. Elemental analysis of the samples was performed on a Perkin Elmer CHNO/S analyzer model 2400 series.

Thermogravimetric Analysis (TGA)

Thermogravimetric analysis is a technique that measures the amount of weight change of a material, either as a function of increasing temperature, or isothermally as a function of time, in an atmosphere of nitrogen, helium, air, other gas, or in vacuum. In this work, the thermal analysis was performed by Perkin Elmer TGA-7. The dye of samples about 10 mg were used and heated in range 25℃ to 700℃ under nitrogen flow with scan rate 20℃ per minute.

APPENDIX B

Mass Spectra

Mass Spectra of free base porphyrins

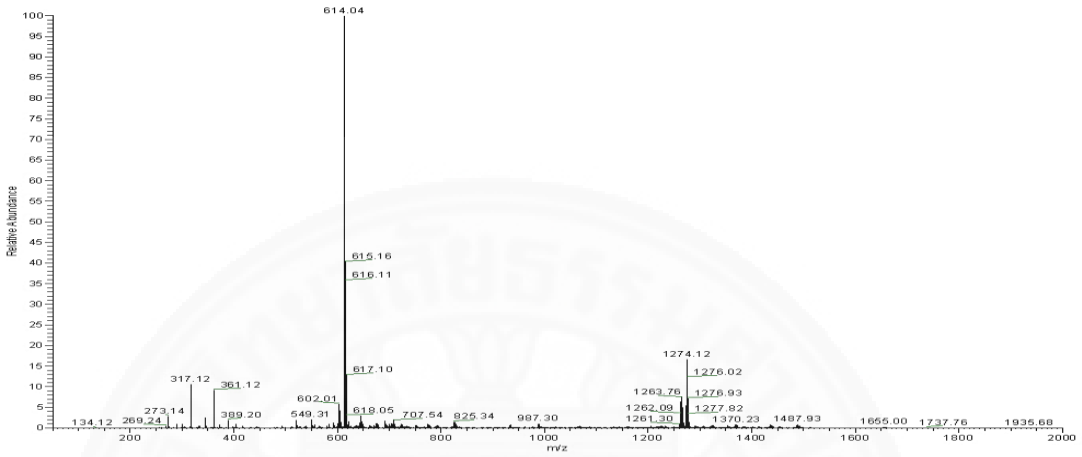

Figure B1. Mass spectrum of TPP from MeTrPP crude in dichloromethane

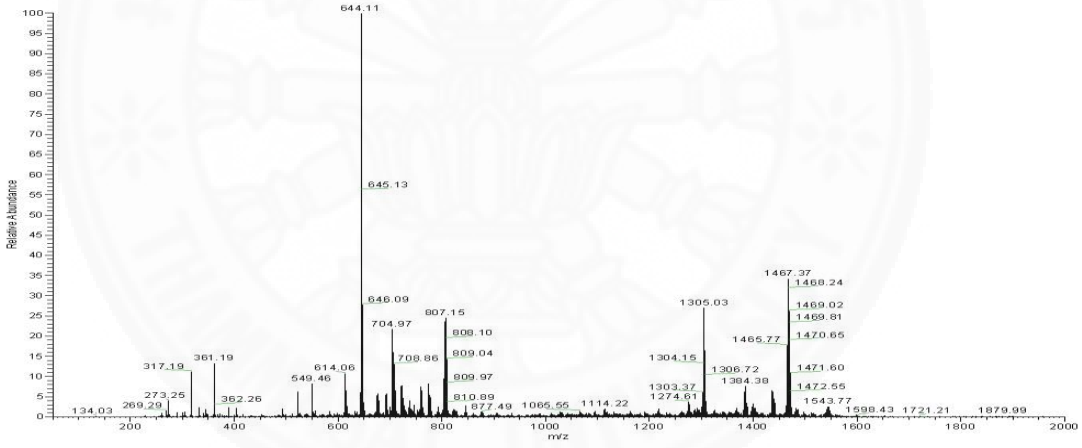

Figure B2. Mass spectrum of MeTrPP in dichloromethane

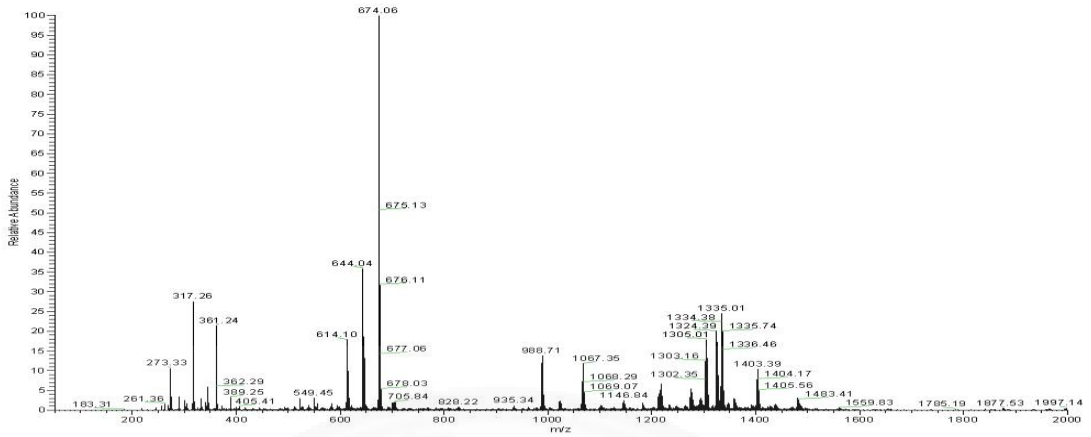

Figure B3. Mass spectrum of MeTrPP-2 in dichloromethane

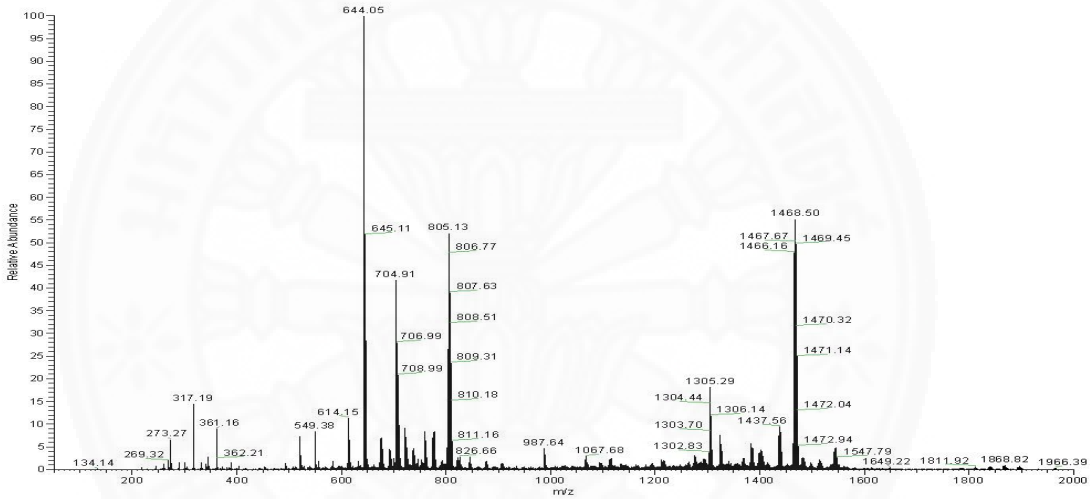

Figure B4. Mass spectrum of MeTrPP-3 in dichloromethane

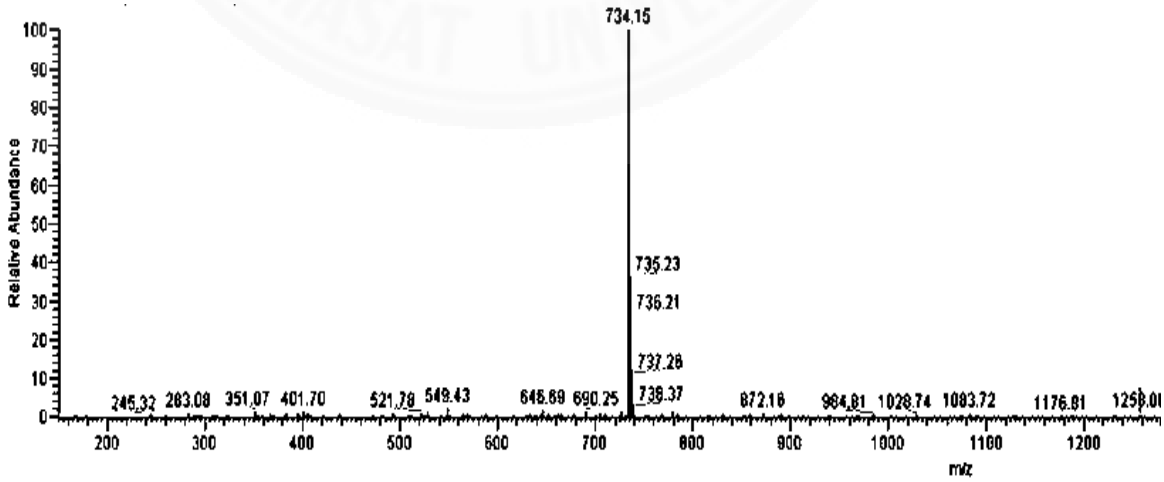

Figure B5. Mass spectrum of TMePP in dichloromethane

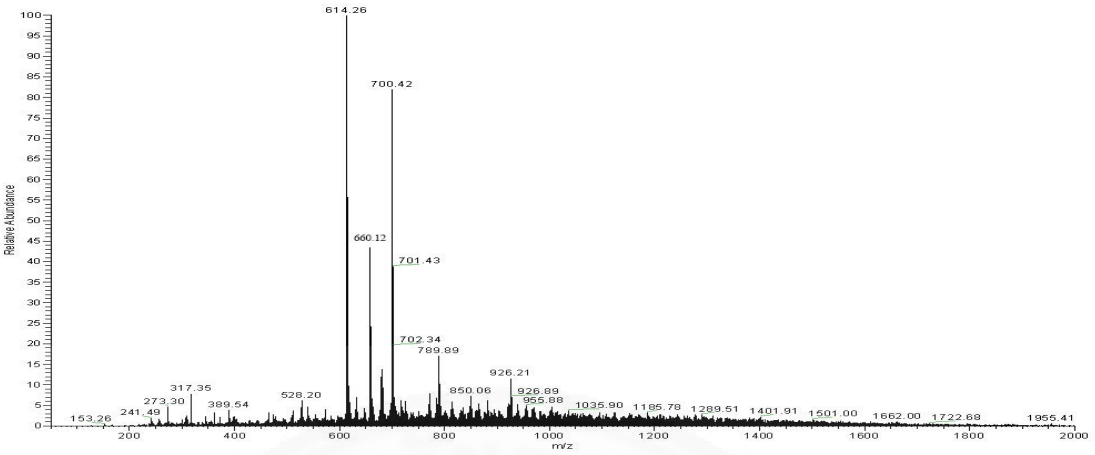

Figure B6. Mass spectrum of CTrPP crude in dichloromethane

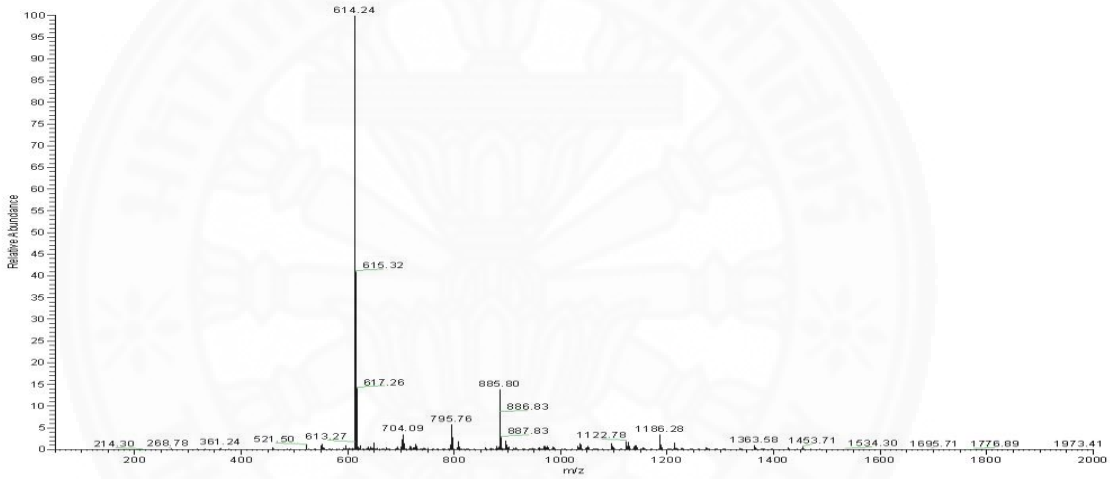

Figure B7. Mass spectrum of TPP from CTrPP crude in dichloromethane

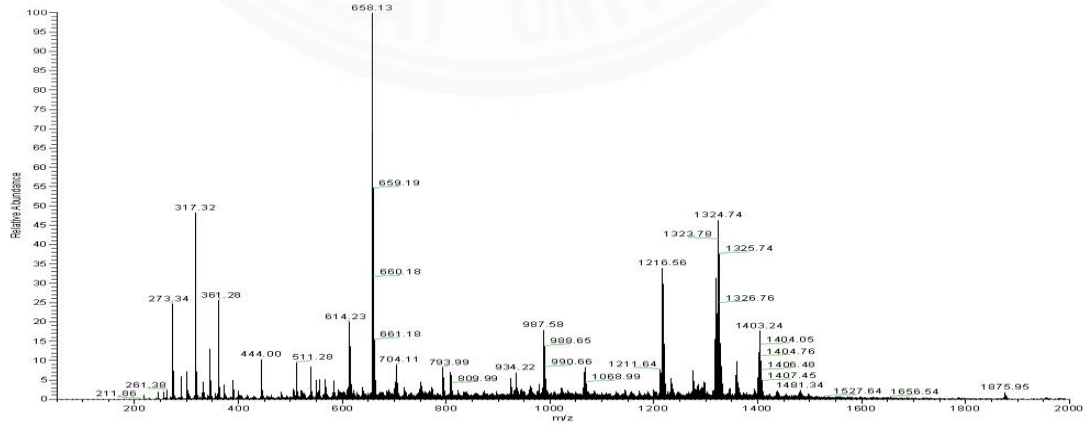

Figure B8. Mass spectrum of CTrPP in dichloromethane

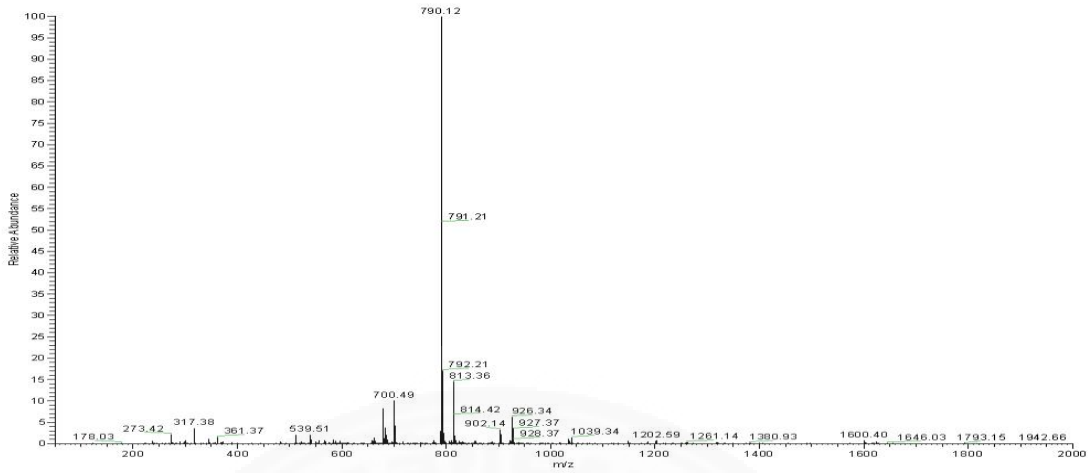

Figure B9. Mass spectrum of TCPP in dichloromethane

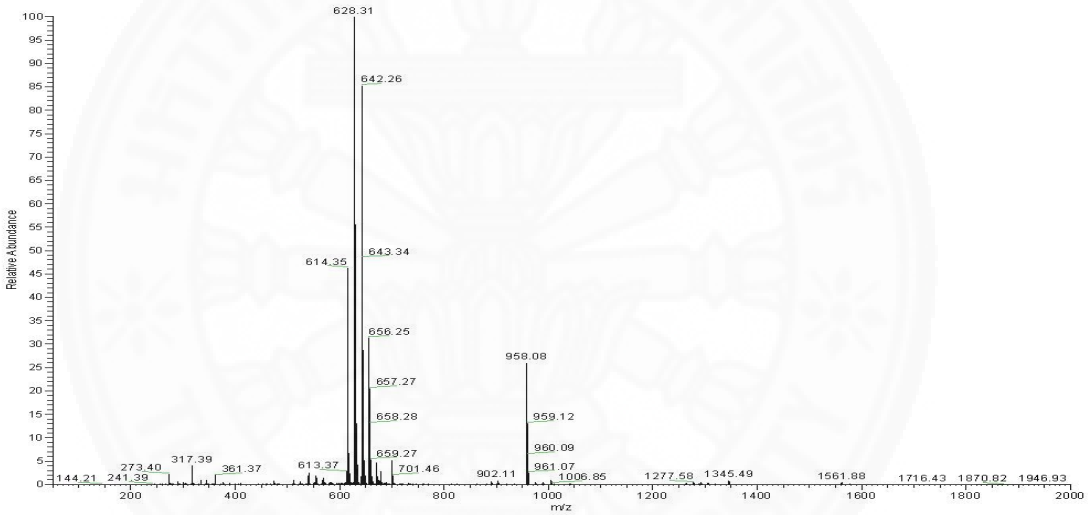

Figure B10. Mass spectrum of MTrPP in dichloromethane

Mass Spectra of Zinc-porphyrins

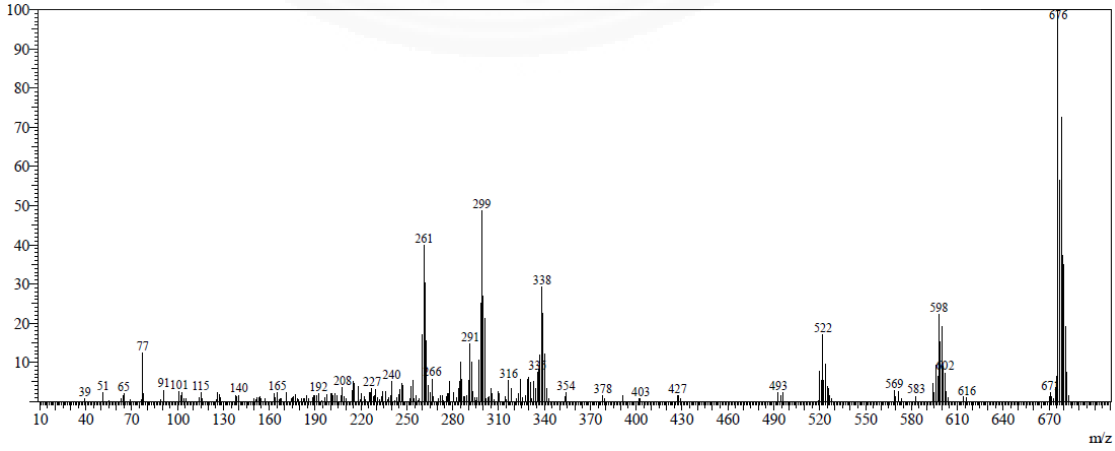

Figure B11. Mass spectrum of ZnTPP in dichloromethane

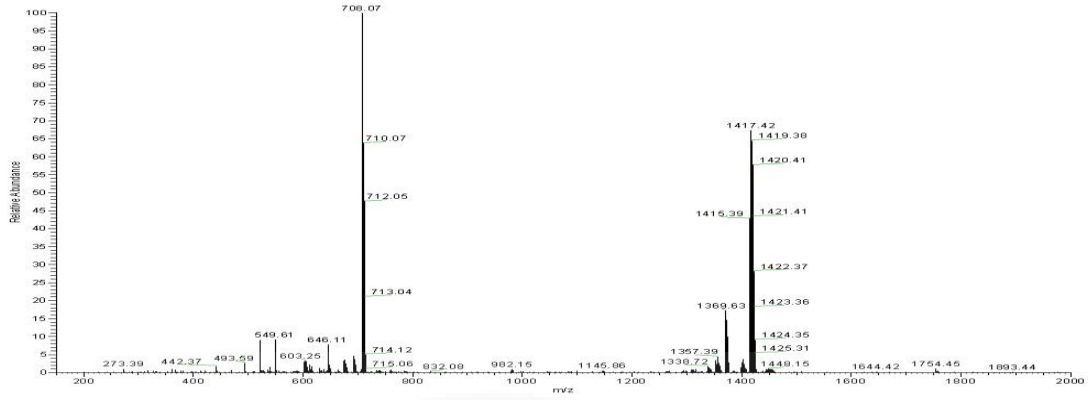

Figure B12. Mass spectrum of ZnMeTrPP in dichloromethane

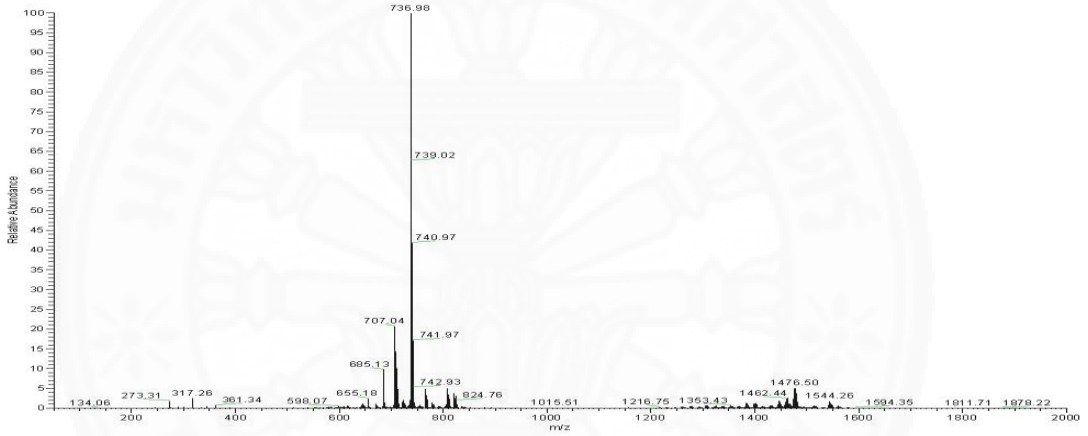

Figure B13. Mass spectrum of ZnMeTrPP-2 in dichloromethane

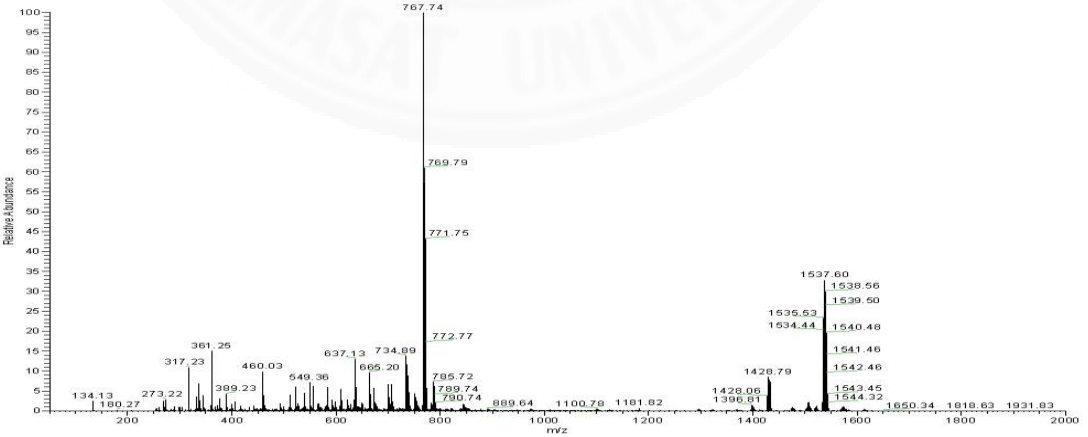

Figure B14. Mass spectrum of ZnMeTrPP-3 in dichloromethane

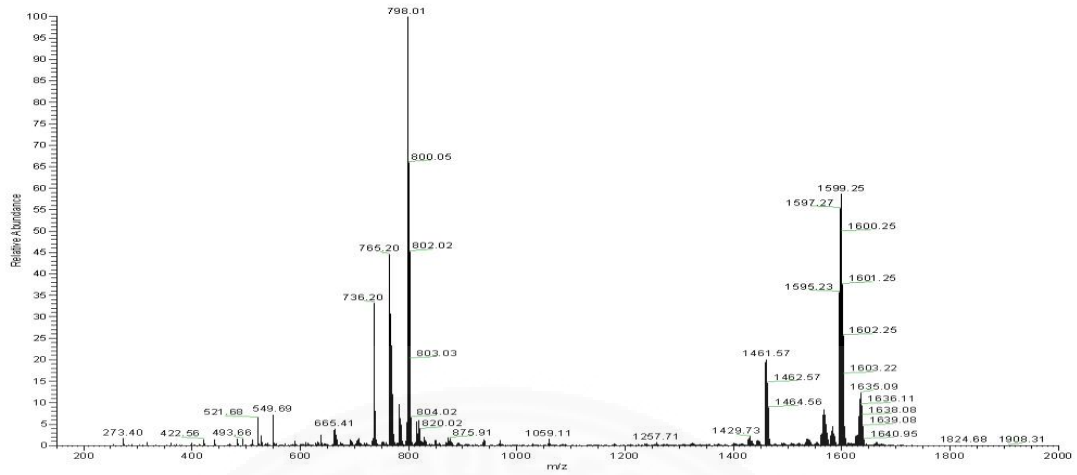

Figure B15. Mass spectrum of ZnTMePP in dichloromethane

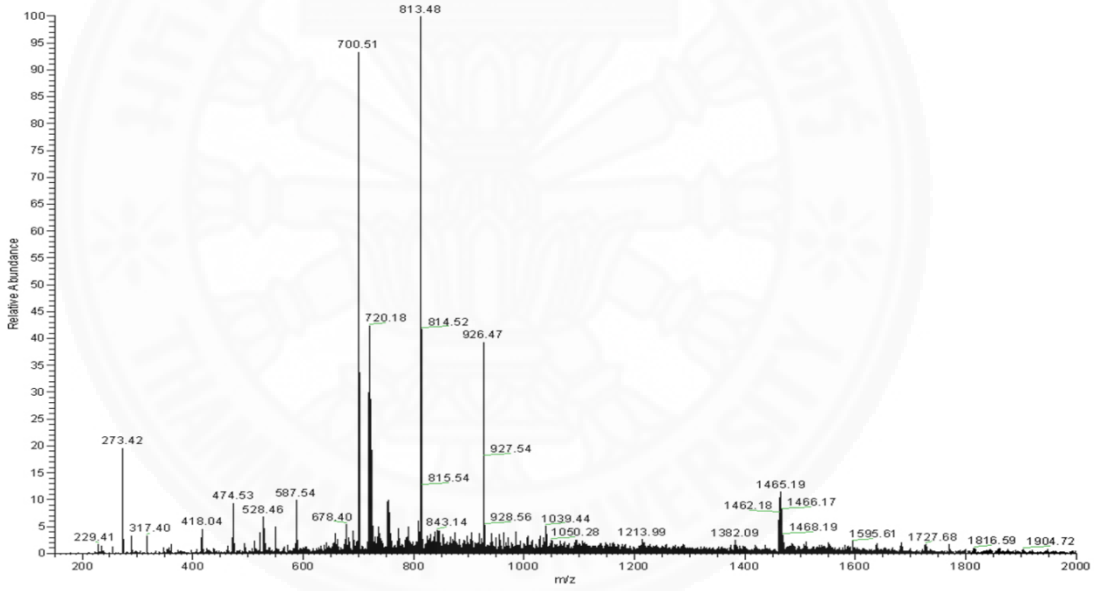

Figure B16. Mass spectrum of ZnCTrPP in dichloromethane

APPENDIX C

NMR SPECTRA

^{1}H- NMR Spectra of free base porphyrins

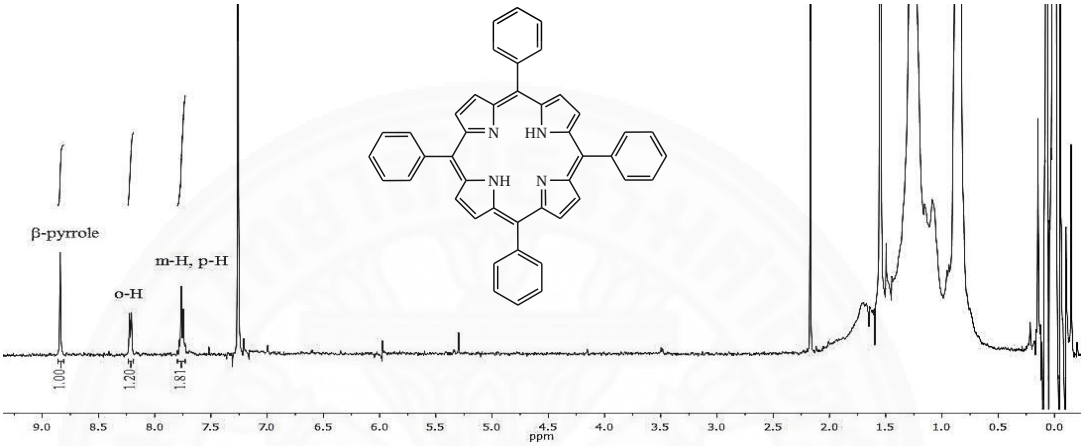

Figure C1. ^{1}H-NMR spectra of TPP taken in $CDCl_3$ solution

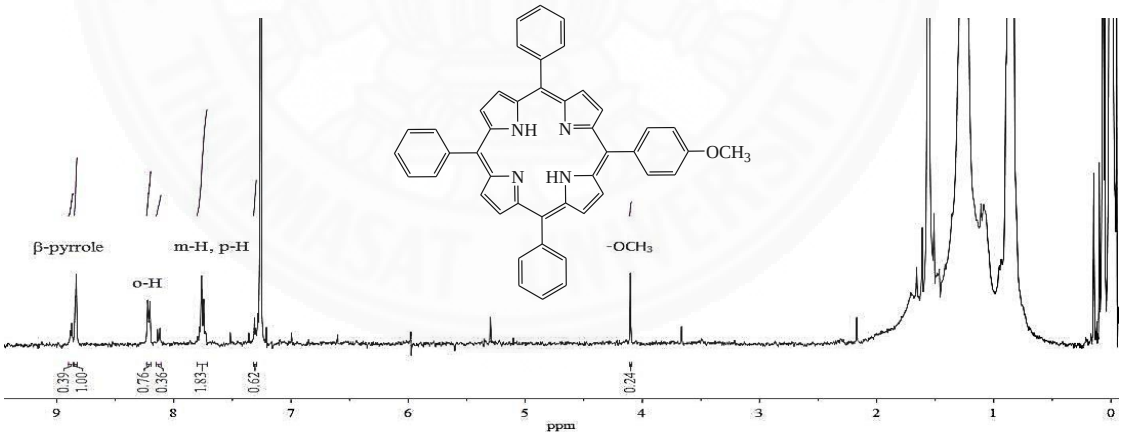

Figure C2. ^{1}H-NMR spectra of MeTrPP taken in $CDCl_3$ solution

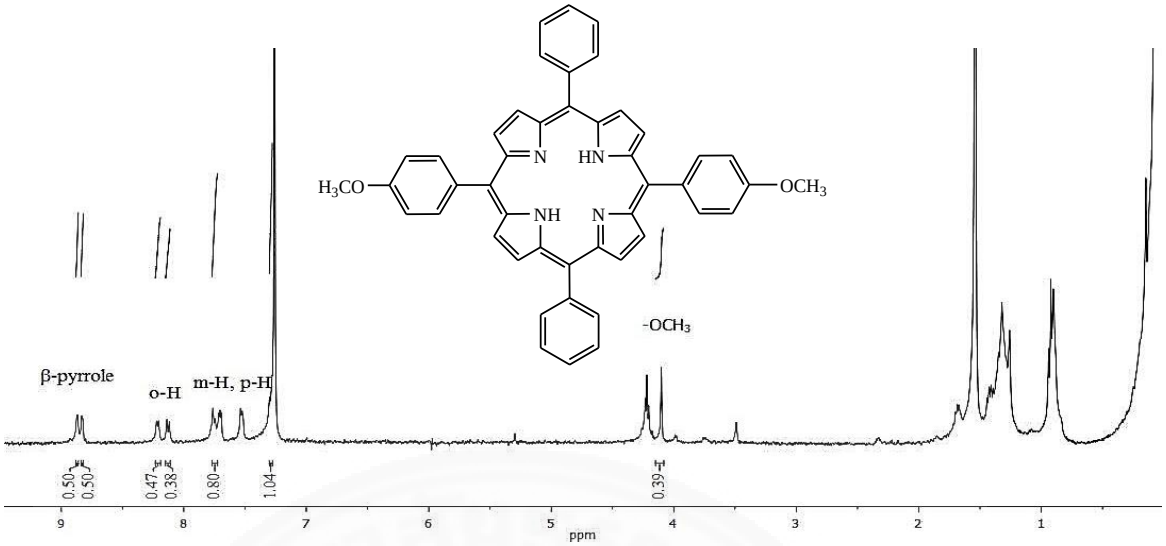

Figure C3. ^{1}H-NMR spectra of MeTrPP-2 taken in $CDCl_3$ solution

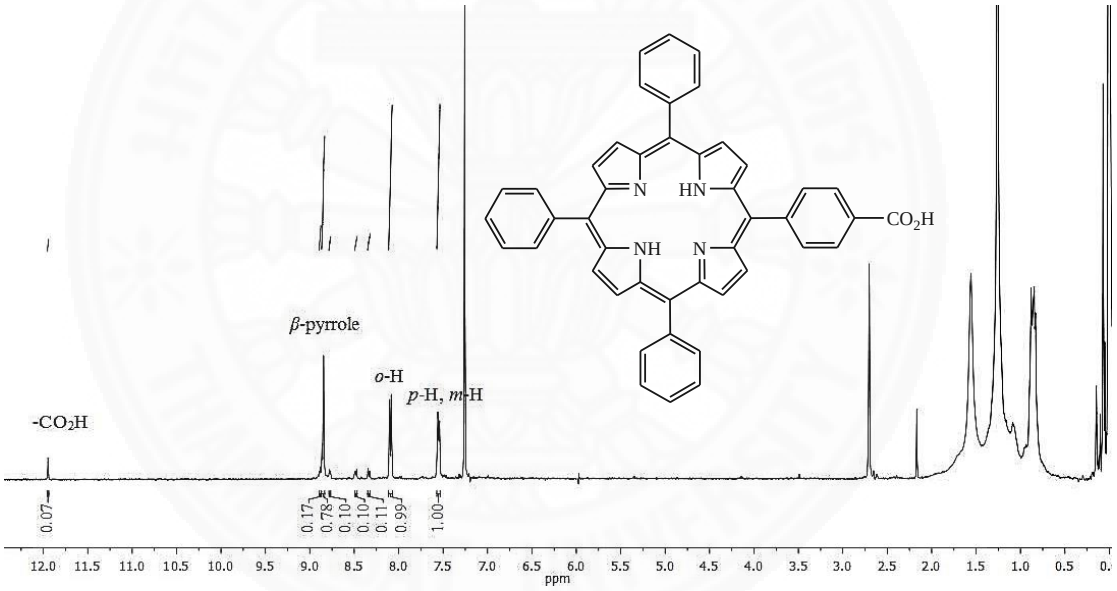

Figure C5. ^{1}H-NMR spectra of CTrPP taken in $CDCl_3$ solution

^{1}H-NMR Spectra of zinc-porphyrins

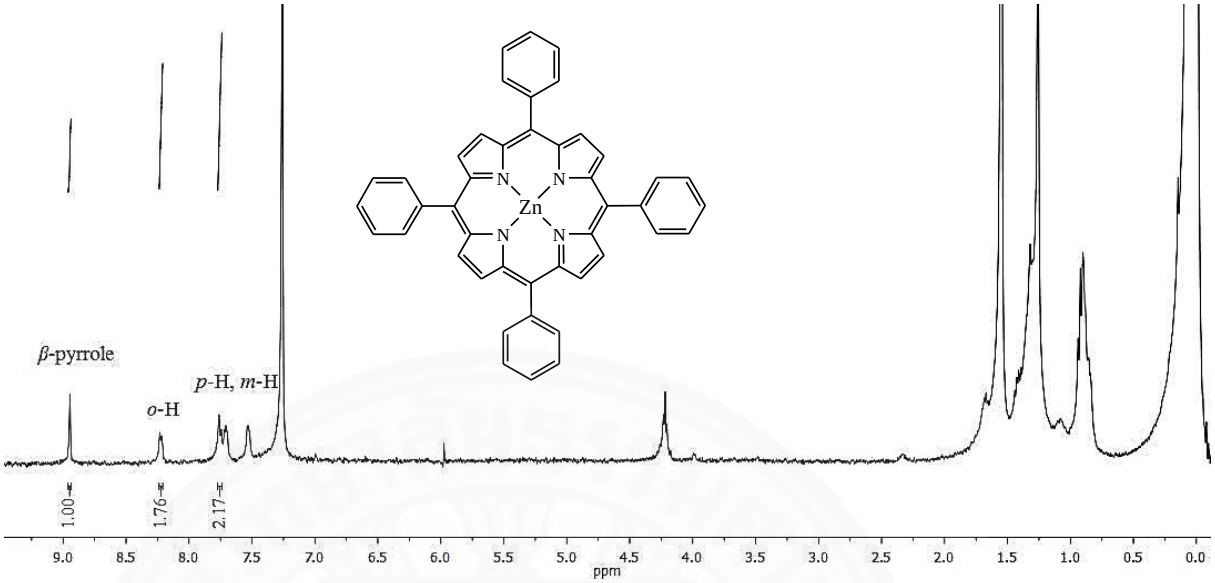

Figure C6. ^{1}H-NMR spectra of ZnTPP taken in $CDCl_3$ solution

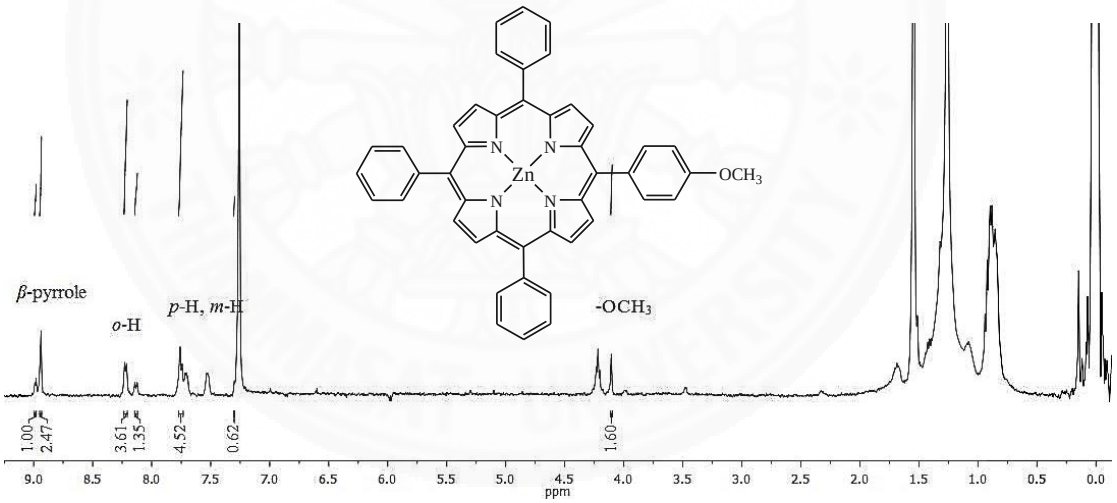

Figure C7. ^{1}H-NMR spectra of ZnMeTrPP taken in $CDCl_3$ solution

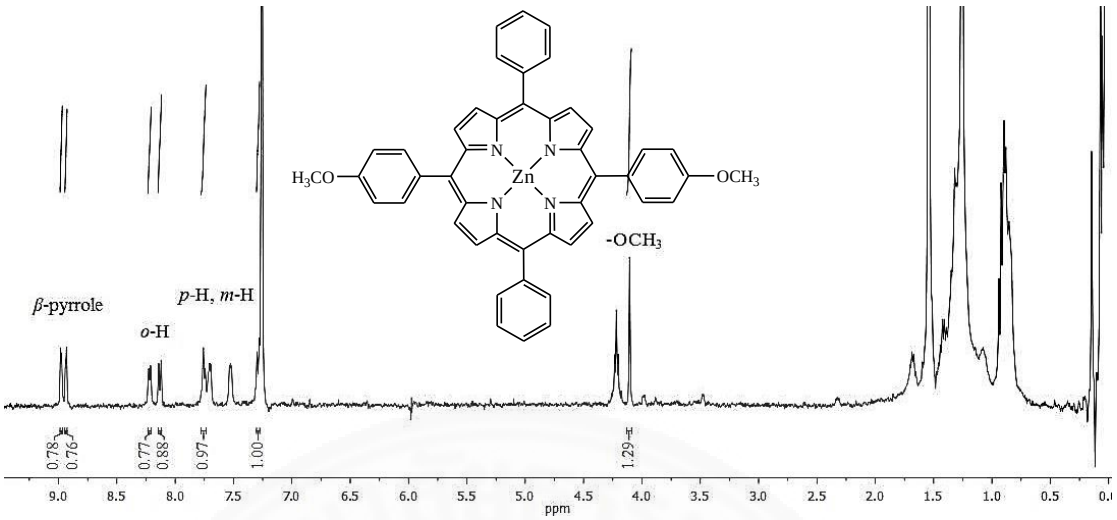

Figure C8. ^{1}H-NMR spectra of ZnMeTrPP-2 taken in $CDCl_3$ solution

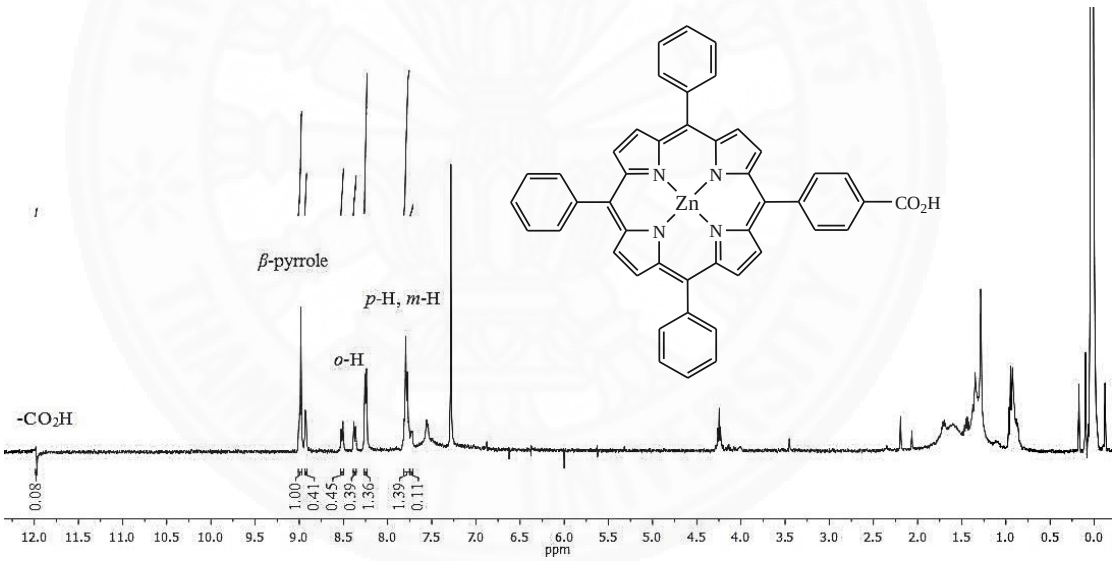

Figure C9. ^{1}H-NMR spectra of ZnCTrPP taken in $CDCl_3$ solution

APPENDIX D

IR spectra

IR spectra of free base porphyrins

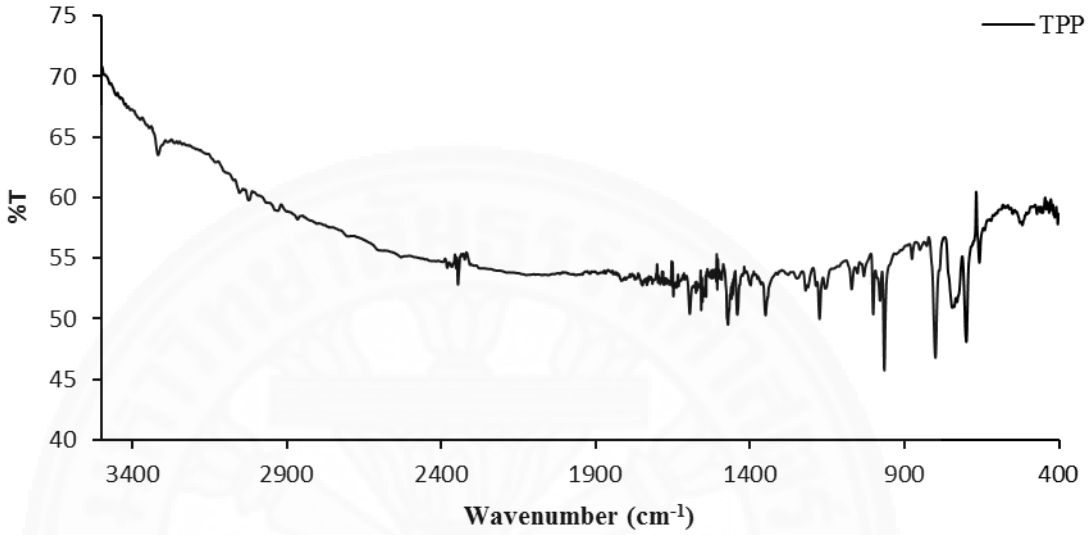

Figure D1. The IR spectrum of TPP in KBr

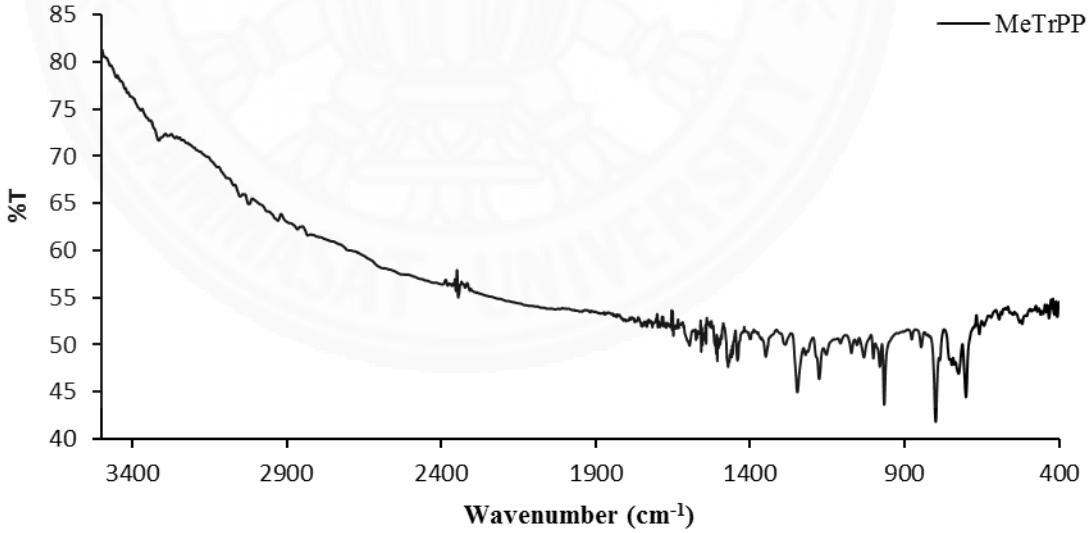

Figure D2. The IR spectrum of MeTrPP in KBr

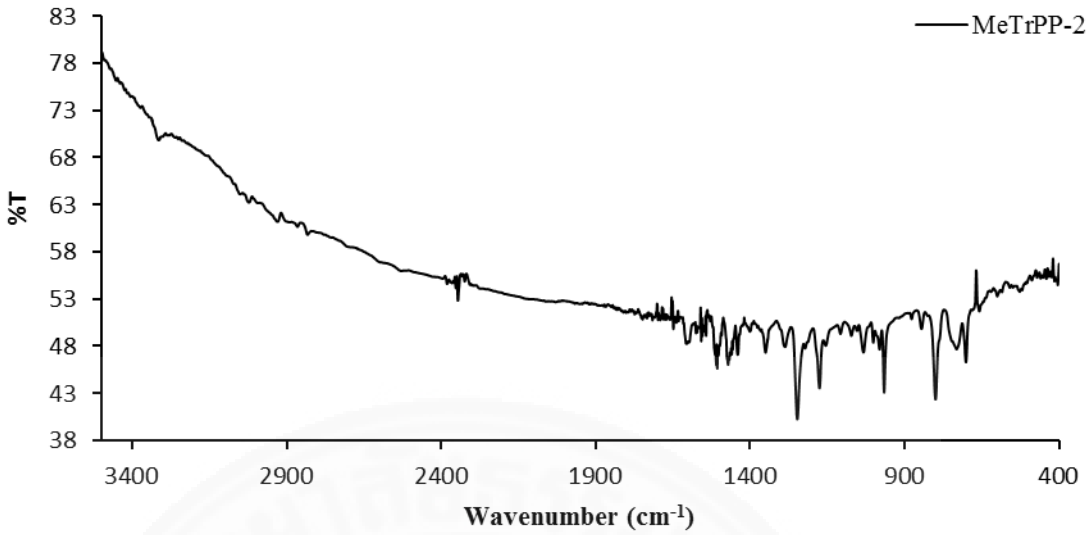

Figure D3. The IR spectrum of MeTrPP-2 in KBr

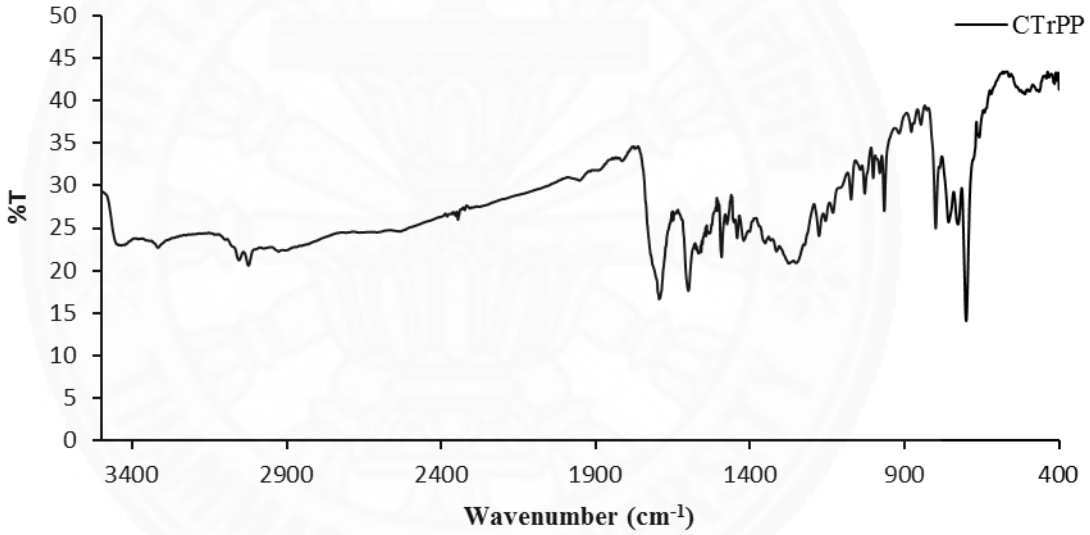

Figure D4. The IR spectrum of CTrPP in KBr

IR spectra of Zinc-porphyrins

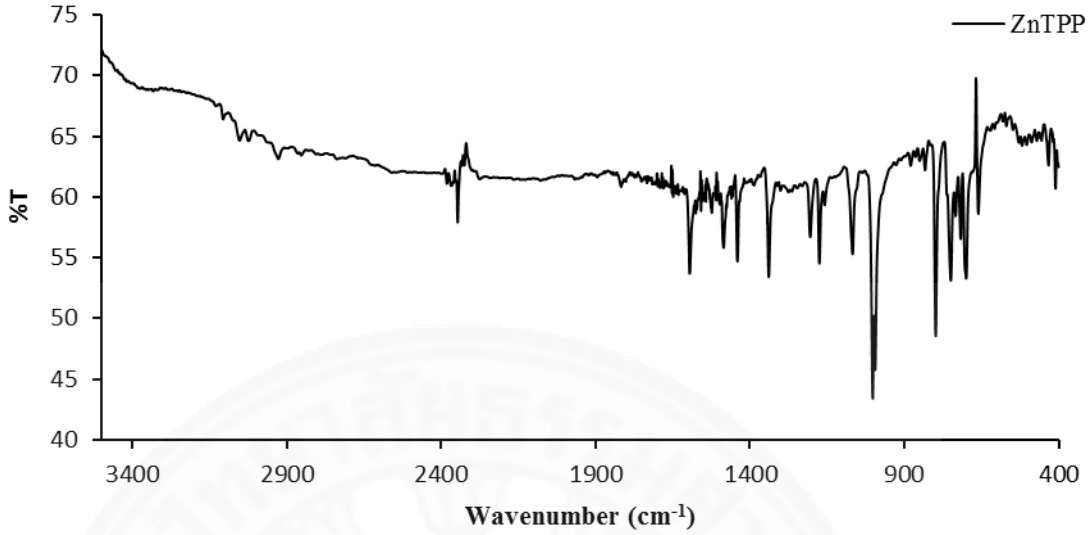

Figure D5. The IR spectrum of ZnTPP in KBr

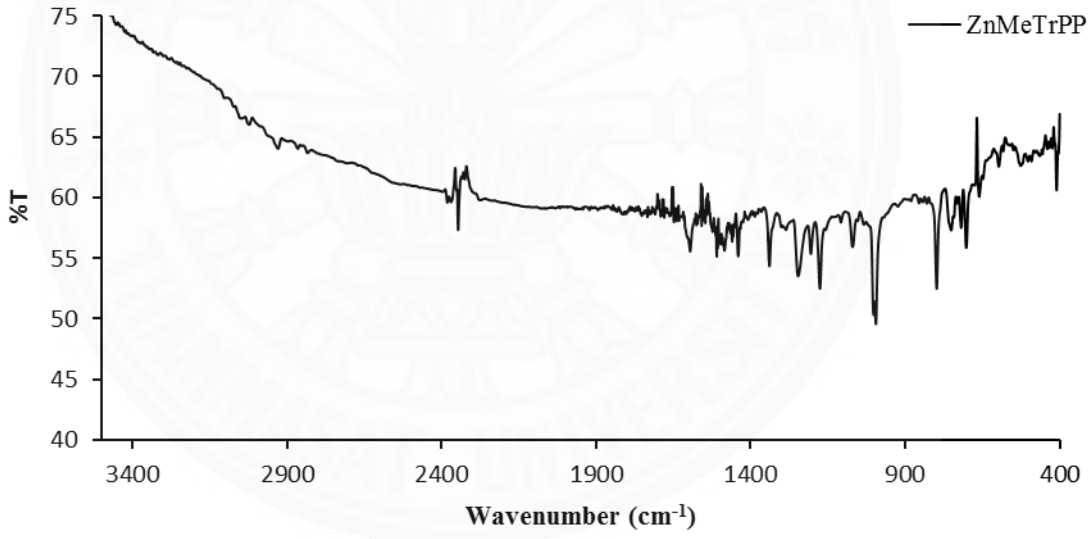

Figure D6. The IR spectrum of ZnMeTrPP in KBr

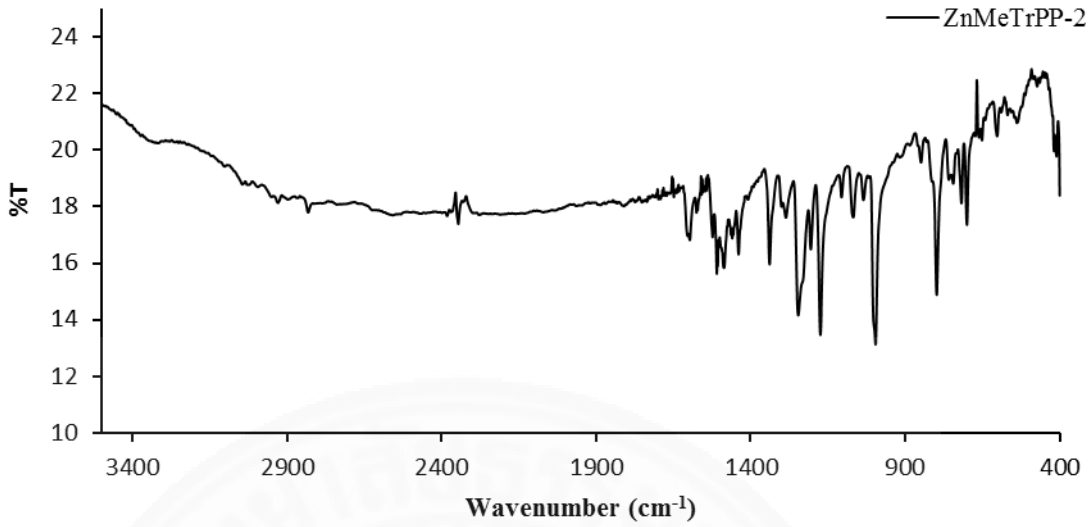

Figure D7. The IR spectrum of ZnMeTrPP-2 in KBr

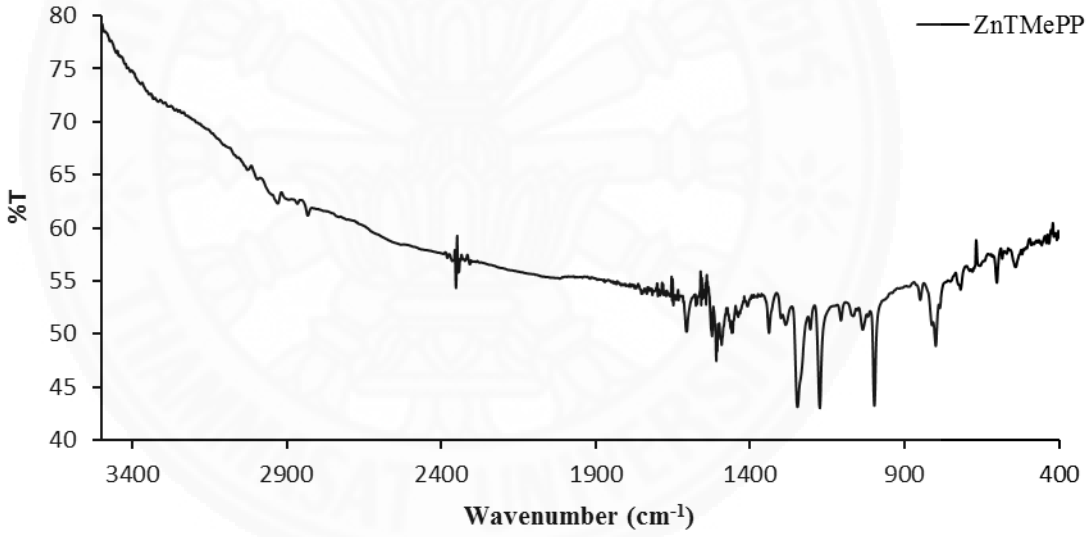

Figure D8. The IR spectrum of ZnTMePP in KBr

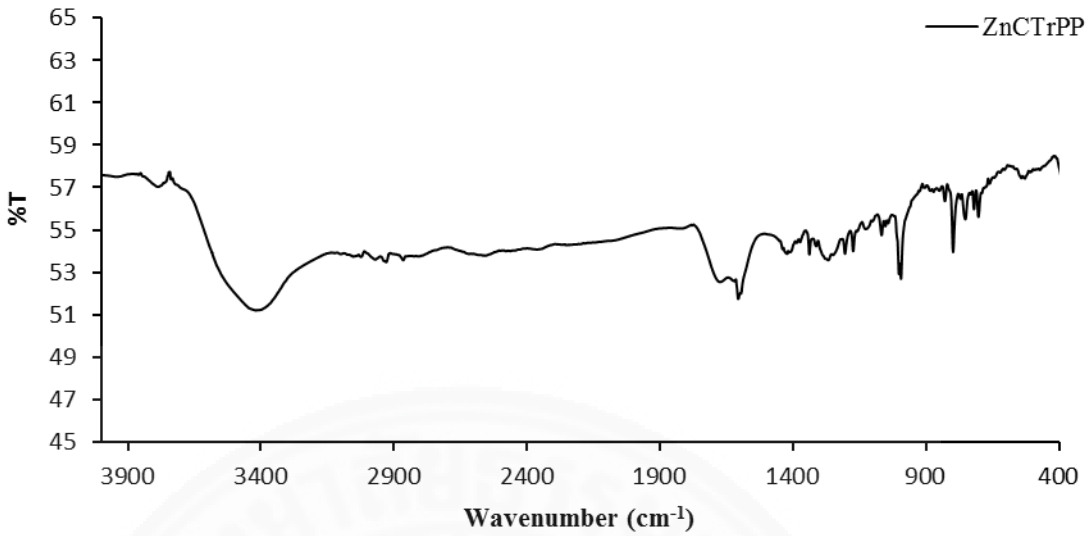

Figure D9. The IR spectrum of ZnCTrPP in KBr

APPENDIX E

UV-Vis absorption spectra

UV-Vis absorption spectra of free base ligands in dichloromethane

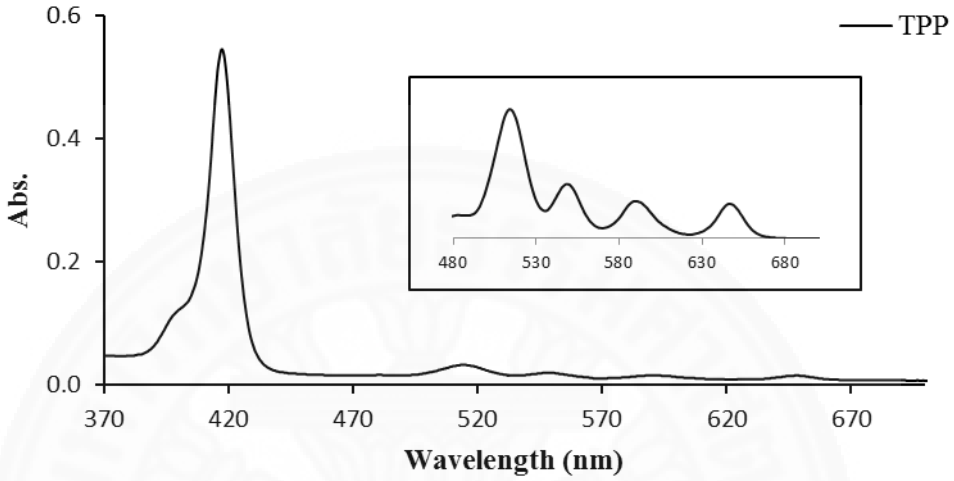

Figure E1. UV-Vis absorption spectrum of TPP with in inserts the enlargement of Q region

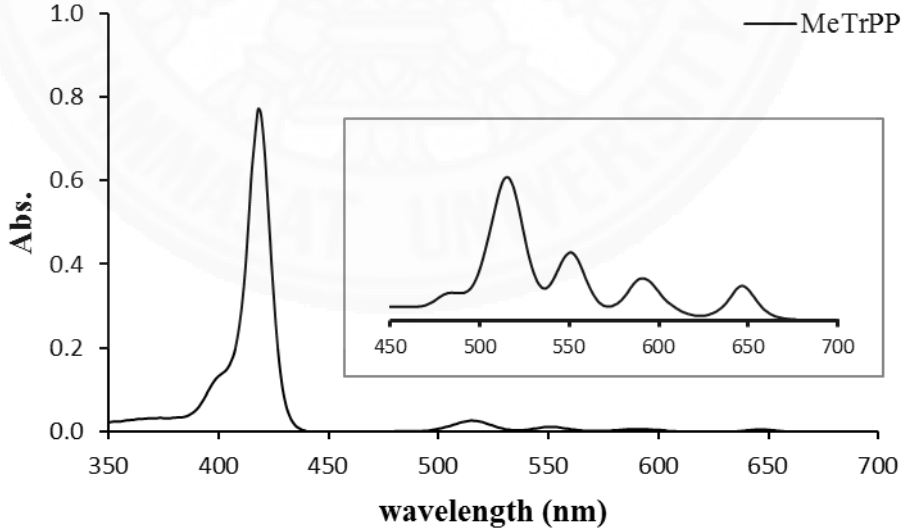

Figure E2. UV-Vis absorption spectrum of MeTrPP with in inserts the enlargement of Q region

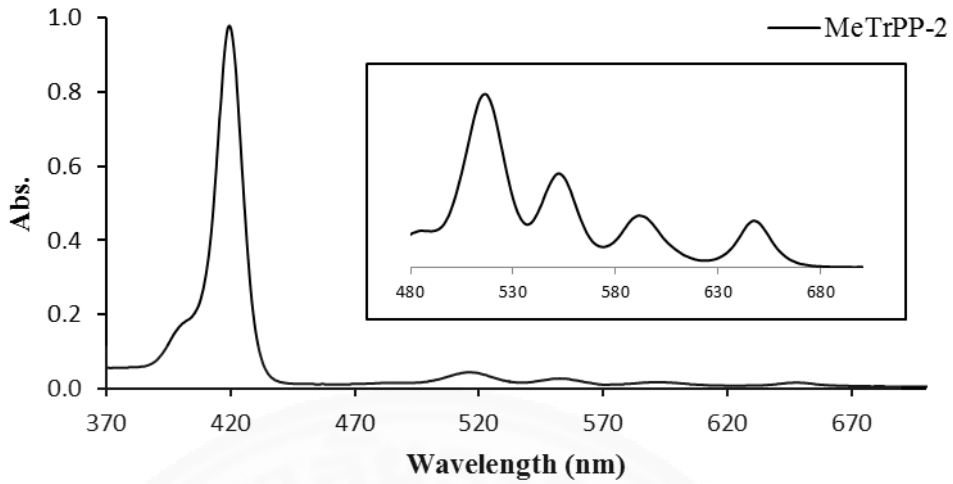

Figure E3. UV-Vis absorption spectrum of MeTrPP-2 with in inserts the enlargement of Q region

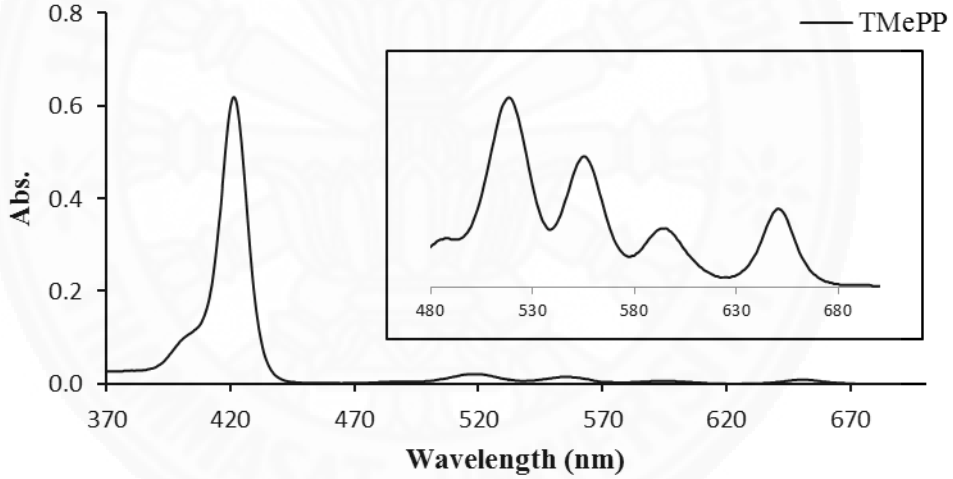

Figure E4. UV-Vis absorption spectrum of TMePP with in inserts the enlargement of Q region

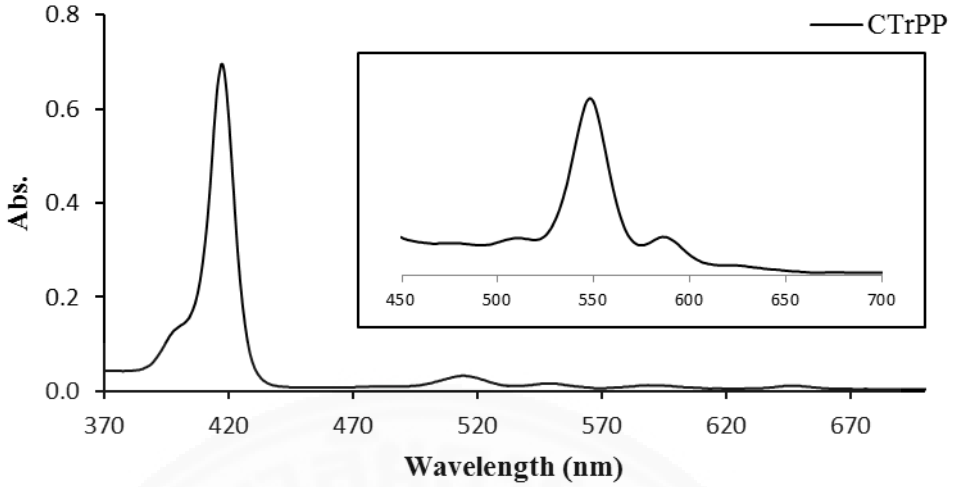

Figure E5. UV-Vis absorption spectrum of CTrPP with in inserts the enlargement of Q region

UV-Vis absorption spectra of Zinc-porphyrins in dichloromethane

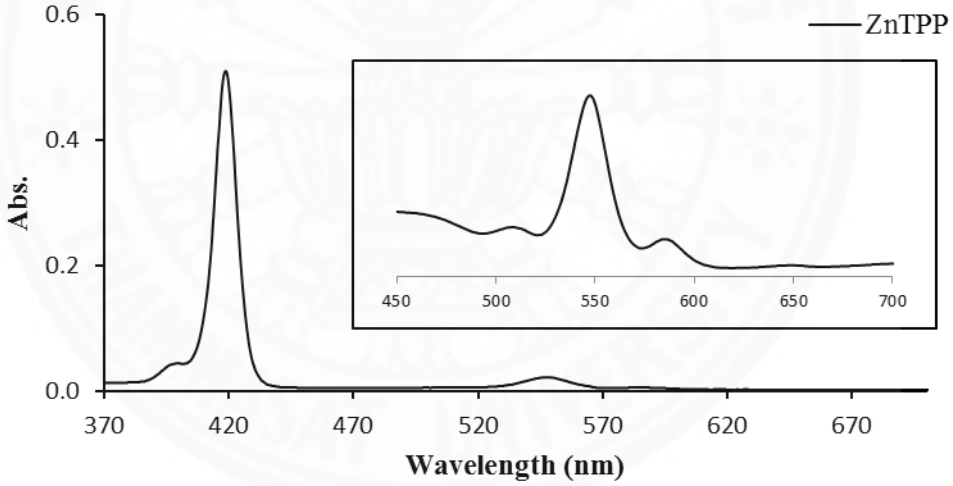

Figure E6. UV-Vis absorption spectrum of ZnTPP with in inserts the enlargement of Q region

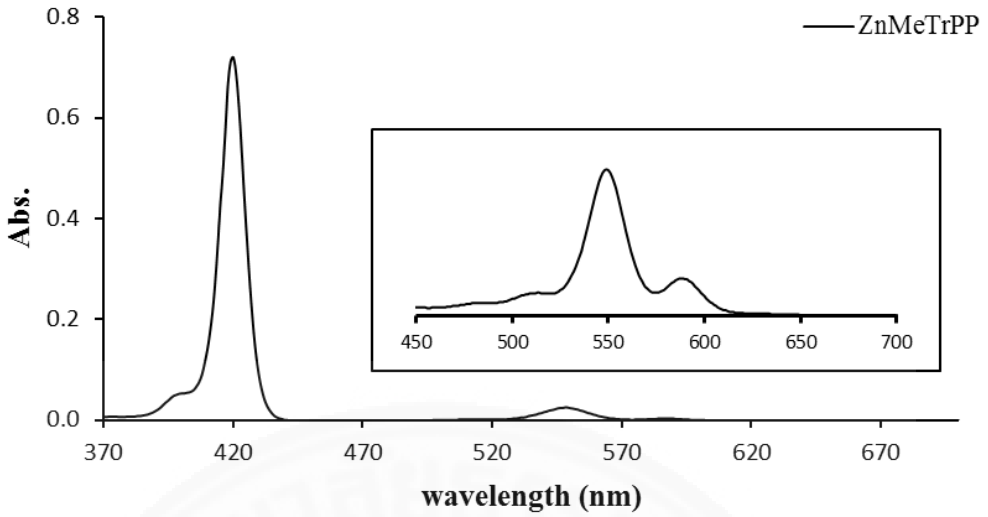

Figure E7. UV-Vis absorption spectrum of ZnMeTrPP with in inserts the enlargement of Q region

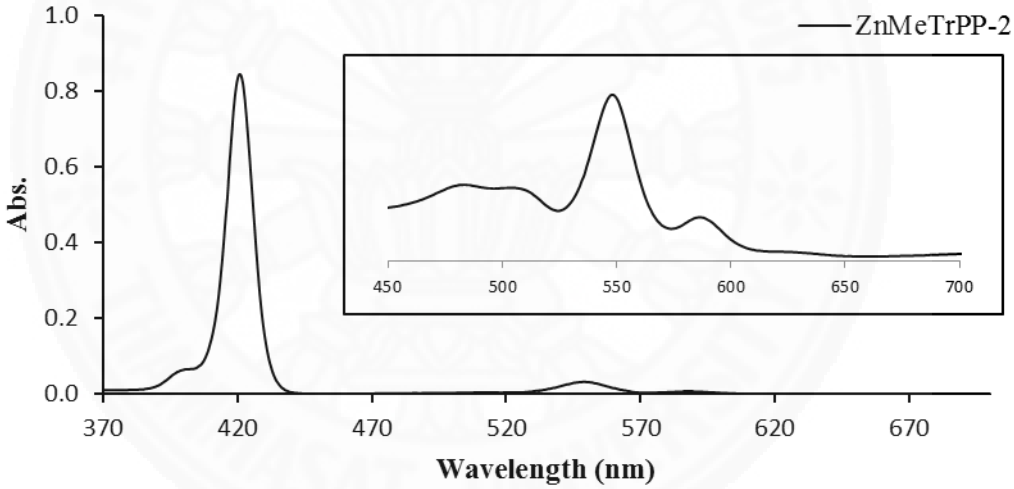

Figure E8. UV-Vis absorption spectrum of ZnMeTrPP-2 with in inserts the enlargement of Q region

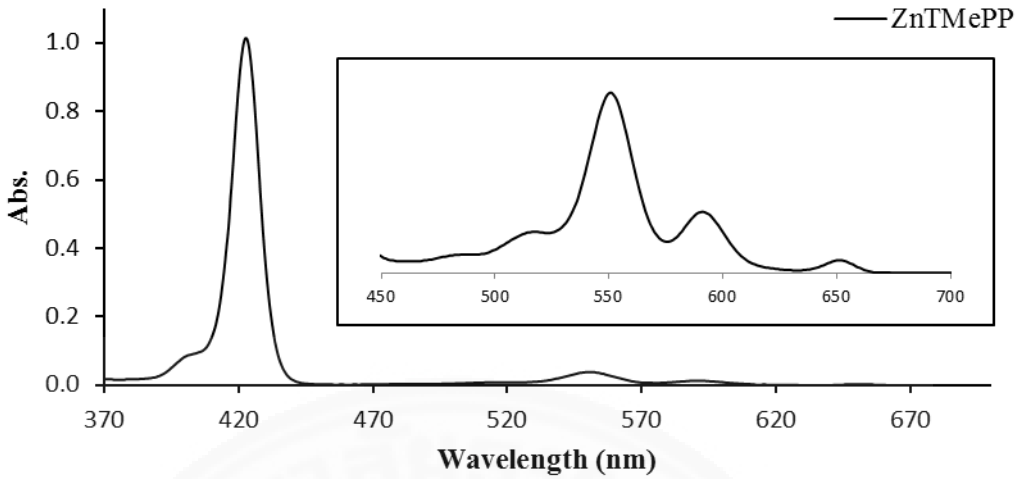

Figure E9. UV-Vis absorption spectrum of ZnTMePP with in inserts the enlargement of Q region

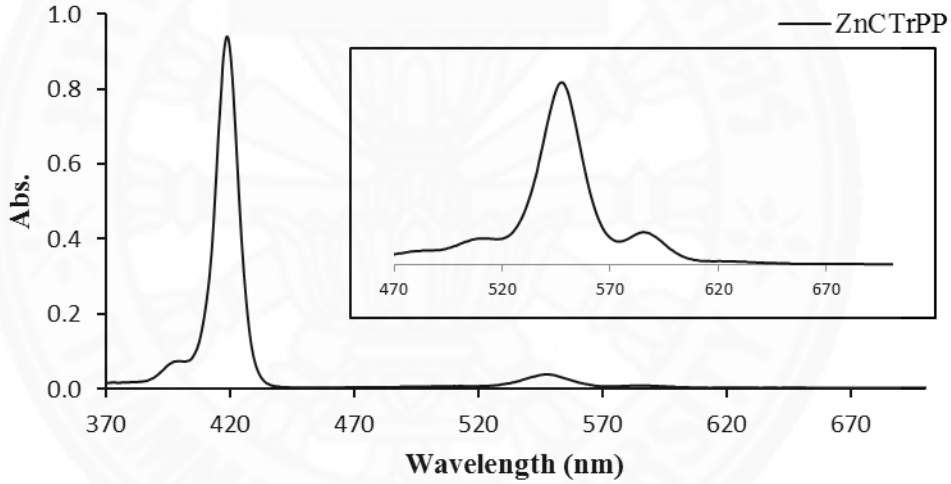

Figure E10. UV-Vis absorption spectrum of ZnCTrPP with in inserts the enlargement of Q region

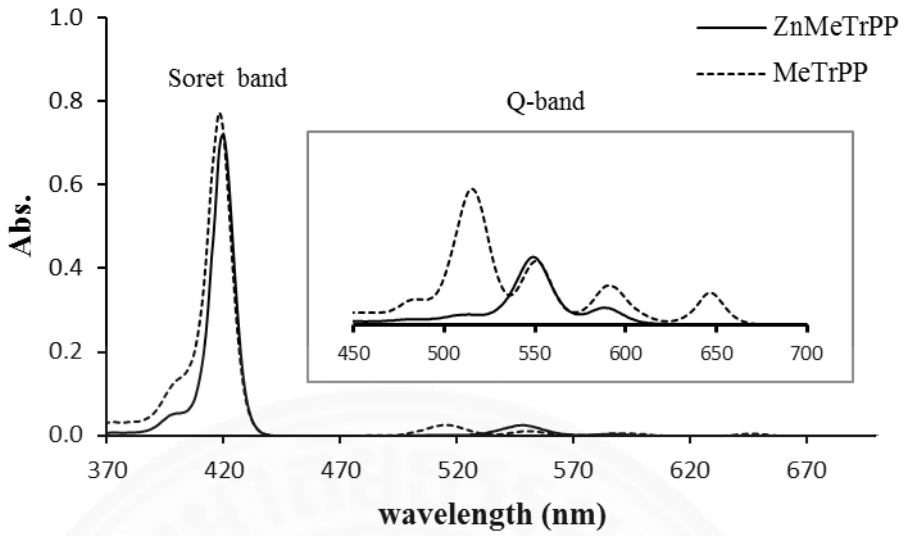

Figure E11. Comparison of UV-Vis absorption spectra of ZnMeTrPP and MeTrPP

APPENDIX F

FLUORESCENCE SPECTRA

Fluorescence spectra of free base ligands in dichloromethane

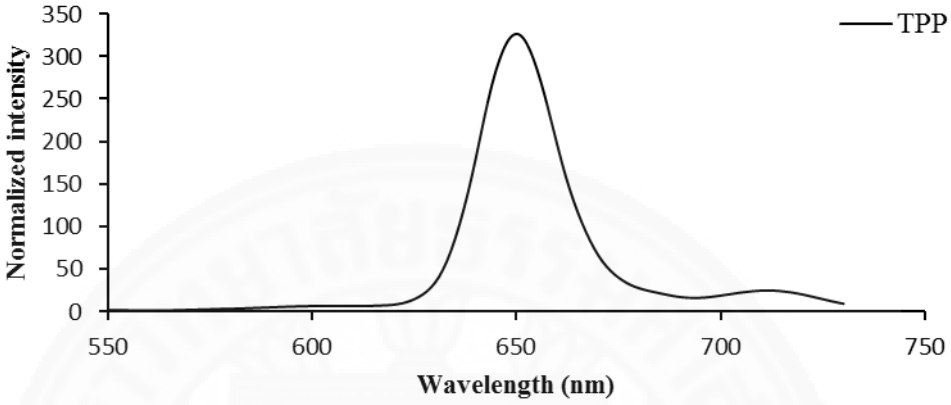

Figure F1. Fluorescence spectrum of TPP in CH_2Cl_2

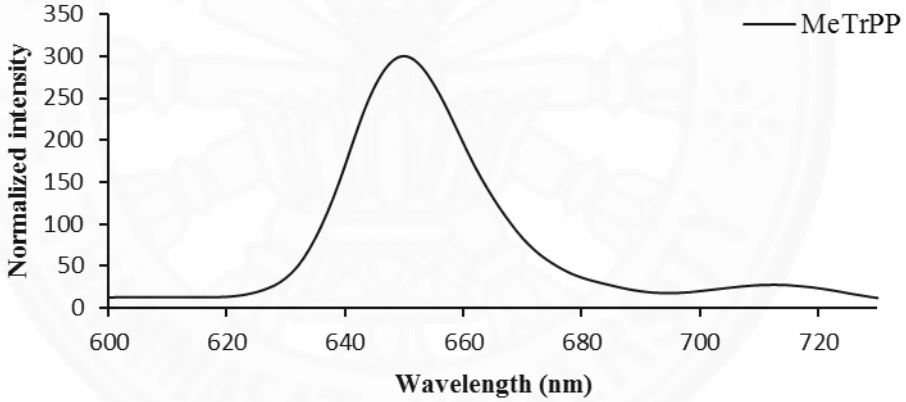

Figure F2. Fluorescence spectrum of MeTrPP in CH_2Cl_2

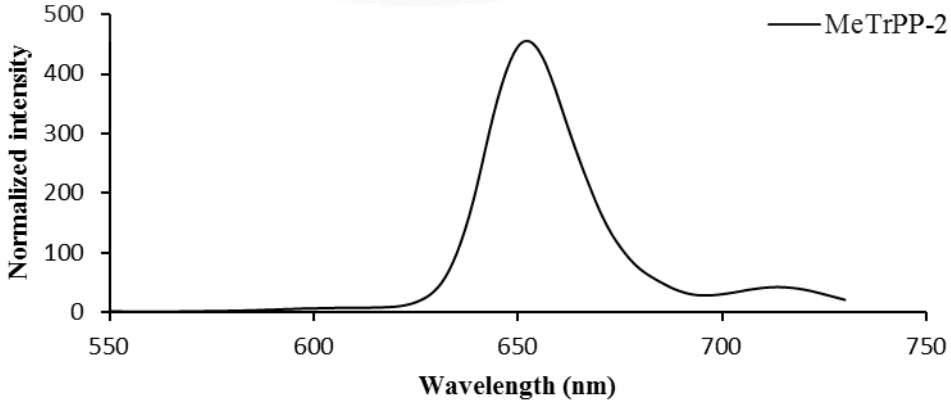

Figure F3. Fluorescence spectrum of MeTrPP-2 in CH_2Cl_2

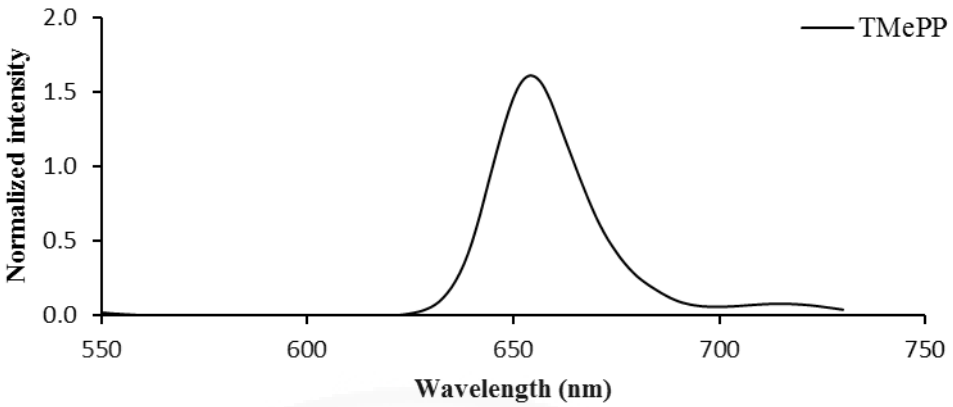

Figure F4. Fluorescence spectrum of TMePP in CH_2Cl_2

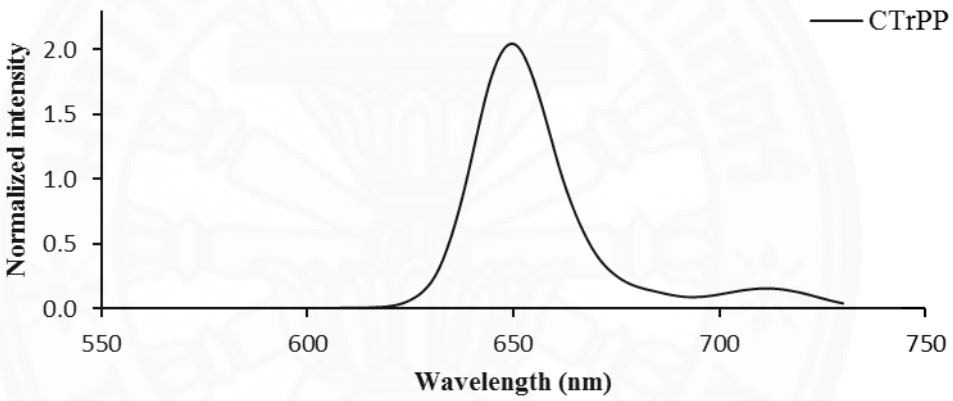

Figure F5. Fluorescence spectrum of CTrPP in CH_2Cl_2

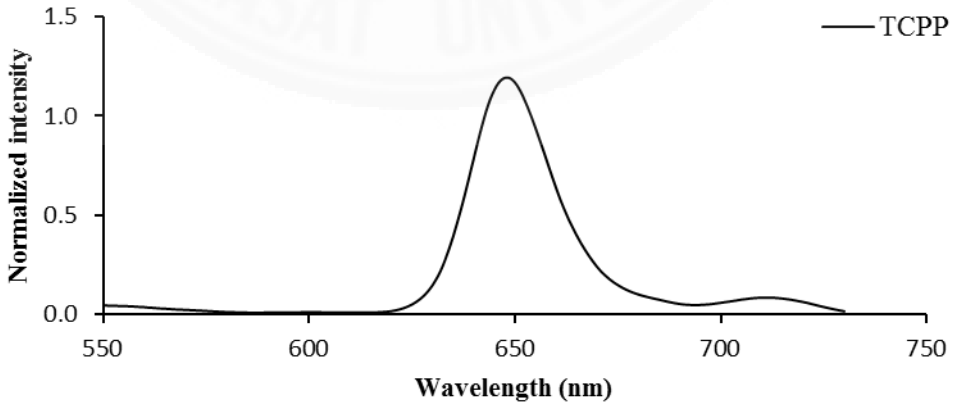

Figure F6. Fluorescence spectrum of TCPP in CH_2Cl_2

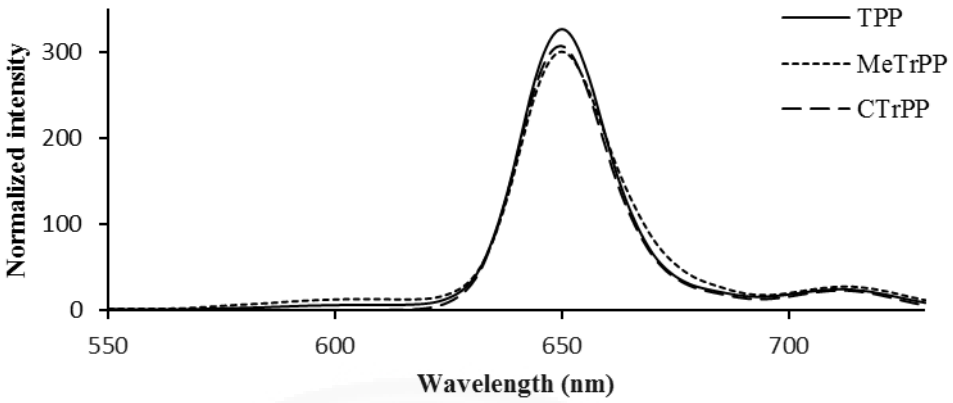

Figure F7. Comparison of Fluorescence spectra of free base porphyrins

Fluorescence spectra of zinc-porphyrins in dichloromethane

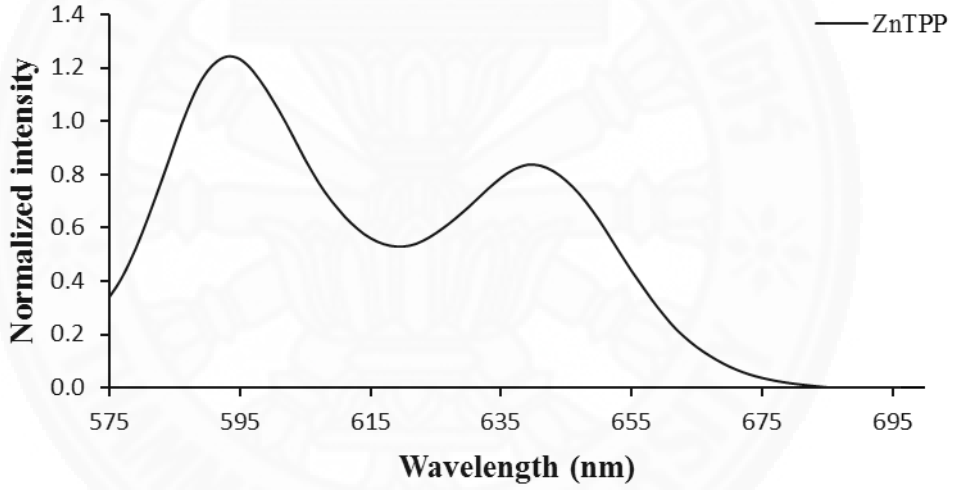

Figure F8. Fluorescence spectrum of ZnTPP in CH_2Cl_2

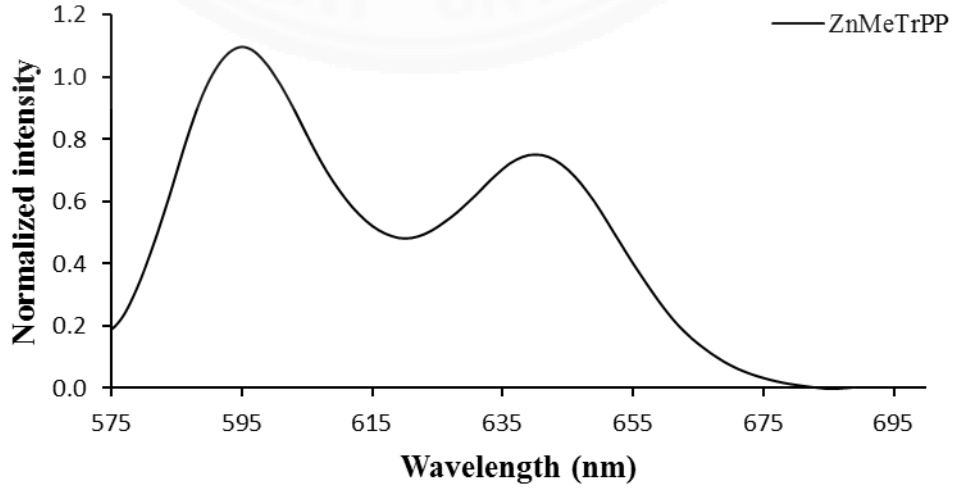

Figure F9. Fluorescence spectrum of ZnMeTrPP in CH_2Cl_2

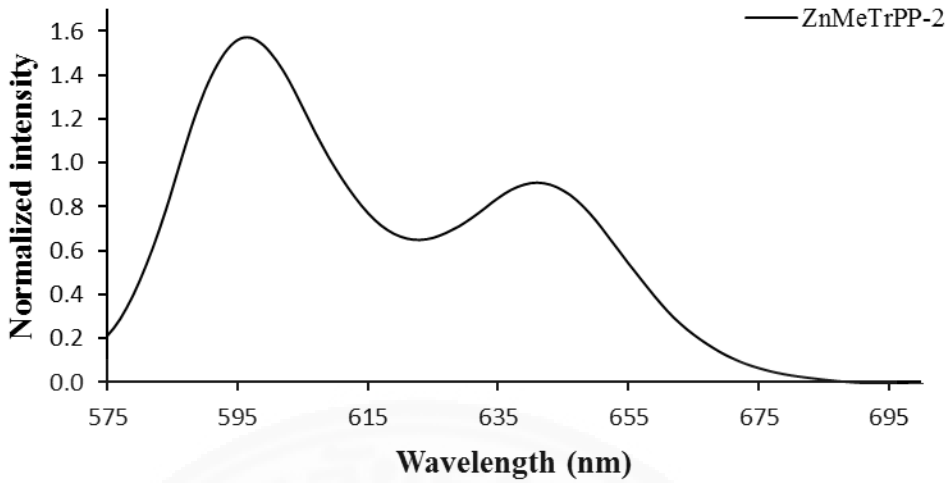

Figure F10. Fluorescence spectrum of ZnMeTrPP-2 in CH_2Cl_2

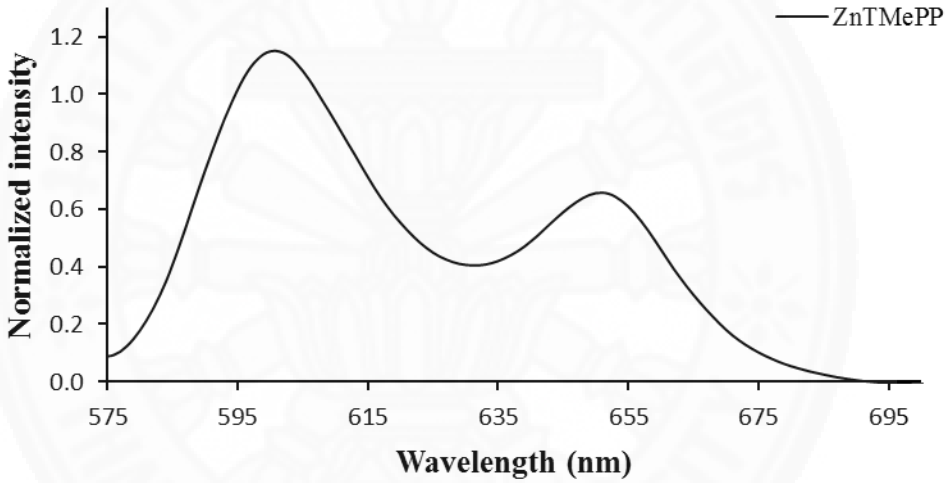

Figure F11. Fluorescence spectrum of ZnTMePP in CH_2Cl_2

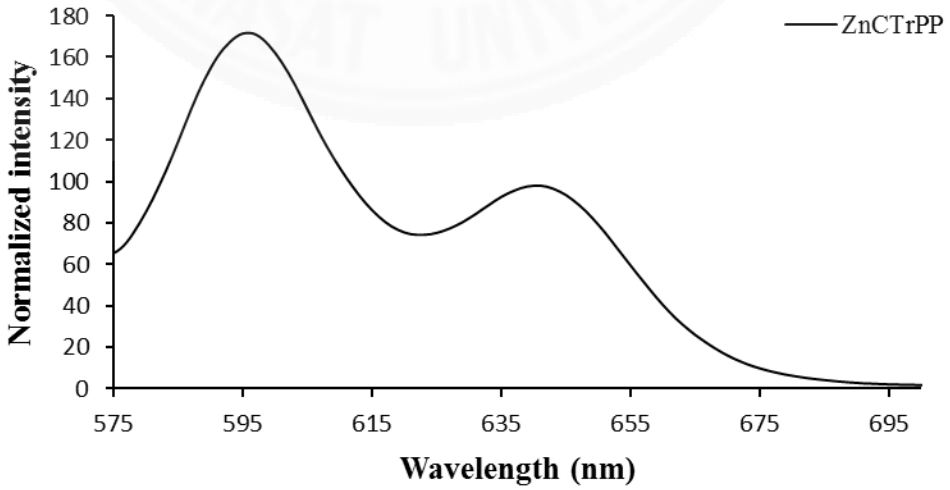

Figure F12. Fluorescence spectrum of ZnCTrPP in CH_2Cl_2

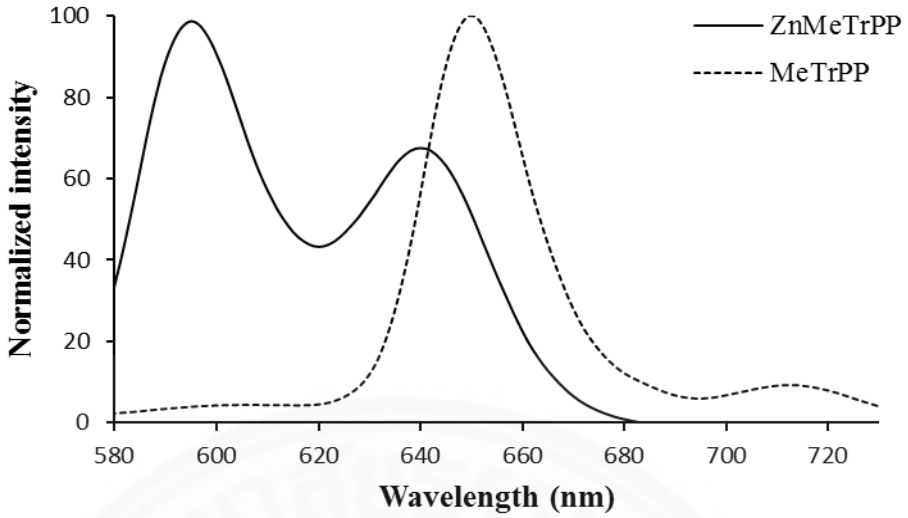

Figure F13. Comparison of Fluorescence spectra of ZnMeTrPP and MeTrPP

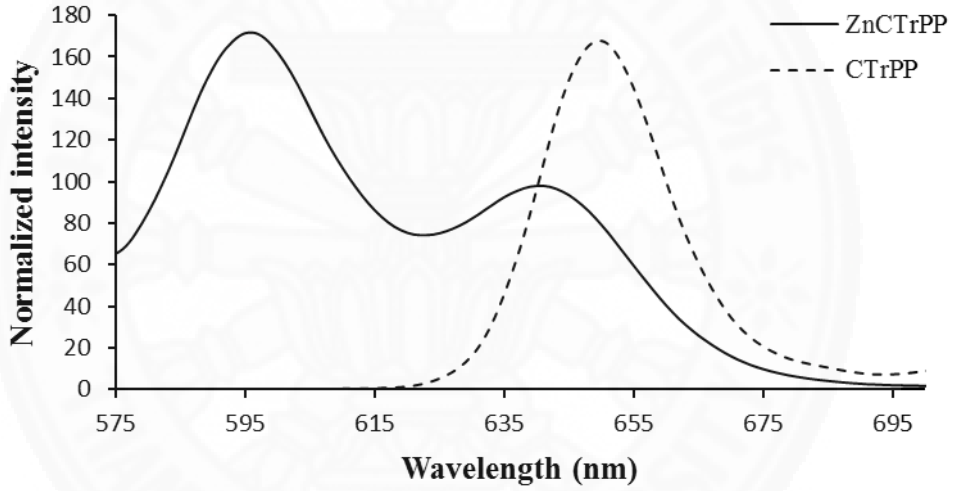

Figure F14. Comparison of Fluorescence spectra of ZnCTrPP and CTrPP

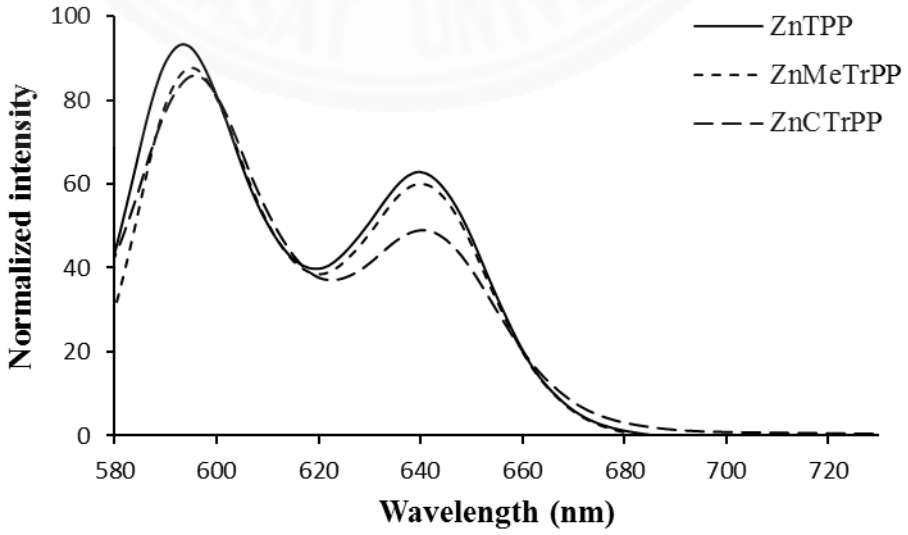

Figure F15. Comparison of Fluorescence spectra of ZnTPP, ZnMeTrPP, ZnCTrPP

APPENDIX G

Thermo Gravimetric Analysis (TGA)

Thermogravimetric analysis (TGA) curves for free base ligands

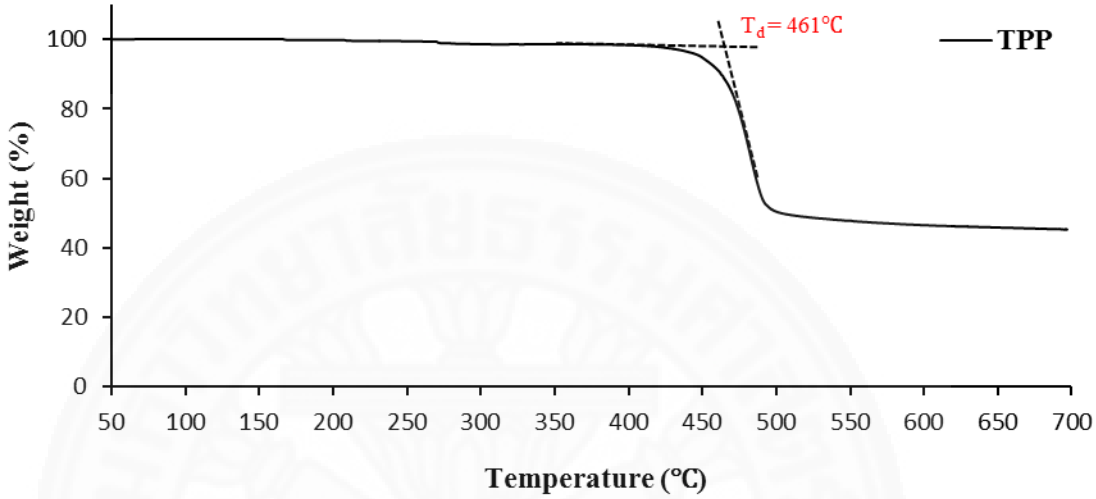

Figure G1. Thermogravimetric analysis (TGA) curves of TPP

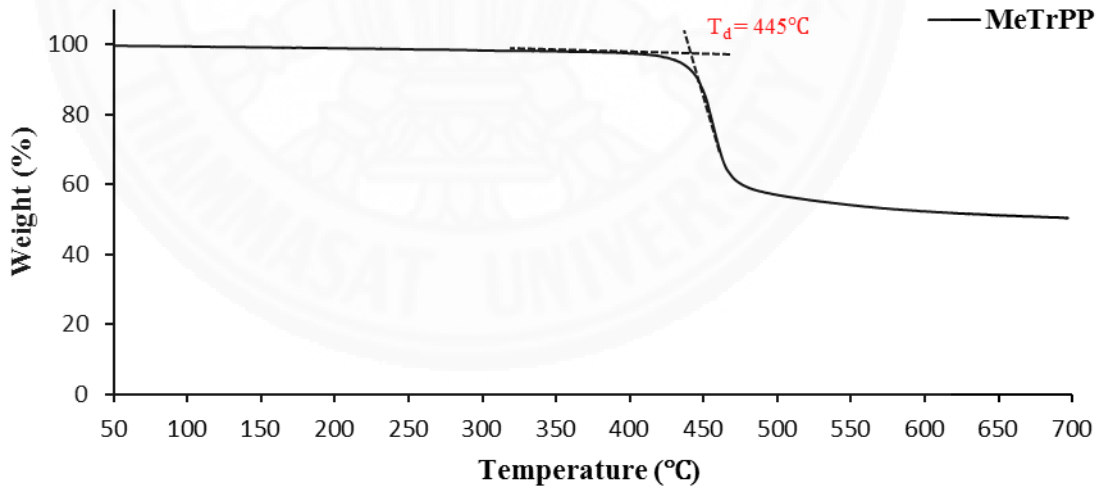

Figure G2. Thermogravimetric analysis (TGA) curves of MeTrPP

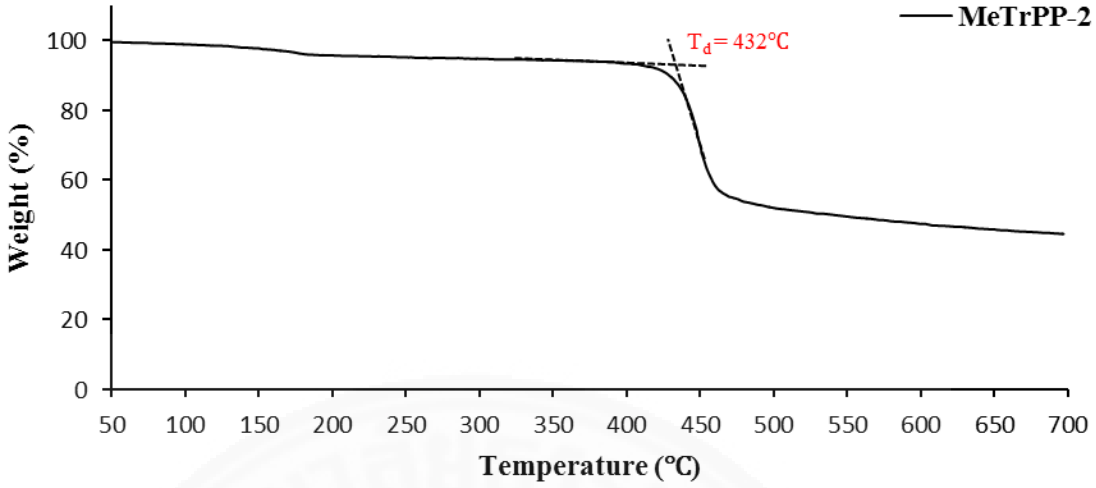

Figure G3. Thermogravimetric analysis (TGA) curves of MeTrPP-2

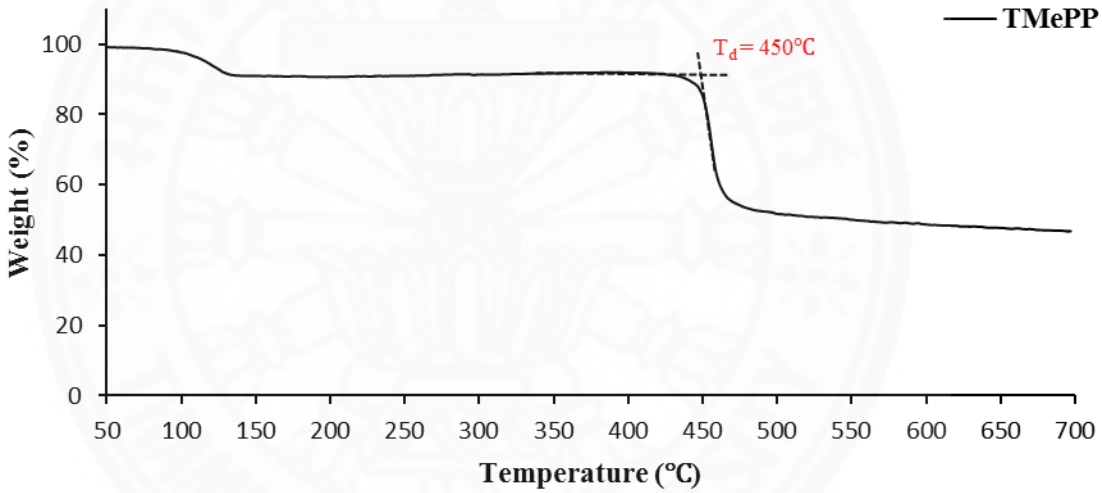

Figure G4. Thermogravimetric analysis (TGA) curves of TMePP

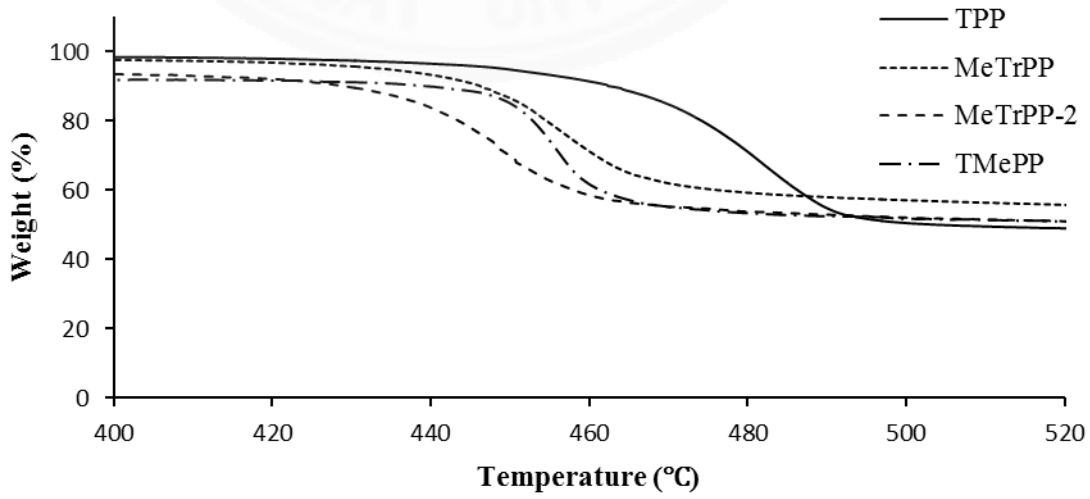

Figure G5. Comparison of TGA curves of TPP, MeTrPP, MeTrPP-2 and TMePP

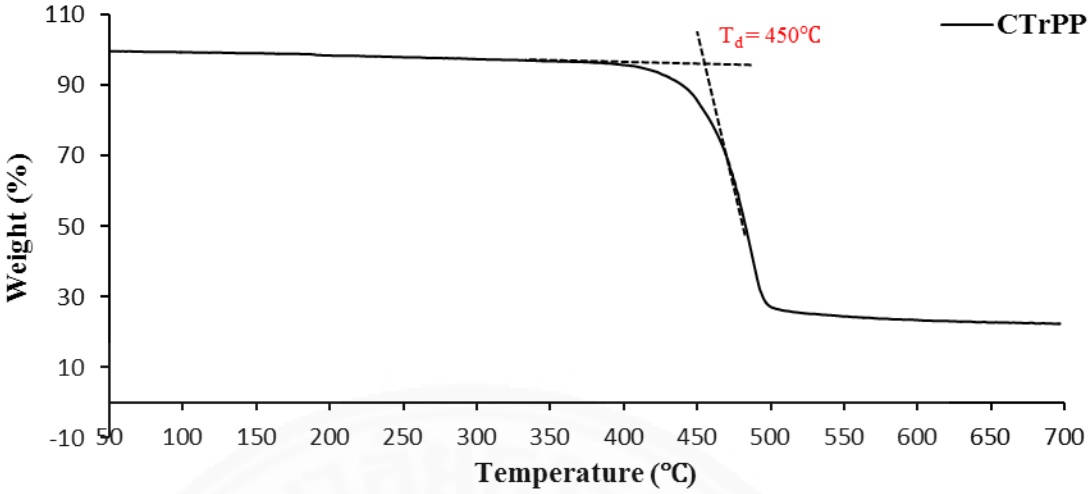

Figure G6. Thermogravimetric analysis (TGA) curves of CTrPP

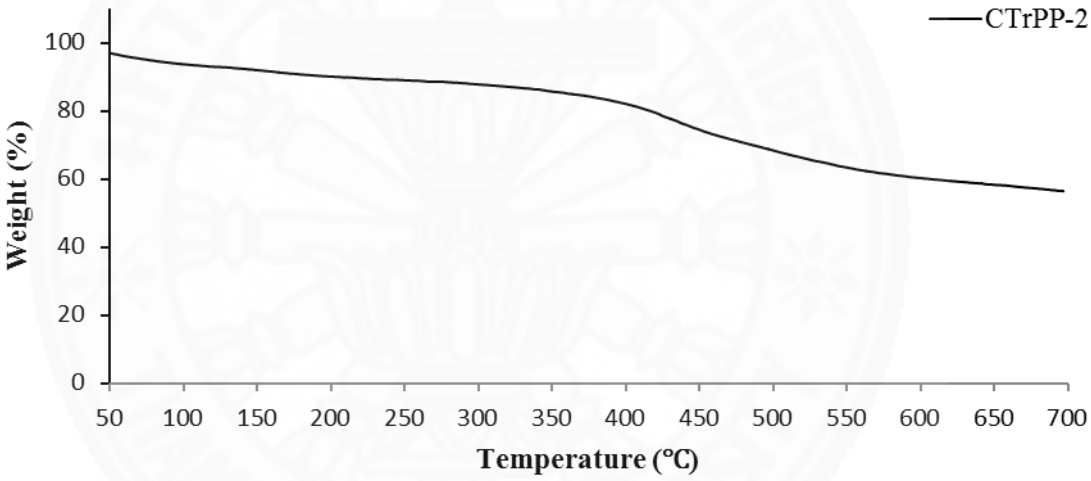

Figure G7. Thermogravimetric analysis (TGA) curves of CTrPP-2

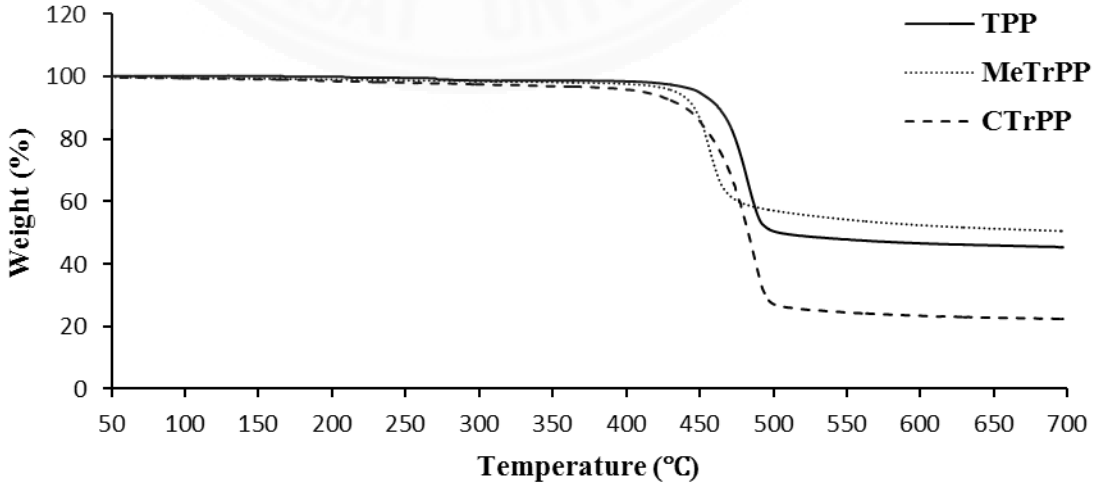

Figure G8. Comparison of TGA curves of TPP, MeTrPP and CTrPP

Thermogravimetric analysis (TGA) curves for Zinc-porphyrins

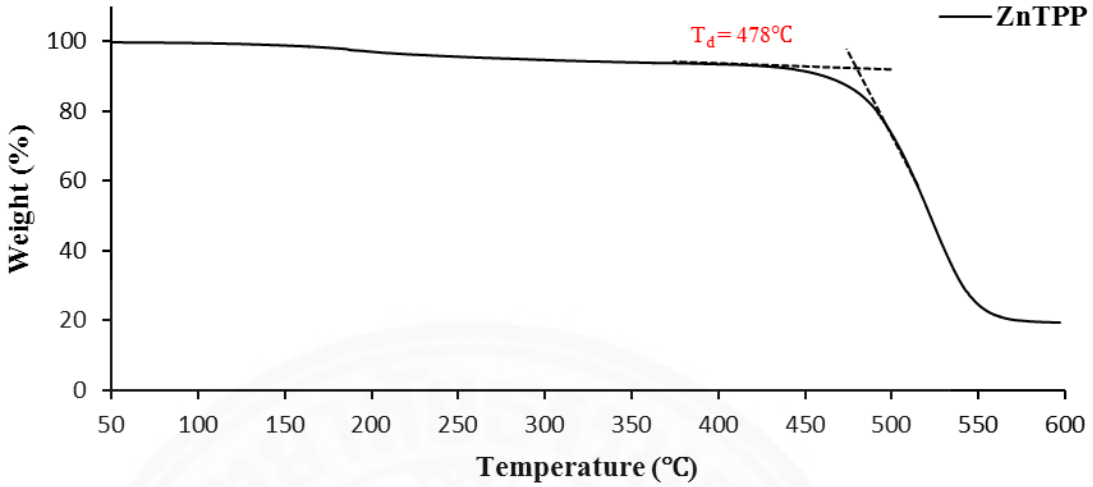

Figure G9. Thermogravimetric analysis (TGA) curves of ZnTPP

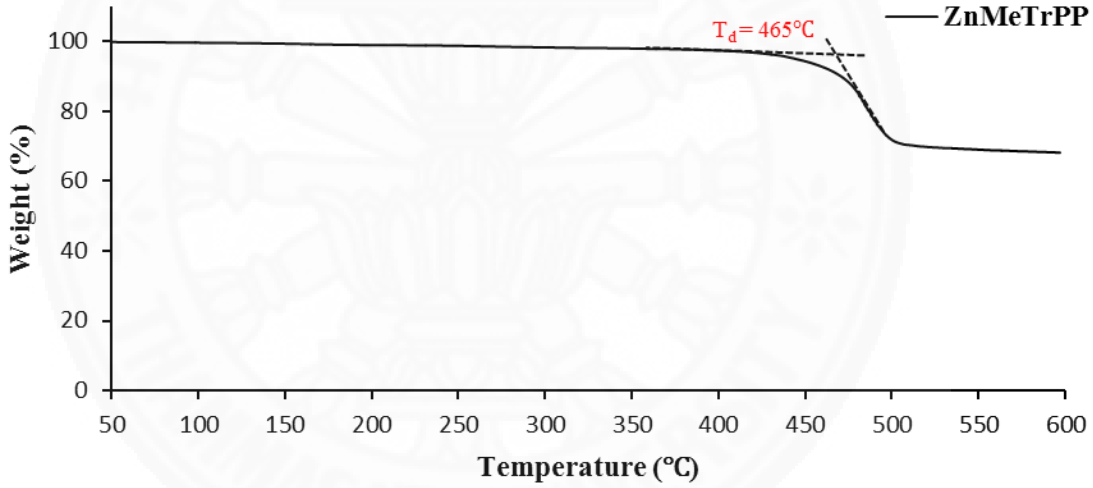

Figure G10. Thermogravimetric analysis (TGA) curves of ZnMeTrPP

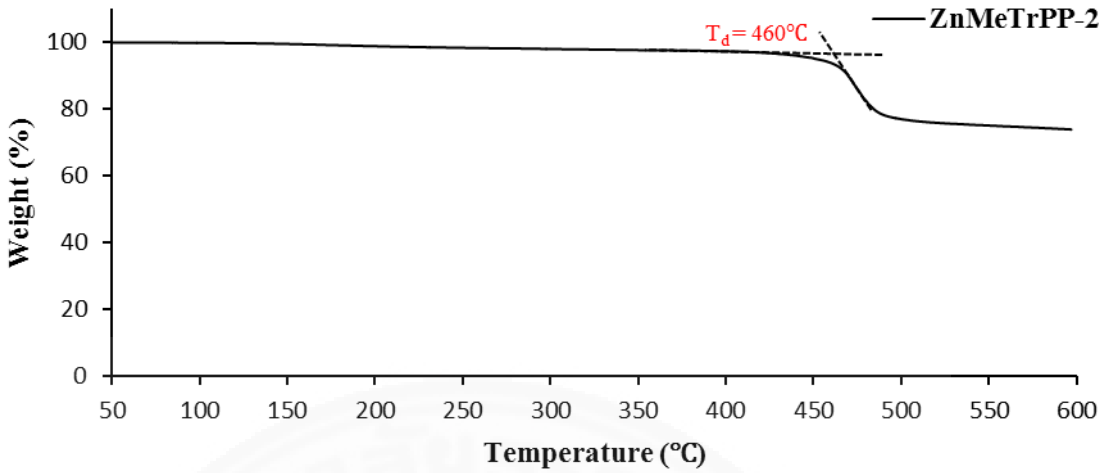

Figure G11. Thermogravimetric analysis (TGA) curves of ZnMeTrPP-2

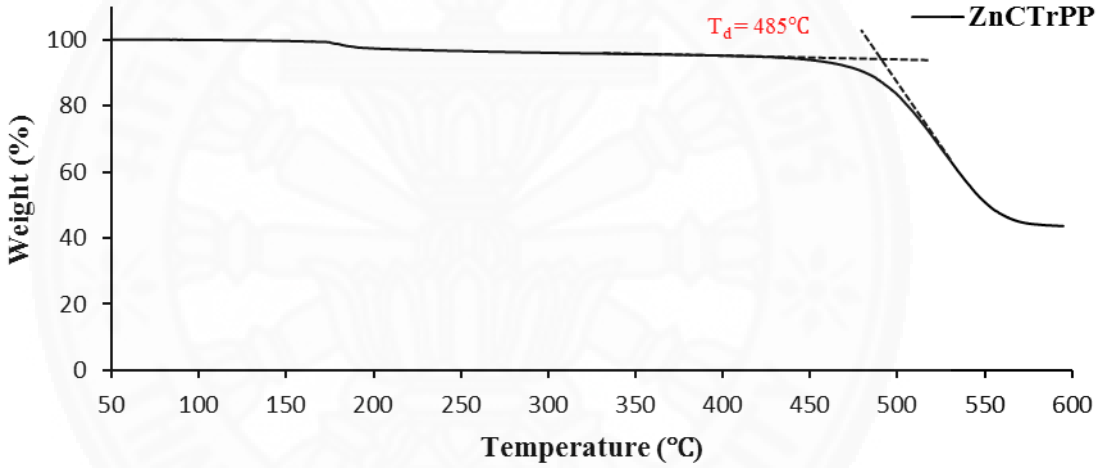

Figure G12. Thermogravimetric analysis (TGA) curves of ZnCTrPP

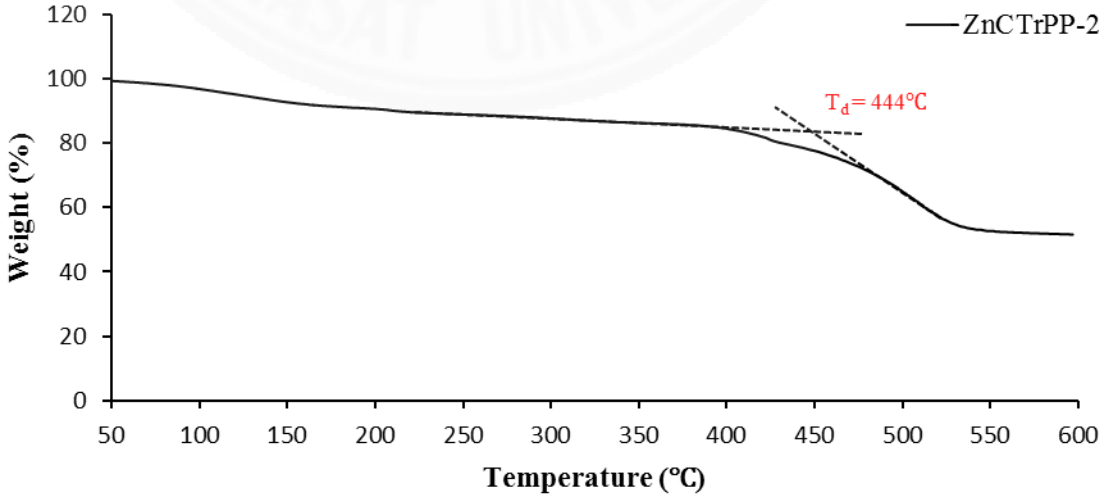

Figure G13. Thermogravimetric analysis (TGA) curves of ZnCTrPP-2

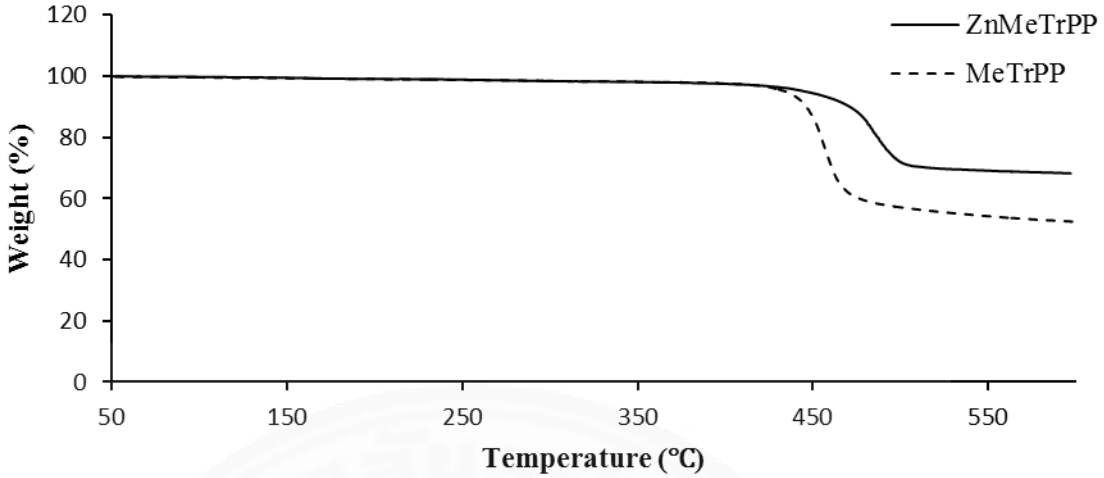

Figure G14. Comparison of TGA curves of ZnMeTrPP and MeTrPP

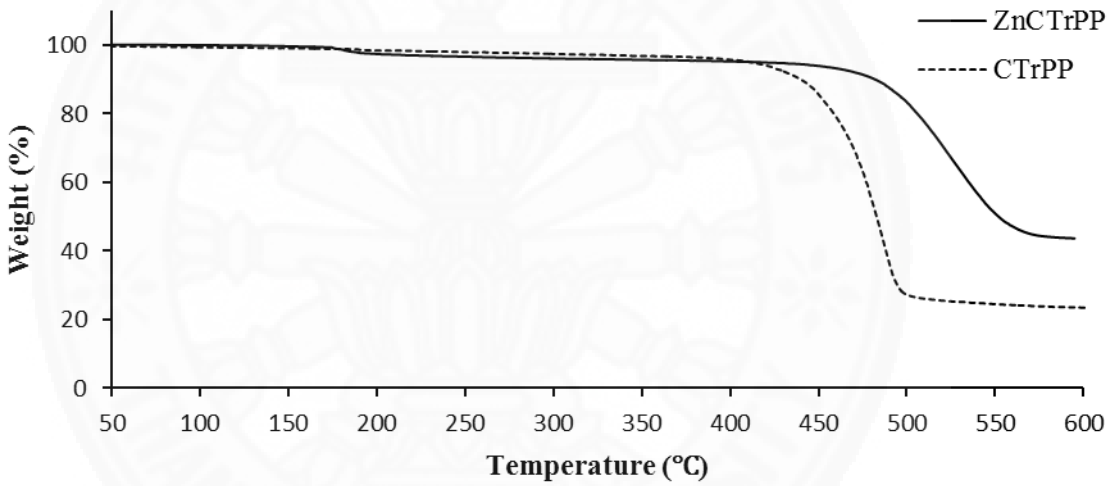

Figure G15. Comparison of TGA curves of ZnCTrPP and CTrPP

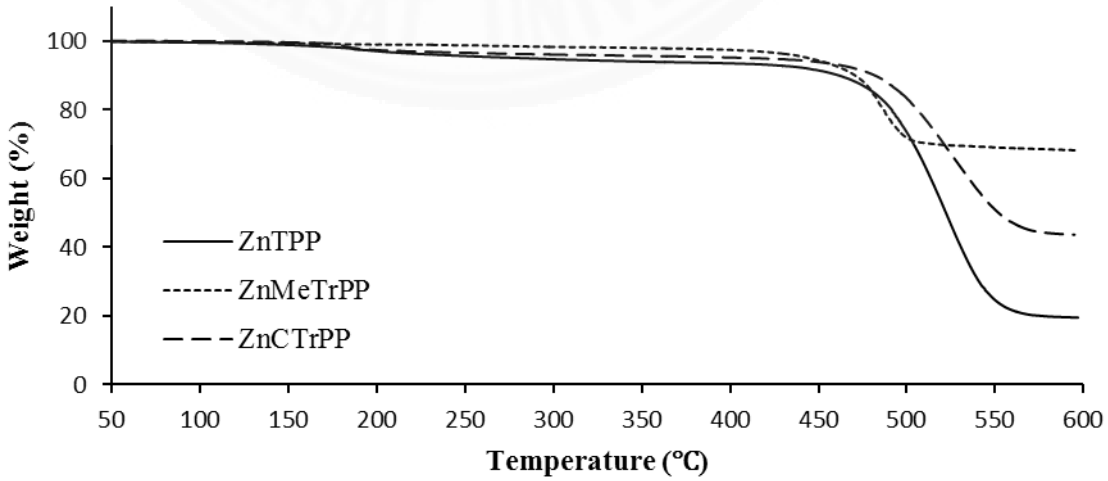

Figure G16. Comparison of TGA curves of ZnTPP, ZnMeTrPP and ZnCTrPP

BIOGRAPHY

Name	Miss Jantima Sukjan
Date of Birth	October 2, 1990
Educational Attainment	2012: Bachelor of Science in Chemistry, Thammasat University
Scholarship	2015: The National Research Council of Thailand (NRCT) "Synthesis and Characterization of Unsymmetrical Porphyrins and Their Complexes"

Publications

Poster presentation at The 39th Congress on Science and Technology of Thailand (STT 39)

Participated in a competition of invention at Institute of Intellectual Property and Business Thammasat University (TUIPI 2013)

Participated in Pure and Applied Chemistry International Conference (PACCON 2013)

Poster presentation at The 40th Congress on Science and Technology of Thailand (STT 40)

Poster Presentation at Pure and Applied Chemistry International Conference (PACCON 2014)

Paper publishing in Thai Journal of Science and Technology 3 (1) January - April (2014)

Paper publishing in Journal of Materials Science and Engineering A 4 (9) (2014) 297-302

Poster Presentation at Pure and Applied Chemistry International Conference (PACCON 2015)